T-577

A DESIGN PROCEDURE UTILIZING CROSSFEEDS FOR COUPLED MULTILOOP SYSTEMS

by

PAUL S. BASILE
B.S.E. Princeton University
(1970)

SUBMITTED IN PARTIAL FULFILLMENT
OF THE REQUIREMENTS FOR THE
DEGREE OF MASTER OF SCIENCE

at the

MASSACHUSETTS INSTITUTE OF TECHNOLOGY

May 12, 1972

Signature of Author _____
Department of Aeronautics and Astronautics, May 12, 1972

Certified by _____
Thesis Supervisor

Accepted by _____
Chairman, Departmental Graduate Committee

This report was prepared under DSR Project 55-23890, sponsored by the Manned Spacecraft Center of the National Aeronautics and Space Administration through Contract NAS 9-4065 with the Draper Laboratory.

A DESIGN PROCEDURE UTILIZING CROSSFEEDS FOR COUPLED MULTILOOP SYSTEMS

by

Paul S. Basile

Submitted to the Department of Aeronautics and Astronautics on May 12, 1972 in partial fulfillment of the requirements for the degree of Master of Science.

ABSTRACT

A design procedure is proposed for the analysis and synthesis of general coupled multiloop systems. Qualitative rules, resulting from the study of a two-output, two-input system, are generated to assist in the successful application of the design procedure to a variety of plant dynamics. Crossfeeds between controls are presented as a means of wholly or partially decoupling the outputs. The potentially conflicting demands made on the crossfeeds to reduce coupling while maintaining other desirable plant characteristics are investigated for a three-output, two-input system, and insights are developed for the successful choice of crossfeeds. Rules for the frequency domain design of feedback compensations to complete the crossfed system are presented. The design procedure is applied to the problem of designing a lateral cruise control system for the space shuttle orbiter. The degree of coupling in this system, as well as the effects of gust disturbances, are evaluated.

Thesis Supervisor: Renwick E. Curry, Ph.D.
Title: Assistant Professor of Aeronautics and Astronautics

ACKNOWLEDGMENTS

The author is indebted to his thesis supervisor, Prof. R. E. Curry, for guidance, support, and encouragement throughout this research. Also, thanks go to Dr. Robert F. Stengel at the Draper Laboratory for his many helpful suggestions and comments.

The generous contributions of interest and expert advice from Alexander Penchuk are greatly appreciated. Also, the investments of time and care by Joan Whittemore in typing the manuscript deserve acknowledgment.

A special note of appreciation is extended to the Charles Stark Draper Laboratory for providing its research facilities, for supporting the author's graduate study at M.I.T., and for providing extremely valuable and rewarding research experience.

TABLE OF CONTENTS

CHAPTER 1

INTRODUCTION

The intelligent design and analysis of complex multivariable systems has been the subject of many investigations over the past several years. As more and better techniques have been developed, systems with greater complexity have appeared. Furthermore, these systems possess, in general, more demanding design objectives than simpler systems. This has resulted in a desire for techniques which might simplify the analysis somewhat. The problem of synthesizing and analyzing a complex multi-input multi-output system is by no means, then, a completely solved one.

Undoubtedly the major complication inherent in multivariable systems over single variable systems is the additional consideration of interaction or coupling among output variables. Many of the measures of performance for single loop systems – stability, realizability, sensitivity, etc. – are equally valid for multiloop systems. However, the evaluation of some of these quantities is made difficult by the complexities of loop couplings.

Study of these couplings has given rise to an analysis and synthesis technique developed by Systems Technology, Inc. (see Ref. 1) which utilizes so-called "coupling numerators". These are unique to mutli-variable systems and are developed briefly in Appendix A. Use is made of coupling numerators at various points in this thesis.

While each specific system will have different desired results, the generally acceptable design objectives for multivariable systems are usually not much different than for single variable systems. That is, it is desired to achieve a good closed loop frequency response. In addition, it is desired that the system achieve a specified degree of decoupling.

Both of these objectives will be satisfied by the design procedure presented. However, the last objective is the central consideration of this thesis. The "desired degree of decoupling" changes, of course,

from system to system. If it is desired, for instance, that there be complete decoupling, then a one-to-one correspondence will exist between input and output variables. That is, each output will be governed by only one input. However, since cases where the number of outputs exceeds the number of controls is fairly common, each control may regulate more than one output variable.

A common procedure in current use is to employ matrix techniques to analyze multivariable systems. For example, the designer might make use of cascade compensation in order to diagonalize – and hence decouple – a system matrix. Kavanagh (1956) has developed in some detail matrix methods for the analysis and synthesis of linear multivariable control systems. The central concept is cancellation compensation, or cancelling the undesired dynamics and replacing them with desired closed loop dynamics. The technique depends, to a large extent, upon knowledge of the matrix of desired closed loop dynamics. Rather than study that matrix, in this thesis each loop in the multiloop system is examined separately and sequentially.

Cox (1965) uses matrix partitioning schemes to directly control the system interaction. His synthesis technique, directly applied to the interaction, concentrates on achieving nonexact low interaction. Complete decoupling (no interaction) is investigated by Morse and Wonham (1970). Use is made in their study of dynamic compensation (an important element of this thesis) in addition to state variable feedback.

A satisfactory multiloop analysis and design procedure should satisfy several requirements. It should provide clear physical appreciation for the analysis, as well as revealing design-oriented insights and intuitions. It should clearly separate the open loop plant characteristics in order that the effects of both may be evaluated separately. Also it would be desirable if use could be made of existing well-developed graphical analysis techniques – so that a "good" system can be achieved by an experienced designer with a minimum of iterations. The "good" system will respond quickly and accurately to commands, be well-damped, and will suppress disturbances. The design procedure presented in this thesis is intended to satisfy all of these requirements.

This thesis examines one possible means of decoupling a system – the use of crossfeeds between loops. It is hoped, in attempting this procedure, that the crossfeed signal between two loops will cancel, or at least reduce, the plant coupling between the two loops. This idea can be viewed as a kind of compensation, where the intent of the compensation is to reduce or eliminate a plant coupling transfer function.

The analysis begins with a presentation of the general two-input, two-output system in Chapter 2. The design procedure to be followed throughout this thesis is outlined and rules are given for the evaluation of coupling effects. Chapter 3 introduces the possibility of crossfeeds to reduce couplings. Generality is increased in Chapter 4 with systems having three outputs. Crossfeeds are designed, in a general qualitative way, for this 3×2 system. Finally, in Chapter 5, the entire design procedure, with crossfeeds, is applied to the lateral atmospheric control of the space shuttle orbiter.

CHAPTER 2

THE GENERAL TWO-INPUT TWO-OUTPUT COUPLED SYSTEM

2.1 Introduction

In order to begin the analysis and design of coupled multiloop systems, a two-input, two-output system will be studied. While this system is relatively simple, it is complex enough to include most of the elements necessary to develop a design procedure. It will be used as a basis for the procedure to evaluate the degree of plant coupling and to design a good closed loop system.

The Laplace-transformed linearized equations of a system may be written as

$$A(s)\underline{x}(s) = B(s)\underline{u}(s) + C(s)\underline{x}_d(s) \qquad (2.1)$$

where $\underline{x}(s)$ and $\underline{u}(s)$ are the vector output and control vectors, respectively, and $\underline{x}_d(s)$ is the disturbance input vector. A(s), B(s) and C(s) are matrices dependent on plant characteristics. Transfer functions for control or disturbance inputs can be obtained from Eq. (2.1) by Cramer's rule. The system could then be equivalently represented as

$$\underline{x}(s) = G(s)\underline{u}(s) + G_d(s)\underline{x}_d(s) \qquad (2.2)$$

where G(s) is the matrix of control input transfer functions and $G_d(s)$ is the matrix of disturbance input transfer functions.

In this chapter, both G(s) and $G_d(s)$ are (2×2). The design procedure to be utilized throughout this paper is described and the various types of plant couplings are evaluated.

2.2 The Design Procedure

The two-dimensional transfer function matrix is

$$G(s) = \begin{bmatrix} G_{11}(s) & G_{12}(s) \\ G_{21}(s) & G_{22}(s) \end{bmatrix}$$

and, according to Eq. (2.1), the system equations are (dropping the notational dependence on s)

$$\begin{aligned} x_1 &= G_{11}u_1 + G_{12}u_2 + G_{11_d}x_{1_d} + G_{12_d}x_{2_d} \\ x_2 &= G_{21}u_1 + G_{22}u_2 + G_{21_d}x_{1_d} + G_{22_d}x_{2_d} \end{aligned} \tag{2.3}$$

This open-loop system may be represented as shown in Fig. 2.1.

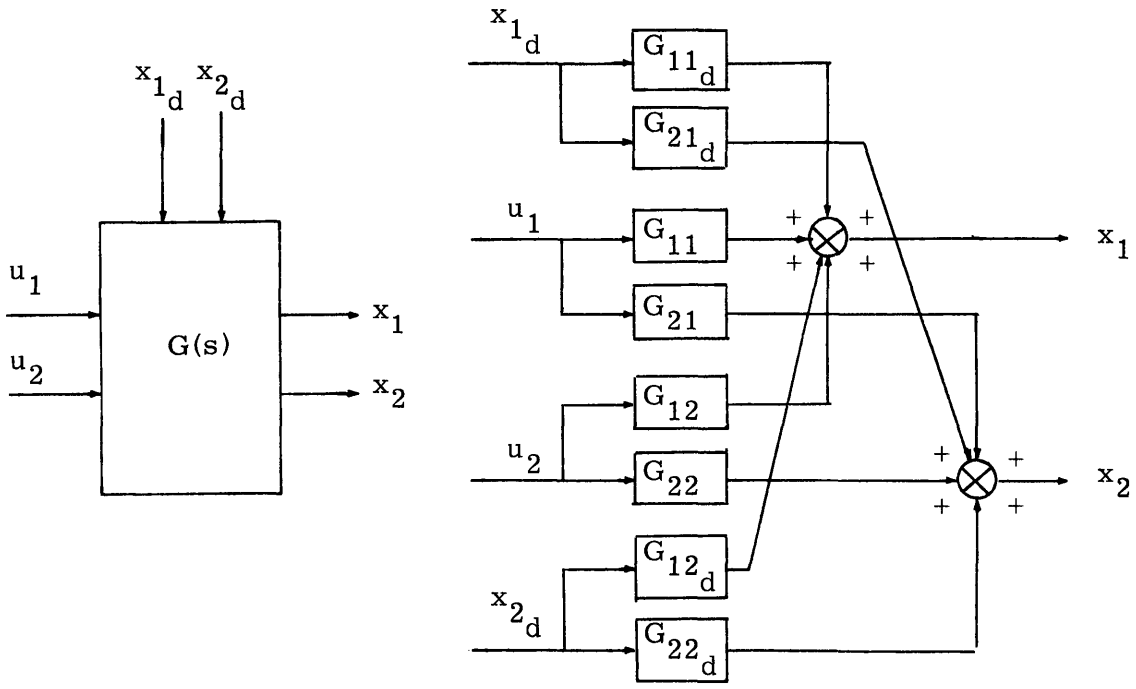

Figure 2.1 The Open Loop Plant

The design is carried out in the frequency domain. To simplify matters for the time being, disturbance inputs are neglected. The intent for this two-output two-control plant is to design two feedback loops as shown in Fig. 2.2, where $x_1 \rightarrow x_{1c}$ is referred to as "loop #1" and $x_2 \rightarrow x_{2c}$ as "loop #2." The effect of one loop upon the other due to plant couplings is investigated in some detail, and it is decided whether this effect has bearing on the design of compensators H_{11} and H_{22}.

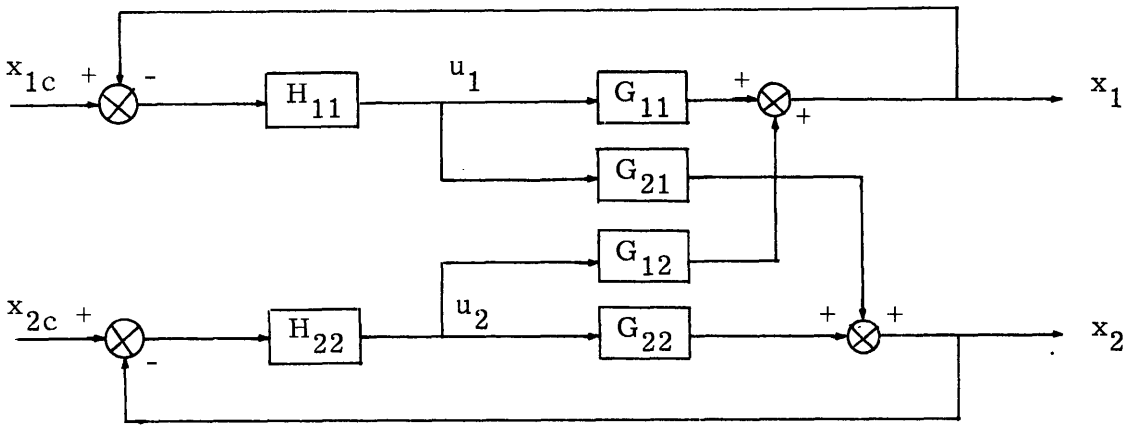

Figure 2.2 General Two-Loop Control System

A convenient way to look separately at the coupling effects of one loop upon the other is afforded by Figs. 2.3 and 2.4. Fig. 2.3 shows best the coupling effects of loop #1 on loop #2 while Fig. 2.4 shows best the effects of loop #2 on loop #1.

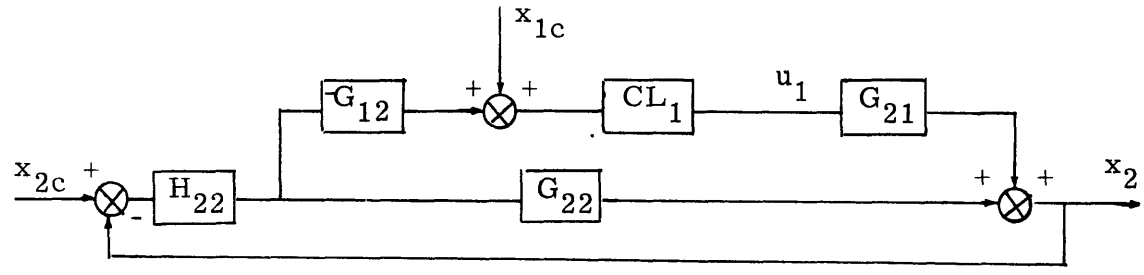

Figure 2.3 Block Diagram of Loop #2 Showing Coupling from Loop #1

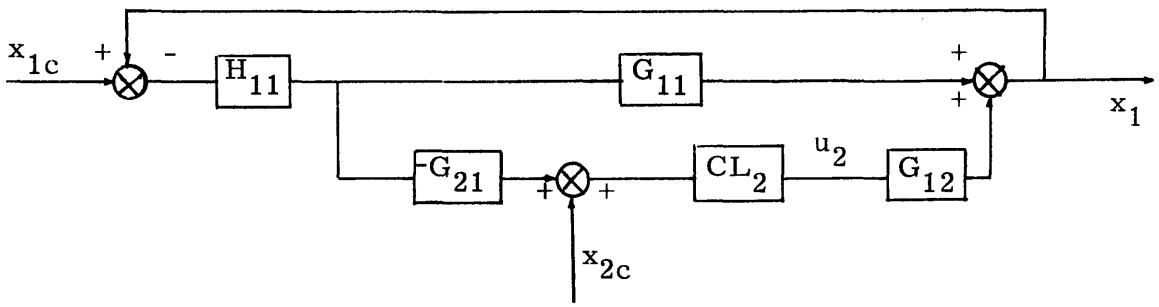

Figure 2.4 Block Diagram of Loop #1 Showing Coupling from Loop #2

In Figs. 2.3 and 2.4,

$$CL_1 = \frac{H_{11}}{1+H_{11}G_{11}} \qquad \text{and} \qquad CL_2 = \frac{H_{22}}{1+H_{22}G_{22}}.$$

The design procedure is as follows:

a) Close loop #1

Design H_{11} so that the closed loop system follows the signal over a desired frequency range (generally from zero frequency up to some desired frequency), i.e., so that

$$\frac{x_1}{x_{1c}} = \frac{H_{11}G_{11}}{1+H_{11}G_{11}} = T_1 \approx 1 \tag{2.4}$$

over the specified frequency range. The "frequency range" referred to here is generally defined as zero frequency up to the bandwidth (ω_B, the half-power frequency for the closed loop) of that particular loop. The approximation that the crossover frequency (ω_c, the frequency where the open loop magnitude equals one) is nearly equal to the bandwidth will be used here. An additional specification for H_{11} is that there be adequate open loop gain margin and phase margin.

b) Analyze and design loop #2 with loop #1 closed

The closed loop transfer function for loop #2 is (see Fig. 2.3)

$$\frac{x_2}{x_{2c}} = \frac{H_{22}(G_{22} - G_{12}CL_1G_{21})}{1+H_{22}(G_{22} - G_{12}CL_1G_{21})}. \tag{2.5}$$

In designing H_{22}, first neglect the plant cross-coupling – the term that represents the signal x_2 passing through loop #1. The transfer function then becomes

$$\frac{\tilde{x}_2}{x_{2c}} = \frac{H_{22}G_{22}}{1 + H_{22}G_{22}} = T_2 \qquad (2.6)$$

Design H_{22}, using Eq. (2.6), to achieve the desired closed loop response for loop #2. Then, after H_{22} is designed, compare the relative sizes of the "direct" term G_{22} and the coupling term $-G_{12}CL_1G_{21}$. Since all transfer functions possess magnitude and phase, one must compare their vector magnitudes over the frequency range of interest. The "parameter plott" given in Appendix B is useful in this regard. An advantage to frequency domain design is that in doing frequency, or Bode plots for the transfer functions involved, the information regarding magnitude and phase as functions of frequency needed for the parameter plot is readily available. By using the parameter plot it can be determined whether the coupling can be neglected. If not, then it may be necessary to redesign H_{22} using the more complicated Eq. (2.5).

c) Determine the effect of loop #2 on loop #1

With both loops now closed, return to loop #1 and determine the effect on x_1 of the coupling caused by the closure of the second loop. This coupling term appears in the two-closed-loop expression (from Fig 2.4)*

$$\left.\frac{x_1}{x_{1c}}\right|_{2CL} = \frac{H_{11}(G_{11} - G_{21}CL_2G_{12})}{1 + H_{11}(G_{11} - G_{21}CL_2G_{12})} \qquad (2.7)$$

Analogously to b) compare, by using the parameter plot, G_{11} and $G_{21}CL_2G_{12}$ – the effect on loop #1 of loop #2. In many applications, the coupling term is quite a bit smaller in vector magnitude than G_{11}, and

---

* The notation $x_{|nCL}$ will be used wherever there is possible ambiguity to indicate that the quantity x is being written for the system with n loops closed.

H_{11} as already designed is satisfactory. However, if the coupling is large, a redesign of H_{11} using Eq. (2.7) may have to be considered.

d) Determine the effects of x_{2c} on x_1 and x_{1c} on x_2

Besides coupling due to the signal of one loop passing through the other loop, there are couplings in each loop due to command inputs in the other. Of course, both these types of couplings result basically from the cross coupling plant transfer functions. The two closed loop "coupling" transfer functions are, again using Figs. 2.3 and 2.4:

$$\frac{x_1}{x_{2c}} = \frac{G_{12} CL_2}{1 + H_{11} G_{11} - H_{11} G_{21} CL_2 G_{12}} \tag{2.8}$$

$$\frac{x_2}{x_{1c}} = \frac{G_{21} CL_1}{1 + H_{22} G_{22} - H_{22} G_{12} CL_1 G_{21}} \tag{2.9}$$

It will be observed throughout this paper that all transfer functions can be written in slightly different forms, each of which reveals different insights into the factors involved in the transfer functions. For instance, by simple algebra on Eq. (2.8)

$$\left.\frac{x_1}{x_{2c}}\right|_{2CL} = \frac{G_{12} CL_2}{1 + G_{12} CL_2 \left[\dfrac{H_{11} G_{11}}{G_{12} CL_2} - H_{11} G_{21}\right]} = \frac{G}{1+GH}$$

$$= \frac{1}{H} \frac{G}{\frac{1}{H} + G}. \tag{2.10}$$

To determine whether either of the coupling transfer functions Eqs. (2.8) or (2.9) is large, the form of Eq. (2.10) is helpful. That is, if at the frequencies of interest, G – i.e., $G_{12} CL_2$ – is much greater

than H – i.e., $\left(\frac{H_{11}G_{11}}{G_{12}CL_2} - H_{11}G_{21}\right)$ – then $\frac{x_1}{x_{2_c}} \approx \frac{1}{H}$, which is small.

If $G \ll \frac{1}{H}$, then $\frac{x_1}{x_{2_c}} \approx 1$. This is no surprise since G represents the plant coupling.

e) Determine the effects of disturbance inputs x_{1_d} and x_{2_d} on x_1 and x_2

The easiest way to obtain the transfer functions for the two-closed-loop system needed for this step in the design procedure is to use the method described in Appendix A. More will be mentioned of this method in later chapters. Here it is sufficient to say that by this technique, the following transfer functions for disturbance inputs can be obtained:

$$\left.\frac{x_1}{x_{1_d}}\right|_{2CL} = \frac{G_{11_d} + H_{22}(G_{22}G_{11_d} - G_{12}G_{21_d})}{1 + H_{11}G_{11} + H_{22}G_{22} + H_{11}H_{22}(G_{11}G_{22} - G_{12}G_{21})}$$

$$= \frac{G_{11_d} - G_{12}CL_2G_{21_d}}{1 + H_{11}G_{11} - H_{11}G_{12}CL_2G_{21}} \qquad (2.11)$$

Similarly,

$$\left.\frac{x_1}{x_{2_d}}\right|_{2CL} = \frac{G_{12_d} - G_{12}CL_2G_{22_d}}{1 + H_{11}G_{11} - H_{11}G_{12}CL_2G_{21}} \qquad (2.12)$$

$$\left.\frac{x_2}{x_{1_d}}\right|_{2CL} = \frac{G_{21_d} - G_{21}CL_1G_{11_d}}{1 + H_{22}G_{22} - H_{22}G_{21}CL_1G_{12}} \qquad (2.13)$$

loop transfer functions Eqs. (2.11) - (2.14) will very likely be small. But of course, if G_{11_d}, G_{12_d}, G_{21_d}, and G_{22_d} are small, disturbances will present no problem in any case. Notice that the denominators of Eqs. (2.11) - (2.14) (as well as the denominators of Eqs. (2.8) and (2.9)) will be large at low frequencies. That is, the denominators will be, at low frequencies, approximately $1 + H_{11}G_{11}$ or $1 + H_{22}G_{22}$ which, for properly designed H_{11} and H_{22}, are large. This result contributes to making the two-closed-loop disturbance transfer functions small.

In order to get a broad view of possible types of plant dynamics and thus generate rules for making more specific predictions about couplings, the design procedure was applied to a variety of different plant dynamics. The following parameters were varied:

1. ratios of bandwidths of G_{11} and G_{22}
2. relative magnitudes of G_{11} and G_{22}
3. ratios of bandwidths of G_{12} and G_{21}
4. relative magnitudes of G_{12} and G_{21}

Also, it should be remembered that it is necessary to achieve small coupling only in the frequency range of interest. This range is generally from zero frequency up to the bandwidth of the loop in question. At much higher frequencies then the loop bandwidth, coupling is immaterial.

It might be of some benefit here to choose one sample case of plant dynamics — i.e., one set of parameters listed above — and apply the design procedure to it. The conclusions which will be drawn from this one qualitative case have been verified by applying the same procedure, as noted above, to many other combinations of parameters.

Consider a 2x2 plant with one high bandwidth transfer function, one low bandwidth transfer function, and two coupling transfer functions which both have moderate gain at all frequencies. Following the design procedure:

$$\left.\frac{x_2}{x_{2_d}}\right|_{2CL} = \frac{G_{22_d} - G_{21}CL_1G_{12_d}}{1 + H_{22}G_{22} - H_{22}G_{21}CL_1G_{12}} \qquad (2.14)$$

These transfer functions should be small in the frequency ranges of interest for a well designed system. There are several possible ways to determine whether they are large or not.

One procedure is to compare the two numerator terms in each transfer function by means of the parameter plot over the frequency range of interest (which is the frequency range of interest for the output variable). Or, the method of Appendix A may be used to obtain the numerical values for the transfer functions Eqs. (2.11) - (2.14). This can be done fairly quickly and easily, and then frequency responses for the entire function may be done. Either way, these transfer functions do not lend themselves easily to the kind of qualitative insight as was possible in steps a) - d).

2.3 A Summary of Qualitative Applications of the Design Procedure

It would definitely be desirable if the designer, given a plant, could know whether the couplings as described previously would be large or not. This a priori information can give clues for desirable loop closure sequence.

By means of just a brief examination of the relevant transfer functions, one fortunate occurrence may be noticed. Often the plant couplings G_{12} and G_{21} appear as a product. If either one of them is small at the right frequencies, the term containing the product will be small.

One unfortunate occurrence can also be easily recognized. It is impossible to generalize — without knowing the particular plant dynamics — as to the size of the disturbance input transfer functions. Partially this is because each transfer function is dependent on two open loop disturbance transfer functions. One obvious conclusion is that, if the open loop transfer functions, G_{11_d}, G_{12_d}, etc. are small, then the two-closed-

a) Close loop #1

Design H_{11} to be a high gain at low frequency ($\omega < \omega_{c_1}$). Perhaps $H_{11} = K_{11}/s$.

b) Analyze and design loop #2 with loop #1 closed

Design H_{22} to be a high gain at low frequency ($\omega < \omega_{c_2}$). Perhaps $H_{22} = K_{22}/s$. Next, use Eq. (2.5) to determine the effect of the coupling due to loop #1 on loop #2. That is, compare G_{22} and $-G_{12}CL_1G_{21}$.

$$CL_1 = \frac{H_{11}}{1 + H_{11}G_{11}} \approx \begin{cases} \frac{1}{G_{11}} & \text{at low frequency } (\omega < \omega_{c_1}) \\ H_{11} & \text{at high frequency } (\omega > \omega_{c_1}) \end{cases}$$

The coupling term $-G_{12}CL_1G_{21}$ is small at frequencies less than the loop #1 crossover if G_{11} has large magnitude in that region. The desire here of course is that the coupling be small over the frequency range of interest for x_2, that is for $\omega < \omega_{c_2}$. So CL_1 should be small in this range. This indicates that it is desirable that $\omega_{c_1} > \omega_{c_2}$ — that is, that the first loop have a higher bandwidth than the second. In other words, G_{11} should be the high frequency transfer function of the plant, and G_{22} the low frequency transfer function. Also, it is helpful if the magnitude of the first loop (G_{11}) is large at low frequencies so that $CL_1 = 1/G_{11}$ is small.

Also, as succeeding loops are closed, the dominant factors of the denominator tend to move toward lower frequency. This, of course, contributes to a reduction in bandwidth for each successive closure. Thus, the first loop closed should be the highest frequency loop. All of these considerations, if satisfied, will make a redesign of H_{22} unnecessary.

c) Determine the effect of loop #2 on loop #1

From Eq. (2.7), compare G_{11} and $-G_{21}CL_2G_{12}$.

$$CL_2 = \frac{H_{22}}{1 + H_{22} G_{22}} \approx \begin{cases} \frac{1}{G_{22}} \text{ at low frequencies } (\omega < \omega_{c_2}) \\ H_{22} \text{ at high frequencies } (\omega > \omega_{c_2}) \end{cases}$$

The coupling term $-G_{21} CL_2 G_{12}$ should be smaller than G_{11} at frequencies less than the loop #2 crossover. However, if — as was tentatively concluded above — $\omega_{c_1} > \omega_{c_2}$, then the frequency range of interest includes higher frequencies than ω_{c_2}. At these higher frequencies ($\omega_{c_2} < \omega < \omega_{c_1}$) $CL_2 \approx H_{22}$ and, since H_{22} is designed as high gain at low frequency ($\omega < \omega_{c_2}$), H_{22} may be small in this range. Also, it would be beneficial, in order to ensure small coupling, if G_{22} were large at low frequency so that $CL_2 \approx 1/G_{22}$ could be small at these frequencies. Thus, if G_{11} is large at low frequencies, then the coupling term $-G_{21} CL_2 G_{12}$ should be small — relative to G_{11} at least — in the frequency range of interest for x_1 and H_{11} will not have to be redesigned.

d) Determine the effects of x_{2c} on x_1 and x_{1c} on x_2

From Eq. (2.8), $\left.\frac{x_1}{x_{2c}}\right|_{2CL}$ will be small if G_{12} is small at frequencies of interest for $x_1 (\omega < \omega_{c_1})$, assuming the smallness of CL_2 as discussed above.

From Eq. (2.9), $\left.\frac{x_2}{x_{1c}}\right|_{2CL}$ will be small if G_{21} is small at frequencies of interest for $x_2 (\omega < \omega_{c_2})$, assuming the smallness of CL_1 as discussed above.

The conclusions resulting from repeated applications of the design procedure (such as the sample one just presented) for several different combinations of plant parameters may be summarized as follows.

1. If at least one of G_{12} or G_{21} is small, or both are moderate in magnitude, and if the "direct" transfer function G_{11} is large at frequencies of interest, then coupling can generally be neglected in the design procedure.* The only notable (and symmetrical) exceptions are the following:

a) If G_{21} is large and has high bandwidth, then — regardless of G_{12} — x_2/x_{1_c} may be significant.

b) If G_{12} is large and has high bandwidth, then — regardless of G_{21} — x_1/x_{2_c} may be significant.

2. The highest frequency loop should be closed first, so that succeeding outer loops — whose bandwidths are somewhat altered by inner loop closures — may have as large bandwidths as possible.

3. The "direct" transfer functions should have large magnitudes over their respective frequency ranges of interest.

In addition, several observations can be made which would indicate rules for a desirable loop closure sequence. This type of conclusion is not easy to draw and results only from insights gained from repeated qualitative applications of the design procedure.

1. Since inner loops alter the dynamics of outer loops, those loops requiring extensive compensation should be made outer loops. In this way, the inner loops may assist in the compensation.

2. Undesirable quantities may be suppressed by being made inner loops. These quantities never appear outside the system — they are effectively nulled by well-designed inner loops.

---

* If any of these conditions are not met, a redesign of H_{11} or H_{22} may be necessary.

3. The outputs of most interest — the outputs for which there will be command inputs — should appear as outer loops.

2.4 Numerical Examples

Admittedly the application of the design procedure in the last section was a qualitative and approximate one. Here, a very simple numerical example will be done using the design procedure. As in Section 2.2, the plant considered has a high frequency transfer function, a low frequency transfer function, and coupling transfer functions that have moderate gain at all frequencies. Consider this plant as

$$G = \begin{bmatrix} G_{11} & G_{12} \\ G_{21} & G_{22} \end{bmatrix} = \begin{bmatrix} \frac{20}{s+10} & 1 \\ 1 & \frac{1}{s+1} \end{bmatrix} \qquad (2.15)$$

The design procedure:

a) Close loop #1

For $H_{11}G_{11}$ to have large low frequency gain, design

$$H_{11} = \frac{5}{s}$$

Then

$$T_1 = \frac{H_{11}G_{11}}{1 + H_{11}G_{11}} = \frac{100}{s^2 + 10s + 100} \approx 1$$

at low frequencies. This choice for H_{11} also puts the bandwidth of loop #1 at $\omega_{B_1} \approx 10$ rad/sec, keeping this loop a high frequency loop.

b) Analyze and design loop #2 with loop #1 closed

First, neglecting coupling, design H_{22} so that $H_{22}G_{22}$ has a large low frequency gain. Thus

$$H_{22} = \frac{1}{s}$$

Then

$$T_2 = \frac{H_{22}G_{22}}{1 + H_{22}G_{22}} = \frac{1}{s^2 + s + 1} \approx 1.$$

at low frequencies. H_{22} is designed so that $\omega_{B_2} \approx \omega_{C_2} = 1$. That is, loop #2 remains a low frequency loop. For this plant, an increase in the gain of H_{22} would effectively increase the bandwidth of loop #2, if desired.

Now consider the effects of loop #1 on loop #2. The coupling term is

$$. \; G_{12}CL_1G_{21} = CL_1 = \frac{5(s+10)}{s^2 + 10s + 100}.$$

So that

$$(G_{22} - G_{12}CL_1G_{21}) = -\frac{4s^2 + 45s - 50}{(s+1)(s^2+10s+100)} \tag{2.16}$$

$$= -4\,\frac{(s-1.02)(s+12.28)}{(s+1)(s+5+j8.66)(s+5-j8.66)}.$$

This coupling is fairly large at low frequency, yet H_{22} as designed for G_{22} alone is still adequate. This is evident in Figs. 2.5a and 2.5b which compare the frequency plots of $H_{22}G_{22}$ and $H_{22}(G_{22} - G_{12}CL_1G_{21})$. In these plots — and in all the frequency plots in this thesis — magnitude is plotted in decibel units (dB), where $|G(j\omega)|_{dB} = 20 \log |G(j\omega)|$ and phase is plotted in degrees, both versus the logarithm of the frequency in radian/second. The phase is determined by noting that each minus sign in the transfer function — due to a negative gain factor or right hand s-plane poles and zeros — contributes -180° of phase angle at dc. The coupling has the effect of reducing the crossover from $\omega_{C_2} = .80$ (no coupling) to $\omega_{C_2} = .50$ (with coupling) and of reducing the phase margin from 57° to 40°. Similarly, the bandwidth is reduced from 1.3 to 1.2. To reduce the coupling, it would be desirable for CL_1 to be

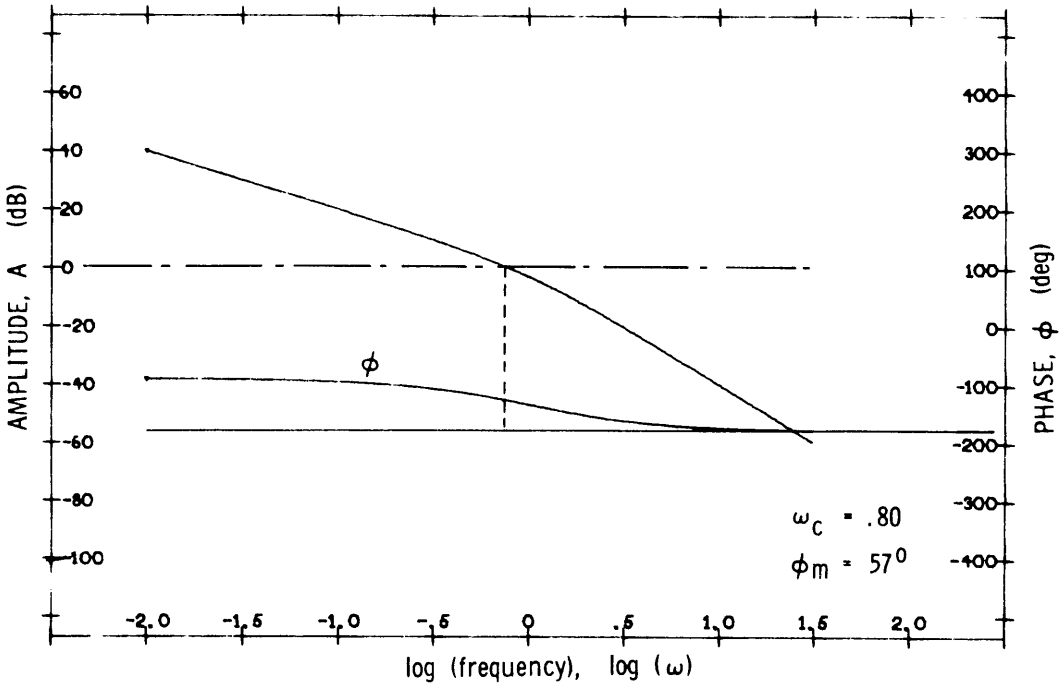

Fig. 2.5a Frequency Plot of $H_{22}G_{22}$

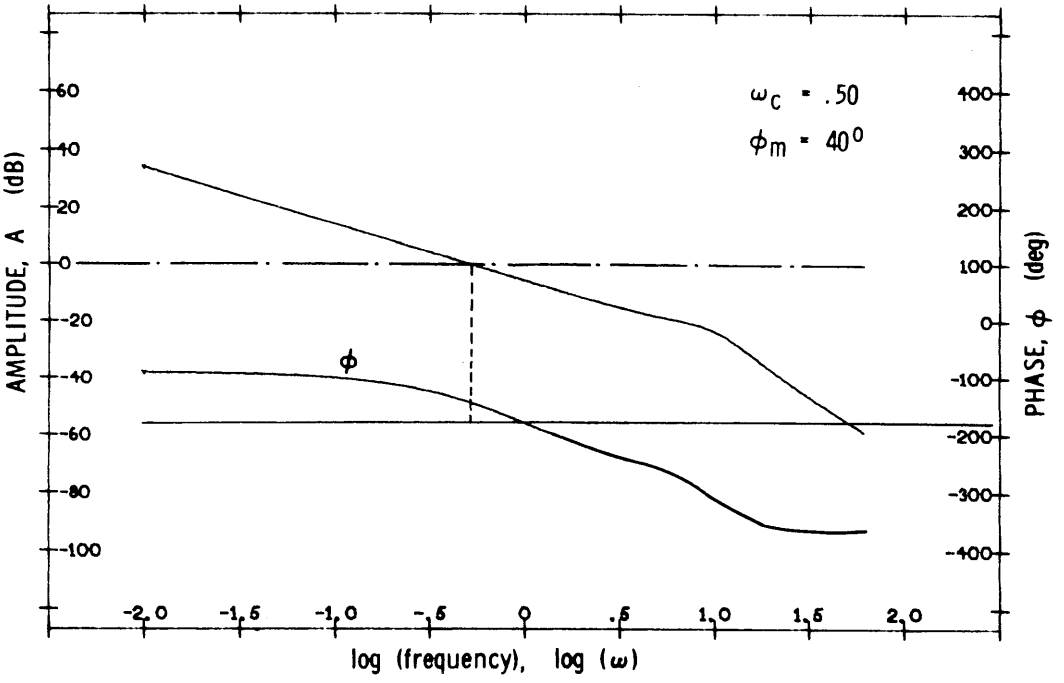

Fig. 2.5b Frequency Plot of $H_{22}(G_{22} - G_{12}CL_1G_{21})$

smaller at low frequencies. Since $CL_1 \approx 1/G_{11}$ at low frequencies, the conclusion of Section 2.3 that G_{11} be large at low frequencies is verified.

c) Determine the effect of loop #2 on loop #1

From Eq. (2.7) the coupling term is

$$G_{21} CL_2 G_{12} = CL_2 = \frac{s + 1}{s^2 + s + 1}.$$

So that

$$(G_{11} - G_{21} CL_2 G_{12}) = \frac{19s^2 + 9s + 10}{(s+10)(s^2+s+1)}. \qquad (2.17)$$

While the coupling here is fairly large, G_{11} is large enough so that there are no difficulties. The crossover frequency and phase margin are virtually unchanged by the addition of coupling. At $\omega = 0$, $G_{11} = 2$ and the coupling term $G_{21} CL_2 G_{12} = 1$. Frequency plots comparing $H_{11} G_{11}$ and $H_{11}(G_{11} - G_{21} CL_2 G_{12})$ are presented in Figs. 2.6a and 2.6b and indicate that the coupling is not large enough to warrant a redesign of H_{11}.

d) Determine the effects of x_{2c} on x_1 and x_{1c} on x_2

From Eq. (2.8)

$$G_{12} CL_2 = \frac{s + 1}{s^2 + s + 1}$$

which is considerably smaller than $H_{11} G_{11}$ at low frequencies. Thus, the coupling effect of x_{2c} on x_1 compared to x_{1c} on x_1 can be neglected at low frequency.

From Eq. (2.9)

$$G_{21} CL_1 = \frac{5(s + 10)}{s^2 + 10s + 100}$$

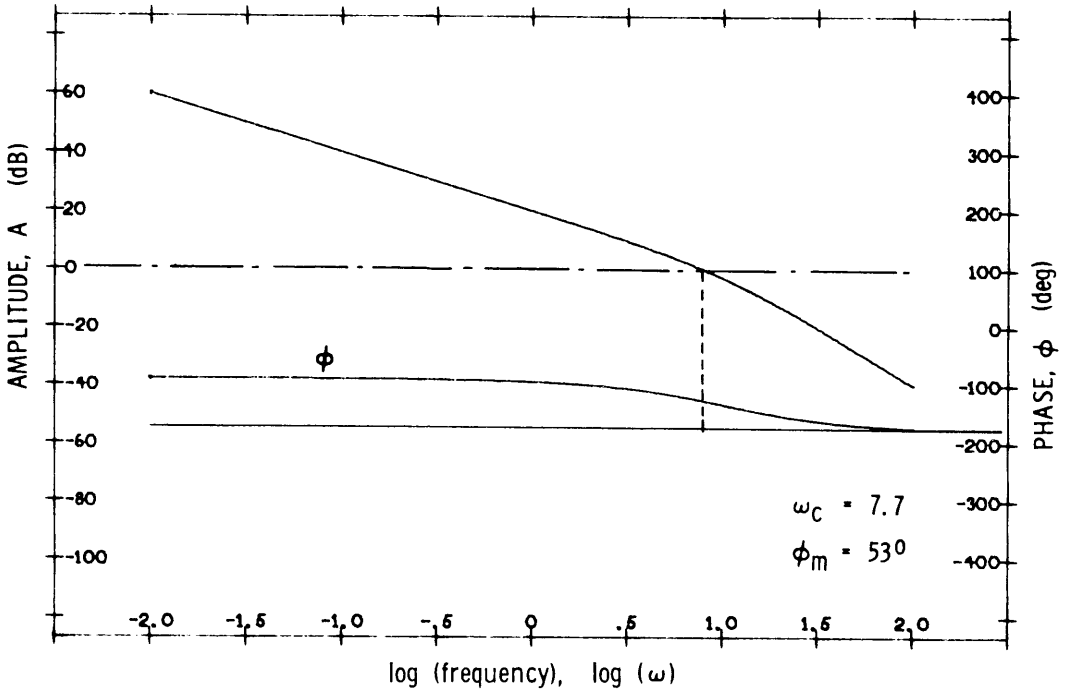

Fig. 2.6a Frequency Plot of $H_{11}G_{11}$

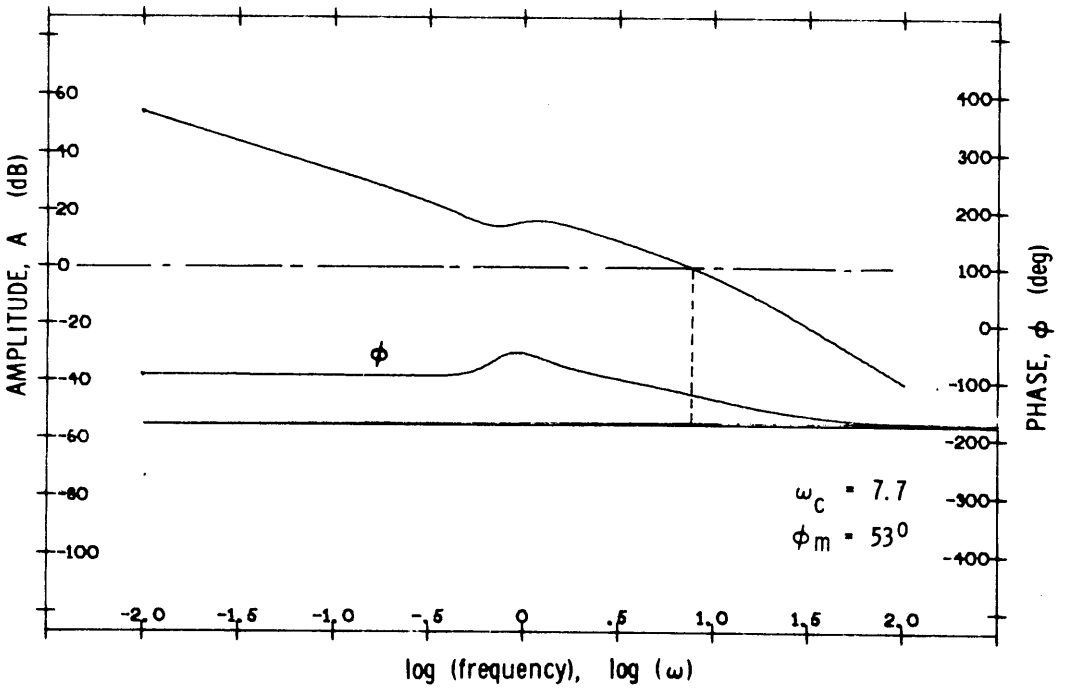

Fig. 2.6b Frequency Plot of $H_{11}(G_{11} - G_{21}CL_2G_{12})$

which is considerably smaller than $H_{22}G_{22}$ at low frequencies. Thus, the coupling effect of x_{1c} on x_2 compared to x_{2c} on x_2 can be neglected at low frequency.

Further evidence confirming this analysis can be found in Figs. 2.7 and 2.8, which compare the time responses $x_1(t)$ and $x_2(t)$ due to unit step commands x_{1c} and x_{2c}. It is seen that, at steady state, the response in each loop to a command in that loop is good — i.e., the command signal is accurately reproduced. In addition, the response in each loop to a command in the other loop is very small (zero at steady state) — indicating the small amount of coupling at low frequency.

Consider now a slightly altered plant so that G_{11}, as recommended, has larger gain at low frequencies.

$$G = \begin{bmatrix} G_{11} & G_{12} \\ G_{21} & G_{22} \end{bmatrix} = \begin{bmatrix} \frac{100}{s+10} & 1 \\ 1 & \frac{1}{s+1} \end{bmatrix} \qquad (2.18)$$

The design procedure, followed in a completely parallel way to the example just concluded, is

a) Close loop #1

$$H_{11} = \frac{1}{s}.$$

Then

$$T_1 = \frac{H_{11}G_{11}}{1 + H_{11}G_{11}} = \frac{100}{s^2 + 10s + 100} \approx 1.$$

at low frequencies, which is exactly the same as the previous example.

b) Analyze and design loop #2 with loop #1 closed

$$H_{22} = \frac{1}{s}.$$

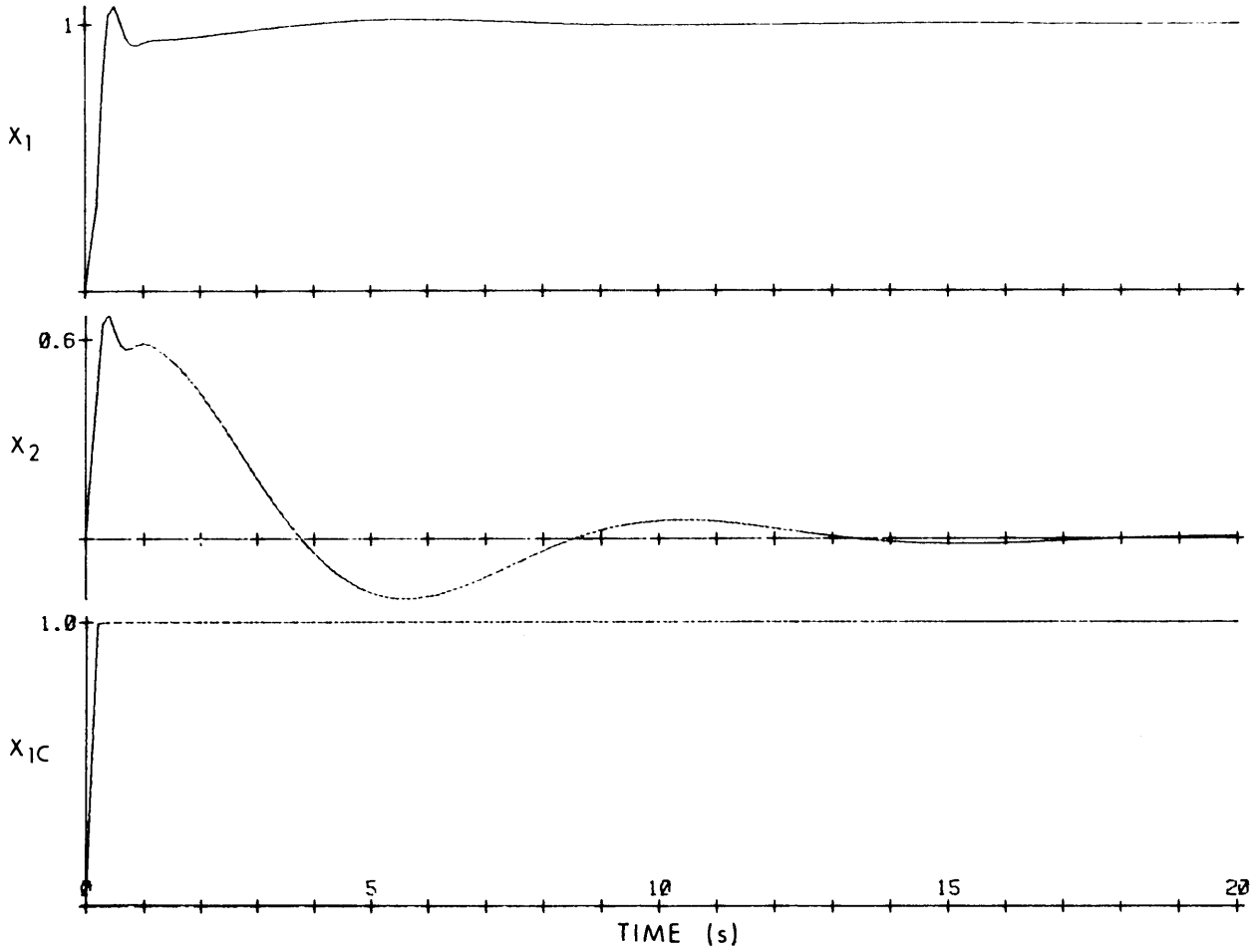

Fig. 2.7 Time Responses of x_1 and x_2 to a Unit Step x_{1c}

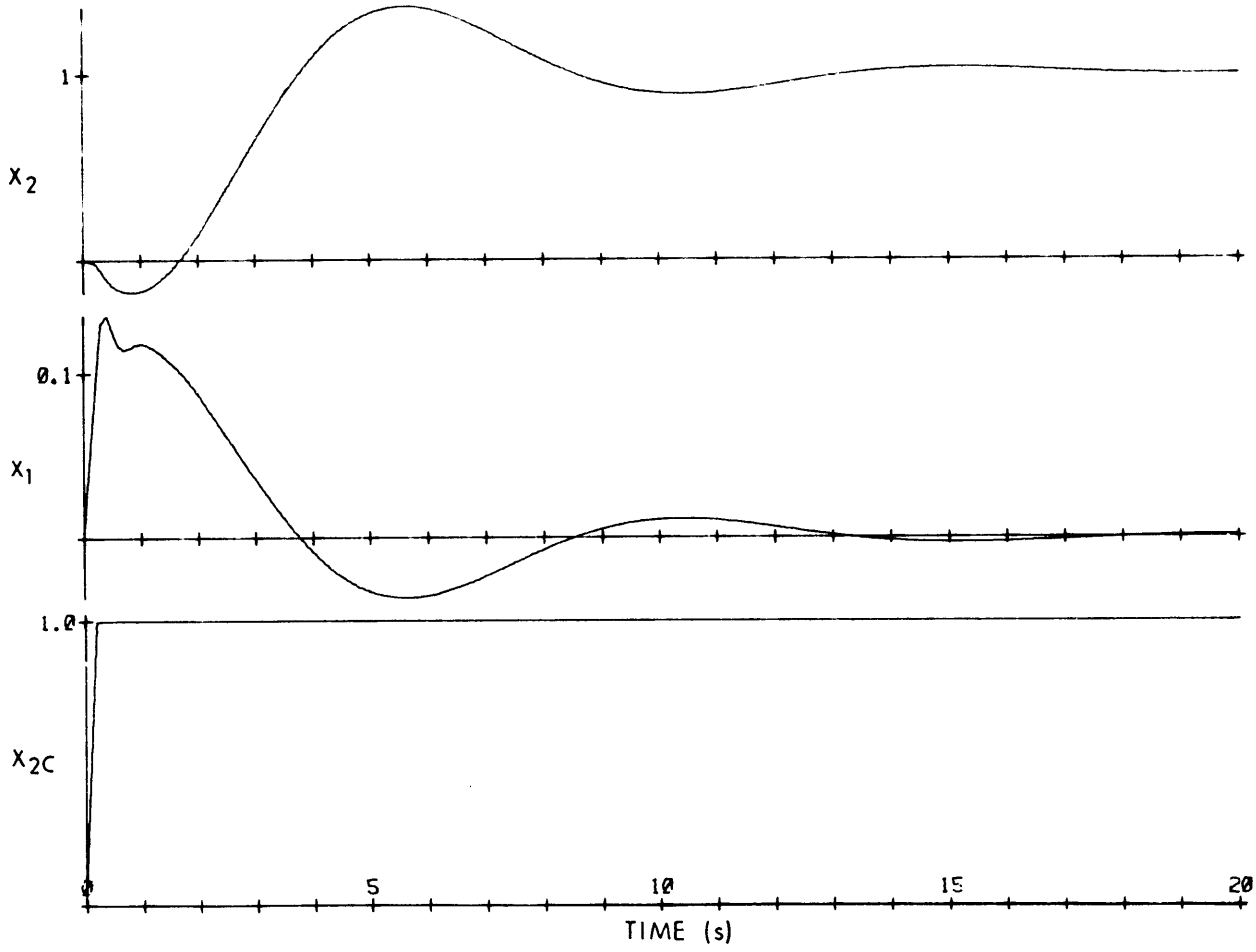

Fig. 2.8 Time Responses of x_1 and x_2 to a Unit Step x_{2c}

Then

$$T_2 = \frac{H_{22}G_{22}}{1 + H_{22}G_{22}} = \frac{1}{s^2 + s + 1} \approx 1.$$

at low frequencies. The frequency plot for $H_{22}G_{22}$ is unchanged from the first example.

The effects of loop #1 on loop #2 are the following.

$$G_{12}CL_1G_{21} = CL_1 = \frac{s + 10}{s^2 + 10s + 100}$$

So that

$$(G_{22} - G_{12}CL_1G_{21}) = \frac{90 - s}{(s+1)(s^2 + 10s + 100)}. \qquad (2.19)$$

A frequency plot of $H_{22}(G_{22} - G_{12}CL_1G_{21})$ is given in Fig. 2.9. $H_{22}G_{22}$ is the same as in the above example, so Fig. 2.9 may be compared with Fig. 2.5a. This comparison indicates that the open loop transfer function for loop #2 is not significantly altered by the coupling from loop #1. The increase in magnitude of G_{11} has made the coupling term so small as to be virtually negligible, as clearly indicated in Fig. 2.9.

c) Determine the effect of loop #2 on loop #1

$$G_{21}CL_2G_{12} = CL_2 = \frac{s + 1}{s^2 + s + 1}$$

So that

$$(G_{11} - G_{21}CL_2G_{12}) = \frac{99s^2 + 89s + 90}{(s + 10)(s^2 + s + 1)} \qquad (2.20)$$

A frequency plot for $H_{11}(G_{11} - G_{21}CL_2G_{12})$ is given in Fig. 2.10. A comparison of this plot and Fig. 2.6a – which is a plot of $H_{11}G_{11}$ for this example also — shows that the coupling is indeed small enough to neglect when designing H_{11}.

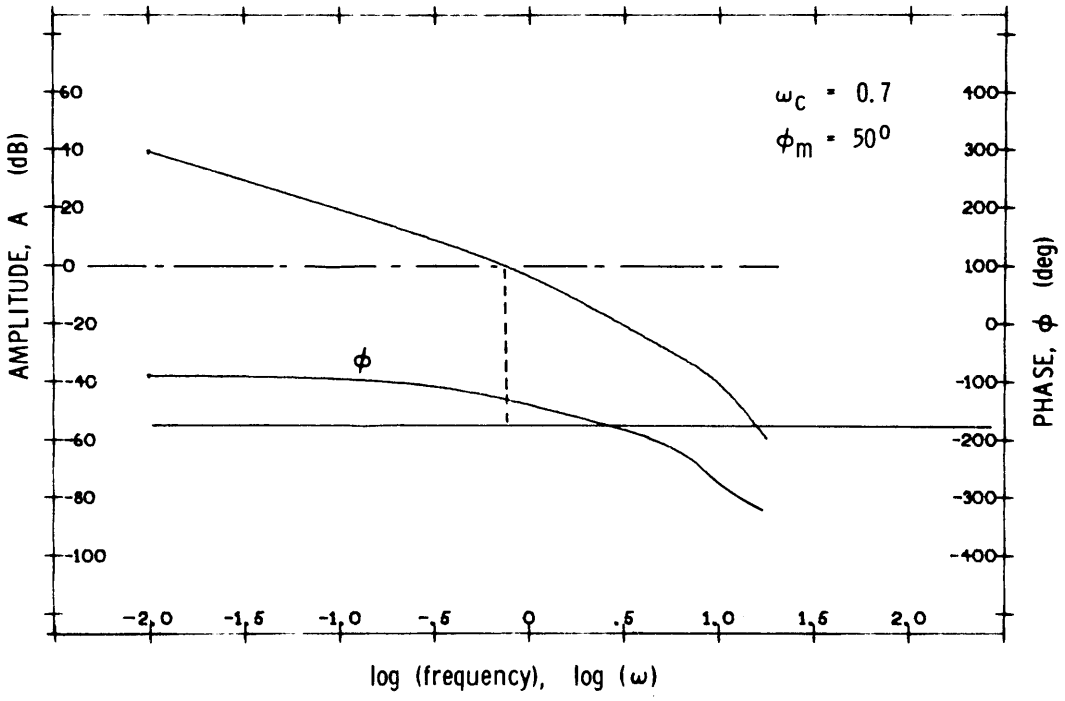

Fig. 2.9 Frequency Plot of $H_{22}(G_{22} - G_{12}CL_1G_{21})$

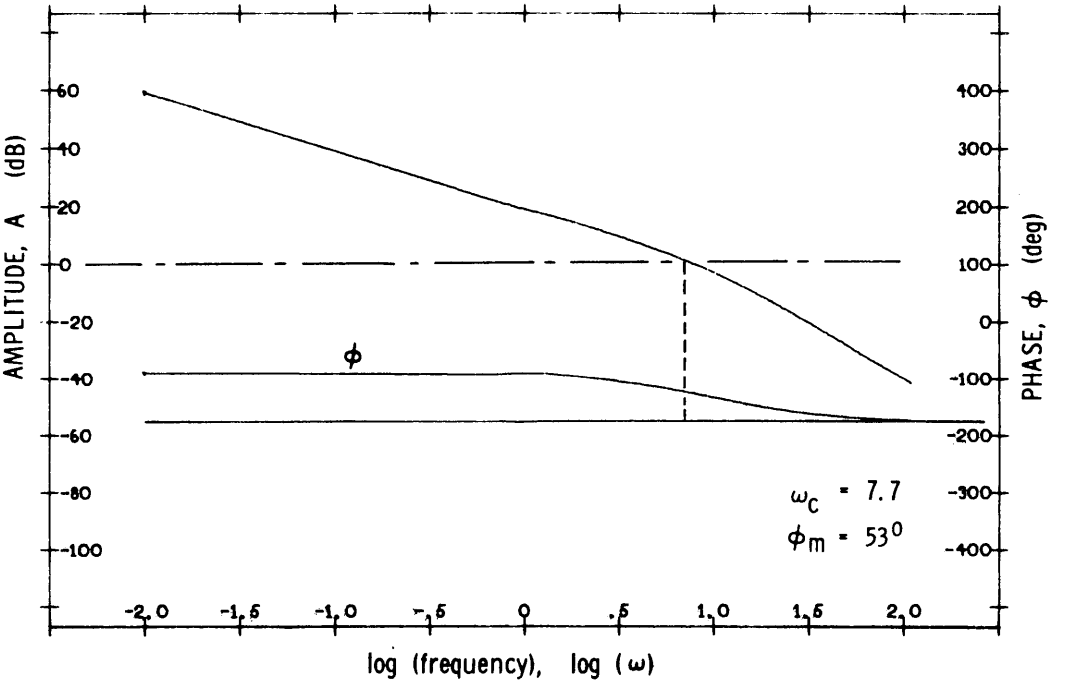

Fig. 2.10 Frequency Plot of $H_{11}(G_{11} - G_{21}CL_2G_{12})$

d) Determine the effects of x_{2c} on x_1 and x_{1c} on x_2

The only change from the conclusions of the above example is that CL_1 is now smaller and thus the effect of x_{1c} on x_2 is even smaller than previously. That is,

$$G_{21}\,CL_1 = \frac{s + 10}{s^2 + 10s + 100}$$

which has a dc gain which is 1/10 of the dc gain of $G_{21}\,CL_1$ in the first example.

It should be noted that these examples are nearly "worst case" situations — the couplings are large and enter at all frequencies. The success of the design procedure for these examples is therefore quite encouraging.

CHAPTER 3

CROSSFEEDING TO ELIMINATE OR DECREASE PLANT CROSSCOUPLING

3.1 Introduction

In certain cases of plant dynamics, as noted in Chapter 2, the coupling between loops may be significant. So that the designer may have more control over the crosscouplings than through just the design compensators H_{11} and H_{22}, crossfeeds between loops are introduced. This is effectively compensation for the open loop coupling transfer functions G_{12} and G_{21}. The addition of crossfeeds to the system is the major advantage of the design procedure as presented in the remainder of this thesis. It gives the designer greater potential in eliminating unwanted couplings between loops.

In this chapter, the design procedure is expanded to include crossfeeds. Also, the factors involved in choosing effective crossfeeds — including potentially conflicting system specifications and tradeoffs — are explored.

3.2 First Attempt — Crossfeeding Between Error Signals

One possible means of using crossfeeds between loops to reduce plant coupling is shown in the diagram of Fig. 3.1. Here, the error signal of each loop is fed to the control of the other. The proposed design procedure for this system is to design the compensators H_{11} and H_{22}, after which the crossfeeds H_{12} and H_{21} would be selected to improve system performance and reduce coupling.

This particular scheme presents a number of obstacles and complexities which eventually result in its abandonment. First, with two-loops closed the system transfer functions are already relatively complex. It is at this point that the crossfeeds H_{12} and H_{21} are to be

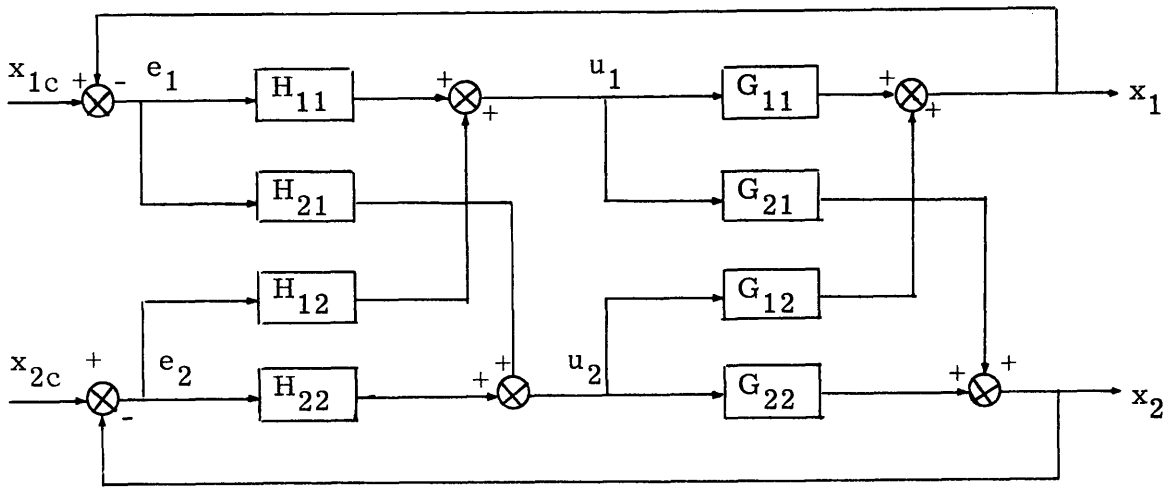

Figure 3.1 Crossfeeding from Errors to Controls in the Two-loop System

chosen. Second, the choice of the first crossfeed, whether it is H_{12} or H_{21}, affects the choice of the second crossfeed. That is, the sequence of crossfeed closure is important. Furthermore, the transfer functions for the system with three loops closed are very difficult to obtain. And once determined, the transfer functions are so complex as to be not readily adaptable to the qualitative insight necessary for intelligent selection of crossfeeds.

In particular, it is found that, for three closed loops — i.e., only one crossfeed chosen — the "direct" transfer functions x_1/x_{1c} and x_2/x_{2c} are in a form in which criteria for the choice of either H_{12} or H_{21} are apparent. For example, if H_{12} is the first crossfeed selected, there is an obvious choice for H_{12} to improve the transfer function $\left.\frac{x_1}{x_{1c}}\right|_{3CL}$. If this choice for H_{12} is made, however, the coupling transfer function $\left.\frac{x_1}{x_{2c}}\right|_{3CL}$ is affected adversely.

Perhaps the degree of complexity in this scheme which makes analysis impractical for real problems can be demonstrated by an example transfer function. One of the transfer functions for the entire system — H_{11}, H_{22}, H_{12} and H_{21} all closed — can be written as

$$\left.\frac{x_1}{x_{1c}}\right|_{4CL} = \frac{N/D}{1 + N/D}$$

where

$$N/D = H_{11}G_{11} - H_{11}G_{12}CL_2G_{21} + \frac{H_{12}}{H_{22}}CL_2G_{21}$$

$$+ \frac{H_{21}}{H_{22}}CL_2G_{12} + \frac{H_{12}H_{21}}{H_{11}H_{22}}CL_2G_{22} . \qquad (3.1)$$

While it is apparent in Eq. (3.1) that the first term is the "direct" term and the latter four are coupling terms, it is not obvious what the best designs for H_{12} and H_{21} are. Also, from the observation above for the three closed-loop system, one might suspect that a good choice (in terms of Eq. (3.1)) for H_{12} and H_{21} might cause difficulties to arise in coupling transfer functions such as $\left.\frac{x_1}{x_{2c}}\right|_{4CL}$. In short, the complexities — in algebra alone — inherent in this scheme for crossfeeding are sufficient to make it impractical for use in analysis and design.

3.3 Crossfeeding Between Controls

3.3.1 Design Procedure for the "New Plant"

An alternate procedure to that described in the previous section is to crossfeed the control signal of each loop to the control signal of the other. Also, if the crossfeeds are chosen first, before any loops are closed, this may simplify some algebraic complexities. Ignoring for the moment disturbance inputs, this new system appears as Fig. 3.2.

The control signal inputs to the plant are still u_1 and u_2. However, u_1 and u_2 are now modified by the crossfeeds H_{12} and H_{21}* in the following manner:

*It may be of interest to note that the H_{12} and H_{21} of the previous section are just $H_{22}H_{12}$ and $H_{11}H_{21}$ respectively, here.

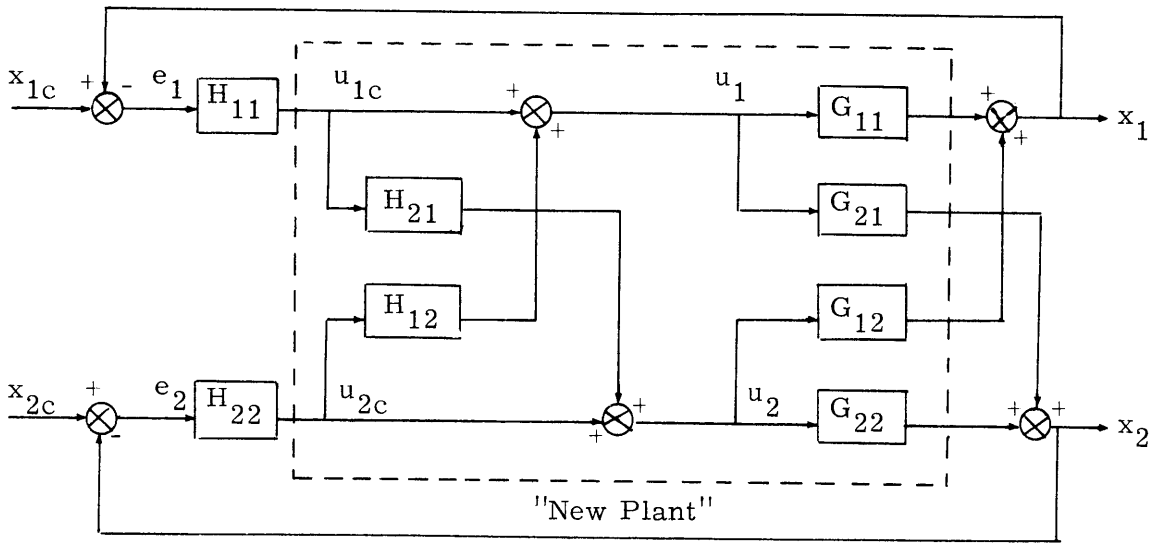

Figure 3.2 Two-loop System with Crossfeeds

$$u_1 = u_{1c} + H_{12}u_{2c} \tag{3.2}$$

$$u_2 = H_{21}u_{1c} + u_{2c}$$

where u_{1c} and u_{2c} are as shown in Fig. 3.2. Therefore, the system equations (2.3) may be rewritten as:

$$\begin{aligned} x_1 &= G_{11}u_1 + G_{12}u_2 \\ &= G_{11}(u_{1c} + H_{12}u_{2c}) + G_{12}(H_{21}u_{1c} + u_{2c}) \\ &= (G_{11} + H_{21}G_{12})u_{1c} + (G_{12} + H_{12}G_{11})u_{2c} \end{aligned} \tag{3.3}$$

$$\begin{aligned} x_2 &= G_{21}u_1 + G_{22}u_2 \\ &= G_{21}(u_{1c} + H_{12}u_{2c}) + G_{22}(H_{21}u_{1c} + u_{2c}) \\ &= (G_{21} + H_{21}G_{22})u_{1c} + (G_{22} + H_{12}G_{21})u_{2c} \end{aligned} \tag{3.4}$$

Eqs. (3.3) and (3.4) indicate that u_{1c} and u_{2c} could be considered as inputs to a "new plant", which is just the original plant modified by the crossfeeds. From these equations it is apparent that the "new plant" open loop transfer functions may be defined as:

$$\begin{aligned} G_{11}' &= G_{11} + H_{21}G_{12} \\ G_{21}' &= G_{21} + H_{21}G_{22} \\ G_{12}' &= G_{12} + H_{12}G_{11} \\ G_{22}' &= G_{22} + H_{12}G_{21} \end{aligned} \tag{3.5}$$

where the control inputs to the "new plant" are u_{1c} and u_{2c}. (The disturbance transfer function matrix G_d of course remains unchanged with crossfeeds between controls.)

The two loop system, with crossfeeds, is now:

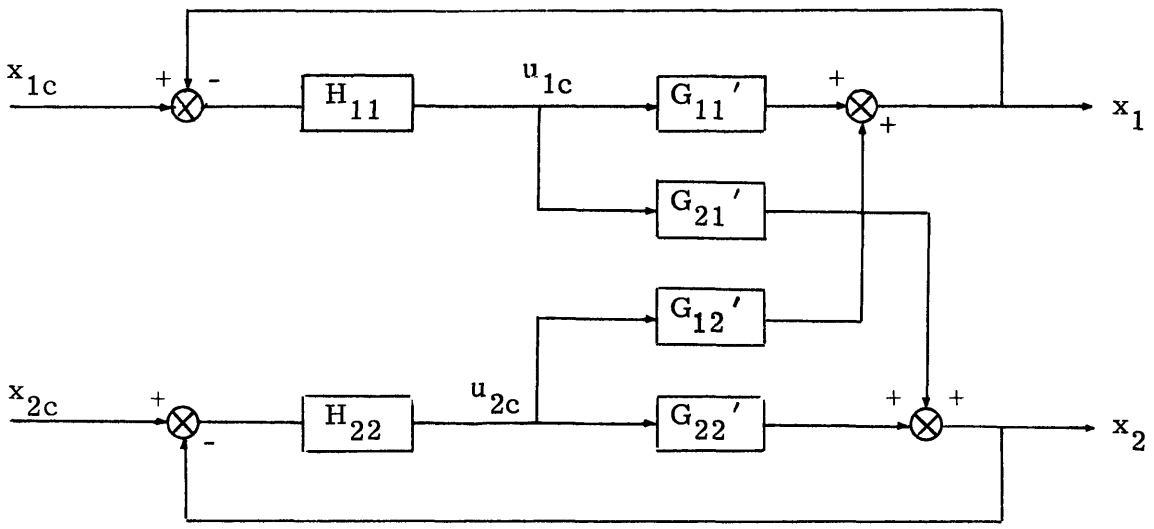

Figure 3.3 Two-loop System for the "New Plant"

Before loop #1 can be closed, the designer must choose values for H_{12} and H_{21} which will achieve a desired degree of decoupling. Once this is accomplished, the design procedure as outlined in Section 2.2 is followed. The only alteration is, of course, that the new plant is used. That is, G_{11}', G_{21}', G_{12}', and G_{22}' replace G_{11}, G_{21}, G_{12}, and G_{22} respectively. Also, by repeating this replacement in Figs. 2.3 and 2.4, those diagrams can continue to be useful in the analysis. If the crossfeeds are designed well, there is justification for expecting the design procedure for the new — and hopefully improved — plant to be very successful.

3.3.2 Choosing the Crossfeeds H_{12} and H_{21}

Obtaining qualitative criteria for the purpose of choosing H_{12} and H_{21} is a rather complex problem of weighing various — sometimes conflicting — factors. Each transfer function of the new plant is the sum of a transfer function of the original plant plus the product of a crossfeed and another original plant transfer function (see Eq. (3.5)). The effect of the crossfeeds on the plant in terms of frequency response is not immediately obvious. However, some conclusions about H_{12} and H_{21} can be drawn from a knowledge of the desired amount of decoupling.

One possible choice for the designer in choosing crossfeeds is the complete elimination of any plant crosscoupling. (However impractical this may seem to be, for the purposes of this analysis one may proceed with this intent in mind.) That is, $G_{12}' = G_{21}' = 0$. The crossfeeds are thus chosen so that:

$$G_{12}' = G_{12} + H_{12}G_{11} = 0 \implies H_{12} = -\frac{G_{12}}{G_{11}} \qquad (3.6)$$

$$G_{21}' = G_{21} + H_{21}G_{22} = 0 \implies H_{21} = -\frac{G_{21}}{G_{22}} \qquad (3.7)$$

This choice of crossfeeds is referred to herein as "exact decoupling". For the 2×2 case, exact decoupling completely decouples the two loops, which may then easily be designed as two separate loops.

If exact decoupling is not desired for a particular system, generally it is advantageous for the crossfeeds to at least reduce the plant cross-coupling. Thus, H_{12} and H_{21} should be designed so that G_{12} and G_{21} are altered in the direction of exact decoupling. In other words, it is desirable that $G_{12}' < G_{12}$ and $G_{21}' < G_{21}$ over frequencies of interest. The crossfeeds should then be chosen so that

$$H_{21} G_{22} < G_{21}$$

and

$$H_{12} G_{11} < G_{12}$$

It should be remembered that the transfer functions, and in general the crossfeeds, possess both magnitude and phase. Therefore only their vector magnitudes can legitimately be compared. The parameter plot (Appendix B) is useful here. In fact, it indicates that, for instance, if the difference in phase (ϕ) between G_{21} and $H_{21} G_{22}$ is less than 90°, then G_{21} and $H_{21} G_{22}$ should be of opposite sign to reduce G_{21}. Conversely, if $90° < \phi < 180°$, then G_{21} and $H_{21} G_{22}$ should have the same sign to achieve the desired reduction in coupling. These considerations determine the signs of H_{12} and H_{21}.

One further caution should be added here. The transfer functions and crossfeeds are generally all frequency dependent, and the design is carried out in the frequency domain. Therefore, it is necessary to satisfy the above specifications concerning vector magnitudes only over the frequency range of interest. If care is not shown in this regard it may happen that, for instance, if H_{21} is chosen so that $G_{21}' < G_{21}$ at zero frequency, the magnitudes and phases of G_{21}, G_{22} and H_{21} change so that $G_{21}' > G_{21}$ at higher — and still operating range — frequencies. Of course, all of the above remarks concerning G_{21}, G_{22}, and H_{21} apply exactly to G_{12}, G_{11}, and H_{12} respectively, by a symmetric change of subscripts.

The frequency range of interest for each loop plays an important role in the choice of crossfeeds. Some of the factors summarized in Section 2.3 help determine what the frequency range of interest is for each loop. Low frequencies are generally of interest — the steady state response is often specified. Also, in terms of restrictions imposed on frequency ranges due to couplings:

1. If G_{21}' is large at frequencies near the loop #2 bandwidth (ω_{B_2}) then x_2/x_{1c} may be significant.

2. If G_{12}' is large at frequencies higher than the loop #2 bandwidth (ω_{B_2}), then x_1/x_{2c} may be significant.

These observations assume that, according to the conclusions of Section 2.3, $\omega_{B_1} > \omega_{B_2}$. Thus the relevant frequency ranges of interest (due to coupling considerations only) may be summarized as:

1. For x_2, H_{21} should be chosen so that G_{21}' remain small at frequencies up to the loop #2 bandwidth.

2. For x_1, H_{12} should be chosen so that G_{12}' remain small at frequencies up to the loop #1 bandwidth.

Since G_{12}' and G_{21}' often appear as a product, one or the other should be small up to the highest bandwidth.

The above criteria might be simplified to state that the desire really is to make G_{12}' or G_{21}' low pass in nature. That occurrence, coupled with reasonably high gains at low frequencies for G_{11}' and G_{22}', will result in the design procedure virtually guaranteeing low frequency decoupling. Condition 2. is actually the most critical, as can be seen by considering the transfer function

$$\frac{x_1}{x_{2c}} = \frac{G_{12}' CL_2'}{1 + H_{11} G_{11}' - H_{11} G_{21}' CL_2' G_{12}'} \tag{3.8}$$

Since loop #2 is the lower bandwidth loop, then at higher frequencies than ω_{B_2}, G_{22}' is small. So, at these higher frequencies — which may be <u>less</u> than ω_{B_1}:

$$CL_2' = \frac{H_{22}}{1 + H_{22} G_{22}'} \approx H_{22}$$

Since H_{22} is designed to make $H_{22}G_{22}'$ large, H_{22} may very well be large at high frequency, for instance, if it supplies only phase lead. In that case, CL_2' will pass high frequencies (i.e., frequencies above ω_{B_2}). But, for the above transfer function, the frequency range of interest extends beyond ω_{B_2} to ω_{B_1}. So unless G_{12}' is low pass (passing signals only up to ω_{B_2}), the high frequency signal will cause the coupling Eq. (3.8) to be very large at frequencies near the loop #1 bandwidth.

Although the crossfeeds are designed to eliminate or reduce crosscoupling, it is apparent from Eq. (3.5) that they also affect the direct terms G_{11} and G_{22}. In fact, it may sometimes occur that the above requirements on the crossfeeds conflict with some limitations on the crossfeeds derived for desirable values for G_{11}' and G_{22}'. For instance, in order for $H_{21}G_{22} < G_{21}$, H_{21} may be of such sign and magnitude that, when $H_{21}G_{12}$ is added to G_{11}, right half s-plane zeros may appear in the resulting G_{11}'. That is, H_{21} may be such that $H_{21}G_{12} > G_{11}$, which could possibly change G_{11} to a most undesirable G_{11}'.* The signs, magnitudes, and phases at relevant frequencies of all terms involved must be considered in order to predict potential conflict between requirements on G_{21}' and G_{11}'. These comments apply in a symmetric way to H_{12}, G_{12}' and G_{22}' of course.

The avoidance of right half s-plane zeros in G_{11}' and G_{22}' is not their only requirement on the crossfeeds. High bandwidths and high gains are generally desirable for G_{11}' and G_{22}'. If possible, the crossfeeds should increase, or at least not decrease, both the open loop crossover frequencies and low frequency gains of G_{11} and G_{22}. High open-loop gain is especially important in view of the need to have $1 + H_{11}G_{11}'$ and $1 + H_{22}G_{22}'$ very large over low frequencies for good closed loop response. If G_{11}' and G_{22}' are large, then H_{11} and H_{22} will not necessarily be

---

* This G_{11}' is "undesirable" because the presence of right half s-plane zeros indicate possible instability. This type of factor adds phase lag to the transfer function, thereby contributing to the possibility of reaching a phase of -180° while the magnitude is greater than one. That is, it may cause the solution of $1 + H_{11}G_{11}' = 0$ to be an s-plane position that has negative damping — i.e., a divergence in the time response.

designed to have excessively large magnitudes in order for $1 + H_{11} G_{11}'$ and $1 + H_{22} G_{22}'$ to be large. This desirable situation is in fact fairly important in coupling transfer functions (see Eqs. (2.8) and (2.9)) where CL_1' and CL_2' should be small. This is of course because $CL_1 \approx 1/G_{11}'$ and $CL_2' \approx 1/G_{22}'$ in the low frequency range.

In choosing crossfeeds, then, care should be taken not only to ensure that the coupling transfer functions are reduced, but also to avoid damaging and, if possible, to improve the direct transfer functions.

CHAPTER 4

DESIGN PROCEDURE FOR A GENERAL THREE-OUTPUT TWO-INPUT SYSTEM

4.1 Introduction

In preceeding chapters, the design procedure was developed for a general two-input, two-output system. The addition of one more output variable to the system in this chapter lends, by itself, considerably more generality to the multiloop analysis. For instance, the implications of two output variables being governed by the same control are revealed. Also, the system — now 3×2 — is not amenable to matrix inversion techniques. Each loop closure and each possible coupling is considered separately. It should be noted that the design procedure as presented assumes a knowledge of the plant.

The design procedure is presented in slightly expanded form for the three-output, two-input system. Factors involved in choosing feedbacks, evaluating couplings, and choosing crossfeeds are discussed. Conclusions are drawn from the design procedure as to exact demands to be made on the crossfeeds.

4.2 Deriving System Transfer Functions

The general 3×2 plant to be considered is shown in Fig. 4.1. For generality, it is assumed that there is a disturbance in each output variable, i.e., that

$$\underline{x}_d = \begin{pmatrix} x_{1d} \\ x_{2d} \\ x_{3d} \end{pmatrix}$$

In order to design this system using techniques developed for the 2×2 system, it must be assumed that two of the outputs are related in some

meaningful way — by a constant factor perhaps, or by simple dynamics. It will be assumed in this chapter that x_3 is closely related to x_2 so that both of them may be governed by the same control u_2.

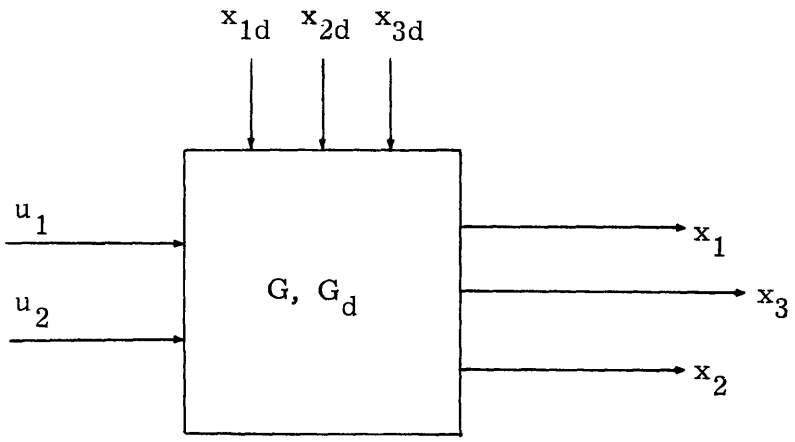

Figure 4.1 The Open Loop 3x2 Plant

For the purposes of designing feedback compensations and to keep the analysis and block diagrams relatively uncomplicated, the disturbance inputs will, for the time being, be neglected. The effects of disturbance inputs on the system will be considered later in this section.

The system will be designed so that x_1 and x_2 are controlled directly by u_1 and u_2, respectively, with minimum coupling. It is assumed in doing this, as noted above, that x_3 is related to x_2 in such a way that by controlling x_2 with u_2, x_3 is also directly controlled. This procedure allows the use of techniques developed above for the 2x2 plant. However, the presence in the system of the third output x_3 implies additional considerations in the design procedure. These additional considerations and complexities will be examined at this point.

As developed in Chapter 3, the crossfeeds between controls u_1 and u_2 are chosen first, resulting in the new plant. Besides their affect on x_1 and x_2, the crossfeeds also modify the additional output x_3.

$$
\begin{aligned}
x_3 &= G_{31}u_1 + G_{32}u_2 \\
&= G_{31}(u_{1c} + H_{12}u_{2c}) + G_{32}(u_{2c} + H_{21}u_{1c}) \\
&= (G_{31} + H_{21}G_{32})u_{1c} + (G_{32} + H_{12}G_{31})u_{2c}
\end{aligned} \tag{4.1}
$$

Therefore, the two new plant transfer functions for x_3 are

$$
\begin{aligned}
G_{31}' &= G_{31} + H_{21}G_{32} \\
G_{32}' &= G_{32} + H_{12}G_{31}
\end{aligned} \tag{4.2}
$$

In Fig. 4.2 is seen the entire control system with crossfeeds chosen. There are now three loops to design.

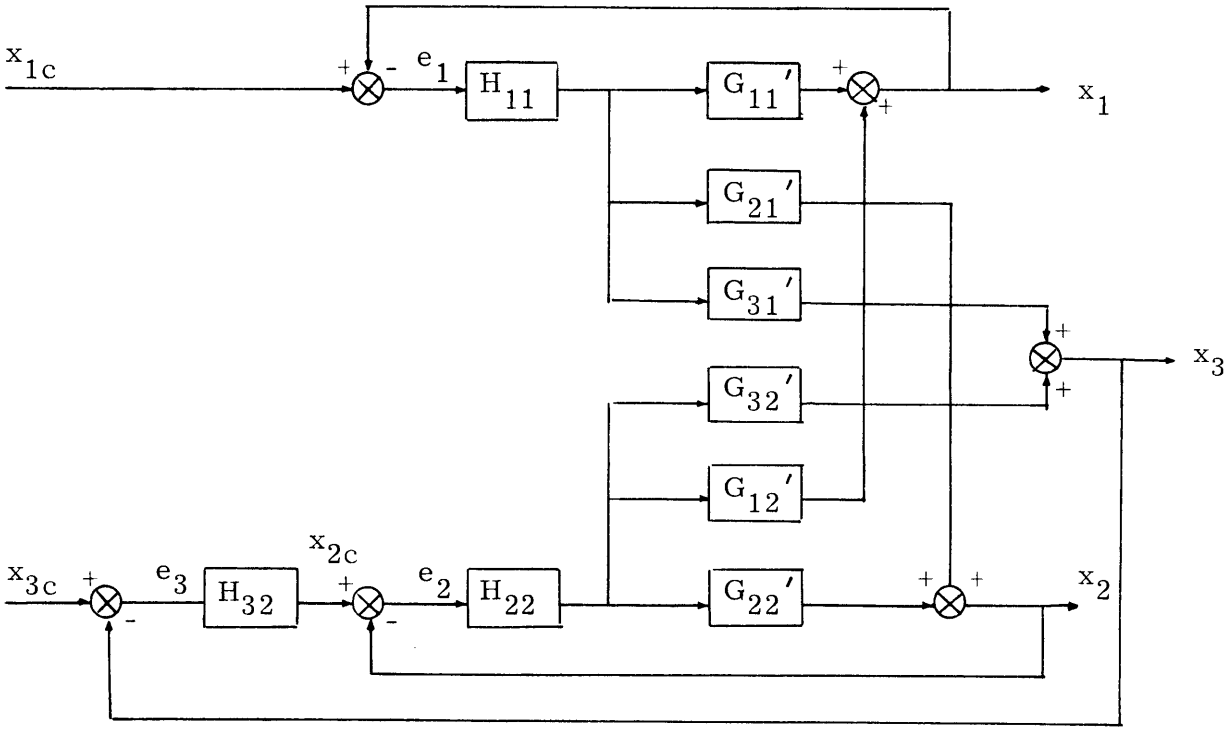

Figure 4.2 Control System for the General 3x2 Plant

In order to proceed with the design procedure, transfer functions are needed for the complete three loop system. These transfer functions are rather complex and the techniques used to derive them will be presented. Two methods were used to derive the transfer functions contained in this thesis. The first of these methods is basically the block diagram approach of Sections 2.2 and 3.3.1. The second method (Ref. 1), referred to herein as "Multiloop Analysis" for lack of any other name, is much simpler — especially numerically — and faster and is described in detail in Appendix A. In addition, the so called "flow graph" rules could be used. However, for this complex system this method offers no simplifications over the two previously mentioned methods.

For the first method, Fig. 4.3 may be used. Analogous to the procedure of Sections 2.2 and 3.3.1, equations for each of the output variables x_1, x_2, and x_3 can be obtained in terms of the command inputs — x_{1c}, x_{2c} and x_{3c}. It is still helpful to neglect the disturbance inputs.

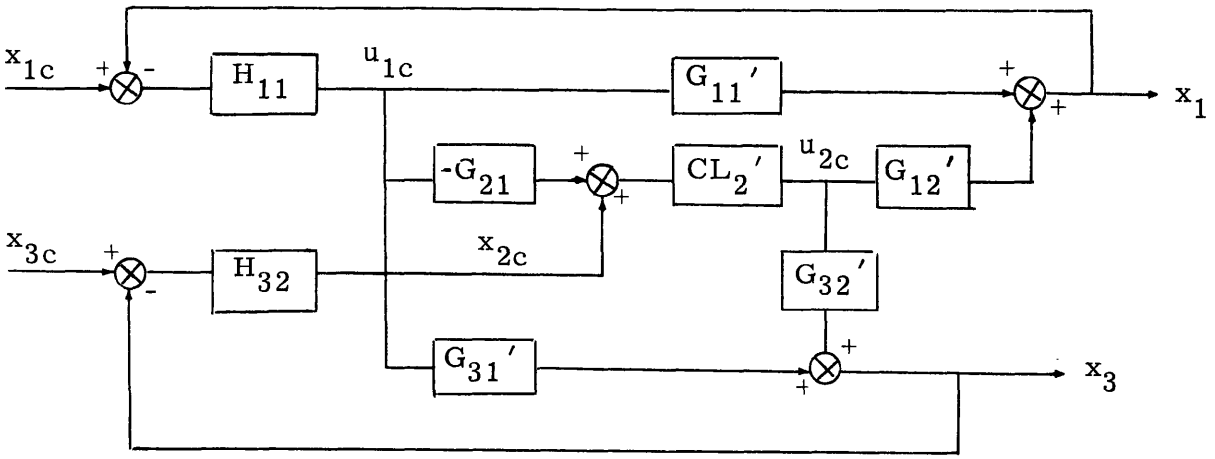

Figure 4.3 Block Diagram of 3×2 System Showing Coupling Paths

The process of using Fig. 4.3 to obtain the overall system equations may be outlined as follows.

First,

$$x_1 = G_{11}' u_{1c} + G_{12}' u_{2c}$$

$$x_2 = G_{21}' u_{1c} + G_{22}' u_{2c} \qquad (4.3)$$

$$x_3 = G_{31}' u_{1c} + G_{32}' u_{2c}$$

Then, using Fig. 4.3,

$$u_{1c} = H_{11} x_{1c} - H_{11}(G_{11}' u_{1c} + G_{12}' u_{2c}) \qquad (4.4)$$

$$u_{2c} = CL_2' x_{2c} - CL_2' G_{21}' u_{1c} \qquad (4.5)$$

It was found to be somewhat easier to continue this process considering only two loops closed, or $H_{32} = 0$. In fact, some of the two-closed-loop transfer functions generated in this way will be helpful in design. Later, since $x_{2c} = H_{32}(x_{3c} - x_3)$, it will be straight-forward to convert to three-closed-loop expressions for the output variables.

Continuing by substituting Eq. (4.5) into Eq. (4.4),

$$u_{1c} = H_{11} x_{1c} - H_{11} G_{11}' u_{1c} - H_{11} G_{12}' \left[CL_2' x_{2c} - CL_2' G_{21}' u_{1c} \right]$$

$$= H_{11} x_{1c} - H_{11} G_{12}' CL_2' x_{2c} + \left(H_{11} G_{12}' CL_2' G_{21}' - H_{11} G_{11}' \right) u_{1c} \qquad (4.6)$$

Finally

$$u_{1c} = \frac{H_{11}}{1 + H_{11} G_{11}' - H_{11} G_{12}' CL_2' G_{21}'} x_{1c}$$

$$- \frac{H_{11} CL_2' G_{12}'}{1 + H_{11} G_{11}' - H_{11} G_{12}' CL_2' G_{21}'} x_{2c} \qquad (4.7)$$

and

$$u_{2c} = CL_2' x_{2c} - CL_2' G_{21}' u_{1c} \tag{4.8}$$

Using Eqs. (4.7) and (4.8) in Eqs. (4.3) results, after considerable algebra, in the following equations for the output variables:

$$x_1\Big|_{2CL} = \frac{1}{\Delta_{2CL}} \left[CL_1' \left(G_{11}' - G_{21}' CL_2' G_{21}' \right) x_{1c} + \frac{CL_2' G_{12}'}{1 + H_{11} G_{11}'} x_{2c} \right] \tag{4.9}$$

$$x_2\Big|_{2CL} = \frac{1}{\Delta_{2CL}} \left[CL_1' G_{21}' \left(1 - CL_2' G_{22}' \right) x_{1c} + CL_2' \left(G_{22}' - G_{12}' CL_1' G_{21}' \right) x_{2c} \right] \tag{4.10}$$

$$x_3\Big|_{2CL} = \frac{1}{\Delta_{2CL}} \left[CL_1' \left(G_{31}' - G_{32}' CL_2' G_{21}' \right) x_{1c} + \left(\frac{CL_2' G_{32}'}{1 + H_{11} G_{11}'} + CL_2' G_{11}' CL_1' G_{32}' - CL_2' G_{31}' CL_1' G_{12}' \right) x_{2c} \right] \tag{4.11}$$

where

$$\Delta_{2CL} = 1 - CL_1' G_{12}' CL_2' G_{21}'$$

Using these equations, any transfer function for any output from either input of the two-closed-loop system can be found by merely setting the other input equal to zero.

By substituting $x_{2c} = H_{32}(x_{3c} - x_3)$ into Eqs. (4.9) - (4.11), three-closed-loop expressions can be obtained for the output variables in terms of the two command inputs x_{1c} and x_{3c}. These complete system equations are:

$$x_1\Big|_{3CL} = \frac{1}{\Delta_{3CL}} \Big\{ CL_1' \Big[G_{11}' - G_{12}' CL_2' G_{21}' + H_{32} CL_2' \big(G_{11}' G_{32}' - G_{12}' G_{31}' \big) \Big] x_{1c} + \Big[\frac{H_{32} CL_2' G_{12}'}{1 + H_{11} G_{11}'} \Big] x_{3c} \Big\} \tag{4.12}$$

$$x_2\Big|_{3CL} = \frac{1}{\Delta_{3CL}} \Big\{ CL_1' \Big[\frac{G_{21}'}{1 + H_{22} G_{22}'} + H_{32} CL_2' \big(G_{32}' G_{21}' - G_{22}' G_{31}' \big) \Big] x_{1c} + \Big[H_{32} CL_2' \big(G_{22}' - G_{12}' CL_1' G_{21}' \big) \Big] x_{3c} \Big\} \tag{4.13}$$

$$x_3\Big|_{3CL} = \frac{1}{\Delta_{3CL}} \Big\{ CL_1' \Big[G_{31}' - G_{32}' CL_2' G_{21}' \Big] x_{1c} + H_{32} \Big[\frac{CL_2' G_{32}'}{1 + H_{11} G_{11}'} + CL_2' CL_1' \big(G_{11}' G_{32}' - G_{12}' G_{31}' \big) \Big] x_{3c} \Big\} \tag{4.14}$$

where

$$\Delta_{3CL} = 1 - CL_1' G_{12}' CL_2' G_{21}' + H_{32} \frac{CL_2' G_{32}'}{1 + H_{11} G_{11}'} + H_{32} CL_2' CL_1' \big(G_{11}' G_{32}' - G_{12}' G_{31}' \big)$$

Transfer functions for any output from either command input can be obtained from these equations.

It should be remembered that, by merely expanding CL_1' and CL_2' and performing some simple algebra, Eqs. (4.9) - (4.14) could be written in several different forms. That is, the terms can be grouped in different ways. The forms for the equations given thus far are intended to be easily amenable to comparisons of direct and coupling terms. As more loops are added to this system, however, and thus more coupling effects contribute to each output, it becomes more difficult to separate the different contributions to coupling. Furthermore, as more loops are added, the derivation of system equations in the way just described becomes algebraically very tedious.

In order to demonstrate the degree of simplification inherent in the second method for obtaining system transfer functions, use will be made of one of the above transfer functions. Consider, for example, from Eq. (4.14),

$$\frac{x_3}{x_{3c}} = \frac{1}{\Delta_{3CL}} H_{32}\left[\frac{CL_2'G_{32}'}{1+H_{11}G_{11}'} + CL_2'CL_1'\left(G_{11}'G_{32}' - G_{12}'G_{31}'\right)\right] \tag{4.15}$$

Substituting $CL_1' = \dfrac{H_{11}}{1+H_{11}G_{11}'}$ and $CL_2' = \dfrac{H_{22}}{1+H_{22}G_{22}'}$ and expanding,

$$\frac{x_3}{x_{3c}} = \frac{H_{32}H_{22}G_{32}' + H_{11}H_{32}H_{22}(G_{11}'G_{32}' - G_{12}'G_{31}')}{1+H_{11}G_{11}' + H_{22}G_{22}' + H_{32}H_{22}G_{32}' + H_{11}H_{22}(G_{11}'G_{22}' - G_{12}'G_{21}')} \cdots$$

$$\cdots \frac{}{+H_{11}H_{32}H_{22}(G_{11}'G_{32}' - G_{12}'G_{31}')} \tag{4.16}$$

The terms in parentheses in Eq. (4.16) are, as it turns out, the so-called "coupling numerators" of Multiloop Analysis (Ref. 1) as described in Appendix A. In the notation of Multiloop Analysis,

$$\Delta(G_{11}'G_{22}' - G_{12}'G_{21}') = N_{u_{1c}\ u_{2c}}^{x_1\ \ x_2}$$

$$\Delta(G_{11}'G_{32}' - G_{12}'G_{31}') = N_{u_{1c}\ u_{2c}}^{x_1\ \ x_3}$$

where Δ is the determinant of the matrix of coefficients of $\underline{x}$. That is, Δ is the "characteristic determinant", where the characteristic equation may be written as $\Delta = 0$. Coupling numerators are very easily determined from open loop plant dynamics and generally are of low order. In fact, it is found that most of the factors in the numerator and denominator of the resultant transfer function $\Delta(G_{11}'G_{22}' - G_{12}'G_{21}')$ exactly cancel.

Using the rules of Multiloop Analysis as outlined in Appendix A, any transfer function may be written quickly and then if desired, be expanded into the form of Eqs. (4.9) - (4.14). Since the coupling numerator is of small order and easy to obtain — in contrast to the laborious task of obtaining terms in the first method — it is almost essential that Multiloop Analysis be used in numerical problems.

The effects of disturbance inputs have, up to this point, been neglected. Due to the addition of the third loop, the system transfer functions given in Section 2.2 for disturbance inputs are somewhat more complicated. These three-closed-loop transfer functions could be obtained by using the first method, i.e., modifying Eqs. (4.3) so that

$$x_1 = G_{11}'u_{1c} + G_{12}'u_{2c} + G_{11d}x_{1d} + G_{12d}x_{2d} + G_{13d}x_{3d}$$

$$x_2 = G_{21}'u_{1c} + G_{22}'u_{2c} + G_{21d}x_{1d} + G_{22d}x_{2d} + G_{23d}x_{3d}$$

$$x_3 = G_{31}'u_{1c} + G_{32}'u_{2c} + G_{31d}x_{1d} + G_{32d}x_{2d} + G_{33d}x_{3d}$$

and continuing with the appropriate terms added to Eqs. (4.4) - (4.14). However, as in Section 2.2, the disturbance input transfer functions will be derived here by using Multiloop Analysis. For example, using the rules in Appendix A,

$$\left.\frac{x_2}{x_{1d}}\right|_{3CL} = \frac{N^{x_2}_{x_{1d}} + H_{11}N^{x_2\ x_1}_{x_{1d}u_{1c}} + H_{32}H_{22}N^{x_2\ x_3}_{x_{1d}u_{2c}} + H_{11}H_{22}H_{32}N^{x_2\ x_3\ x_1}_{x_{1d}u_{2c}u_{1c}} \cdots}{\Delta + H_{11}N^{x_1}_{u_{1c}} + H_{22}N^{x_2}_{u_{2c}} + H_{22}H_{32}N^{x_3}_{u_{2c}} + H_{11}H_{22}N^{x_1\ x_2}_{u_{1c}u_{2c}}}$$

$$\cdots \frac{}{+ H_{11}H_{22}H_{32}N^{x_1\ x_3}_{u_{1c}u_{2c}}}$$

$$= \frac{G_{21d} + H_{11}(G_{21d}G_{11}' - G_{21}'G_{11d}) + H_{32}H_{22}(G_{21d}G_{32}' - G_{22}'G_{31d})}{1 + H_{11}G_{11}' + H_{22}G_{22}' + H_{22}H_{32}G_{32}' + H_{11}H_{22}(G_{11}'G_{22}' - G_{12}'G_{21}')} \cdots$$

$$\cdots \frac{+ H_{11}H_{22}H_{32}(G_{21d}G_{32}'G_{11}' - G_{31}'G_{12}'G_{21d} - G_{32}'G_{21}'G_{11d}}{+ H_{11}H_{22}H_{32}(G_{11}'G_{32}' - G_{12}'G_{31}')} \cdots$$

$$\cdots \underline{- G_{11}'G_{22}'G_{31d})}$$

where

$$\Delta(G_{21d}G_{32}'G_{11}' - G_{31}'G_{12}'G_{21d} - G_{32}'G_{21}'G_{11d} - G_{11}'G_{22}'G_{31d})$$

$$= N^{x_2\ x_3\ x_1}_{x_{1d}u_{2c}u_{1c}}$$

which is a so called "coupling-coupling numerator". After combining terms and making some cancellations, this transfer function may be written in the same form as Eqs. (4.11) - (4.14)

$$\left.\frac{x_2}{x_{1d}}\right|_{3CL} = \frac{1}{\Delta_{3CL}}\left\{\frac{G_{21d}}{1+H_{22}G_{22}'} + H_{32}CL_2'\left(G_{32}' - CL_1'G_{31}'G_{12}'\right)G_{21d}\right.$$

$$- \frac{CL_1'G_{21}'}{1+H_{22}G_{22}'}G_{11d} - H_{32}CL_1'CL_2'G_{21}'G_{32}'G_{11d}$$

$$\left. - H_{32}CL_2'G_{22}'G_{31d}\right\} \qquad (4.17)$$

Similarly, the other transfer functions may be written as:

$$\left.\frac{x_1}{x_{1d}}\right|_{3CL} = \frac{1}{\Delta_{3CL}}\left\{\frac{1}{1+H_{11}G_{11}'}\left[\left(1+H_{32}CL_2'G_{32}'\right)G_{11d}\right.\right.$$

$$\left.\left. - CL_2'G_{12}'\left(G_{21d}+H_{32}G_{31d}\right)\right]\right\} \qquad (4.18)$$

$$\left.\frac{x_1}{x_{2d}}\right|_{3CL} = \frac{1}{\Delta_{3CL}}\left\{\frac{1}{1+H_{11}G_{11}'}\left[\left(1+H_{32}CL_2'G_{32}'\right)G_{12d}\right.\right.$$

$$\left.\left. - CL_2'G_{12}'\left(G_{22d}+H_{32}G_{32d}\right)\right]\right\} \qquad (4.19)$$

$$\left.\frac{x_1}{x_{3d}}\right|_{3CL} = \frac{1}{\Delta_{3CL}}\left\{\frac{1}{1+H_{11}G_{11}'}\left[\left(1+H_{32}CL_2'G_{32}'\right)G_{13d}\right.\right.$$

$$\left.\left. - CL_2'G_{12}'\left(G_{23d}+H_{32}G_{33d}\right)\right]\right\} \qquad (4.20)$$

$$\left.\frac{x_2}{x_{2d}}\right|_{3CL} = \frac{1}{\Delta_{3CL}} \left\{ \frac{G_{22d}}{1+H_{22}G_{22}'} + H_{32}CL_2'\left(G_{32}' - CL_1'G_{31}'G_{12}'\right)G_{22d} \right.$$

$$- \frac{CL_1'G_{21}'}{1+H_{22}G_{22}'} G_{12d} - H_{32}CL_1'CL_2'G_{21}'G_{32}'G_{12d}$$

$$\left. - H_{32}CL_2'G_{22}'G_{32d} \right\} \qquad (4.21)$$

$$\left.\frac{x_2}{x_{3d}}\right|_{3CL} = \frac{1}{\Delta_{3CL}} \left\{ \frac{G_{23d}}{1+H_{22}G_{22}'} + H_{32}CL_2'\left(G_{32}' - CL_1'G_{31}'G_{12}'\right)G_{23d} \right.$$

$$- \frac{CL_1'G_{21}'}{1+H_{22}G_{22}'} G_{13d} - H_{32}CL_1'CL_2'G_{21}'G_{32}'G_{13d}$$

$$\left. - H_{32}CL_2'G_{22}'G_{33d} \right\} \qquad (4.22)$$

$$\left.\frac{x_3}{x_{1d}}\right|_{3CL} = \frac{1}{\Delta_{3CL}} \left\{ G_{31d} - CL_1'CL_2'G_{12}'G_{21}'G_{31d} \right.$$

$$\left. - CL_1'G_{31}'G_{11d} - CL_2'G_{32}'G_{21d} \right\} \qquad (4.23)$$

$$\left.\frac{x_3}{x_{2d}}\right|_{3CL} = \frac{1}{\Delta_{3CL}} \left\{ G_{32d} - CL_1'CL_2'G_{12}'G_{21}'G_{32d} \right.$$

$$\left. - CL_1'G_{31}'G_{12d} - CL_2'G_{32}'G_{22d} \right\} \qquad (4.24)$$

$$\left.\frac{x_3}{x_{3d}}\right|_{3CL} = \frac{1}{\Delta_{3CL}} \left\{ G_{33d} - CL_1 'CL_2 'G_{12} 'G_{21} 'G_{33d} \right.$$

$$\left. - CL_1 'G_{31} 'G_{13d} - CL_2 'G_{32} 'G_{23d} \right\} \qquad (4.25)$$

Notice that, for each output, the only difference among the transfer functions with different inputs is the appropriate G_{ijd}. Eqs. (4.17) - (4.25) together with Eqs. (4.12) - (4.14), give all the transfer functions of the complete three loop system.

4.3 Design Procedure for a General 3x2 System

4.3.1 Designing Feedback Compensations

The design procedure is expanded somewhat to include the third loop, along with the included greater complexity of couplings, as exhibited in Eqs. (4.12) - (4.25). The steps, contained in this and the next subsection, will be listed sequentially first, then remarks concerning the effects of crossfeeds and loop #3 on each step will be included.

The design procedure:

a) Choose the crossfeeds and derive the "new plant"

b) Close loop #1

c) Analyze and design loop #2 with loop #1 closed

d) Analyze and design loop #3 with loop #1 and loop #2 closed

e) Determine the effect of loop #2 on loop #1, and loop #3 on loop #1

f) Determine the coupling effects: x_{3c} on x_1, and x_{1c} on x_2 and x_3

g) Determine the effects of disturbance inputs

a) Choose the crossfeeds and derive the "new plant"

While it is true that in actually designing a system the crossfeeds must be chosen first, in the present qualitative discussion it will be assumed that the "new plant" is already available. Criteria will be developed for the choice of crossfeeds as the design procedure is carried out. These criteria will be useful in step a) of the design procedure as applied to a real physical system in Chapter 5.

b) Close loop #1

This step is unchanged from Section 2.2 — other than G_{11}' replacing G_{11}. That is,

$$\frac{x_1}{x_{1c}} = \frac{H_{11}G_{11}'}{1 + H_{11}G_{11}'} .$$

c) Analyze and design loop #2 with loop #1 closed

Again, the only change from Section 2.2 is G_{ij}' replacing G_{ij}.

d) Analyze and design loop #3 with loop #1 and loop #2 closed

Analogous to the procedure for step b), first loop #3 is closed ignoring the coupling effects from loops #1 and #2. Then the compensator H_{32} is designed following the same criteria as used to design H_{11} and H_{22}. That is, so that

$$\frac{x_3}{x_{3c}} = \frac{H_{32}CL_2'G_{32}'}{1 + H_{32}CL_2'G_{32}'} \approx 1$$

over the frequency range of interest. Also, as was the case in the design of H_{11} and H_{22}, H_{32} should be designed so that there is little overshoot in the closed loop frequency response and so that there is adequate open loop phase margin.

After H_{32} is designed, compare the relative sizes (vector magnitudes) of the "direct term" and coupling terms by using the complete x_3/x_{3c} transfer function Eq. (4.15). After taking out some common factors, the numerator of Eq. (4.15) is

$$\frac{H_{32}CL_2'}{1+H_{11}G_{11}'}\left[G_{32}' + H_{11}G_{11}'G_{32}' - H_{11}G_{12}'G_{31}'\right].$$

The third term above is actually the coupling term and should be compared in magnitude to $G_{32}'(1 + H_{11}G_{11}')$ over the frequency range of interest. If the coupling term is not small, a redesign of H_{32} may be necessary.

It may be of interest to observe here that, since

$$H_{11}(G_{11}'G_{32}' - G_{12}'G_{31}') = H_{11}\frac{N_{u_{1c}u_{2c}}^{x_1\ x_2}}{\Delta},$$

the "coupling numerator" includes both coupling and direct effects.

If the crossfeeds are chosen, as specified above, to make G_{12}' and G_{21}' small and to maintain G_{11}' large, then the coupling term $-G_{12}'G_{31}'$ possibly will be small. It is apparent that a large G_{32}' and small G_{31}' are desirable, and this fact is noted for the benefit of future requirements to be made on H_{12} and H_{21}.

If the coupling is indeed small, then the term $-CL_1'G_{12}'CL_2'G_{21}'$ in Δ_{3CL} will also be small. Thus, for effective crossfeeds,

$$\frac{x_3}{x_{3c}} \approx \frac{\frac{H_{32}CL_2'}{1+H_{11}G_{11}'}\left[G_{32}' + H_{11}G_{11}'G_{32}'\right]}{1 + H_{32}\frac{CL_2'G_{32}'}{1+H_{11}G_{11}'} + H_{32}CL_2'CL_1'G_{11}'G_{32}'}$$

Simplifying,

$$\frac{x_3}{x_{3c}} \approx \frac{H_{32}CL_2'G_{32}'}{1+H_{32}CL_2'G_{32}'} \tag{4.26}$$

Note that the coupling term $-CL_2'CL_1'G_{12}'G_{31}'$ is just the effect of loop #1 on the output of loop #3. This effect is made small by reducing the coupling between the output for loop #1 (x_1) and the control for loop #3 (u_2) — i.e., by reducing G_{12}'.

Another important factor concerning the size of the coupling term enters the design of H_{32}. The terms CL_1' and CL_2' are small (approximately $1/G_{11}'$ and $1/G_{22}'$ respectively) over the frequency range of interest — which is zero frequency to ω_{B_1} for CL_1' and zero frequency to ω_{B_2} for CL_2'. However, above the frequencies ω_{B_1} and ω_{B_2}, $H_{11}G_{11}'$ and $H_{22}G_{22}'$ respectively begin to get small. In that case, then $CL_1' \approx H_{11}$ and $CL_2' \approx H_{22}$. This occurrence offers a possibility that the coupling term may begin to get large near ω_{B_2}, the smaller of ω_{B_1} and ω_{B_2}. Thus, in order to avoid this potential increase in the coupling term (which may or may not be offset by a similar increase in the "direct" term), the loop #3 bandwidth should be as much lower than ω_{B_2} as possible. This condition amounts to another design specification for H_{32}.

4.3.2 Evaluating Couplings

Steps e) - g) of the design procedure are concerned with coupling and disturbance effects.

e) Determine the effect of loop #2 on loop #1, and loop #3 on loop #1

Having designed loop #3, now return to loop #1 and see in what way it has been affected by this closure. Notice that, since loop #2 and loop #3 are governed by the same control, the effect of loop #3 on loop #2 is a direct, and not a coupling one. In any case, it can be seen by comparing the x_{2c} and x_{3c} portions of Eqs. (4.10) and (4.13) respectively, that the only effect of loop #3 on loop #2 is to add terms to the denominator, while the command input changes from x_{2c} to $H_{32}x_{3c}$.

To evaluate how much coupling has been added to x_1 by the closing of loop #3, Eq. (4.12) is used. The relevant transfer function is:

$$\left.\frac{x_1}{x_{1c}}\right|_{3CL} = \frac{CL_1'G_{11}' - CL_1'CL_2'G_{12}'G_{21}' + H_{32}CL_1'CL_2'(G_{11}'G_{32}'}{1 + H_{32}\dfrac{CL_2'G_{32}'}{1+H_{11}G_{11}'} + H_{32}CL_1'CL_2'(G_{11}'G_{32}' - G_{12}'G_{31}')} \cdots$$

$$\cdots \frac{-G_{12}'G_{31}')}{-CL_1'CL_2'G_{12}'G_{21}'}$$

This can be rewritten in a more suitable form:

$$\left.\frac{x_1}{x_{1c}}\right|_{3CL} = \frac{1}{\Delta_{3CL}}\left[CL_1'G_{11}'\left(1 + H_{32}CL_2'G_{32}'\right) - CL_1'CL_2'G_{12}'\left(G_{21}' + H_{32}G_{31}'\right)\right]$$

As will shortly be demonstrated, the only couplings in this transfer function are the last two terms. The term $-CL_1'CL_2'G_{12}'G_{21}'$ represents coupling in loop #1 due to loop #2 and is small for small G_{12}' and G_{21}'. Since the crosscouplings appear here as a product, there is an excellent chance of effective decoupling. The term $-CL_1'CL_2'G_{12}'H_{32}G_{31}'$ represents coupling in loop #1 due to loop #3. The specification observed in step c) – that G_{31}' be small — appears again. If H_{21} can be chosen so that G_{31}' is small, then the presence of the product $G_{12}'G_{31}'$ indicates that this final coupling will probably also be small. It might be noted here that, for the purposes of step c) above, G_{31}' should be small at frequencies up to ω_{B_3} (the loop #3 bandwidth). However, to assist in decoupling loop #3 from loop #1, G_{31}' should be small at frequencies up to ω_{B_1}.

In any case, if the coupling terms discussed above are neglected, then:

$$\left.\frac{x_1}{x_{1c}}\right|_{3CL} \approx \frac{CL_1'G_{11}' + H_{32}CL_1'CL_2'G_{11}'G_{32}'}{1 + H_{32}\dfrac{CL_2'G_{32}'}{1+H_{11}G_{11}'} + H_{32}CL_1'CL_2'G_{11}'G_{32}'} \qquad (4.27)$$

$$= \frac{H_{11}G_{11}'(1 + H_{32}CL_2'G_{32}')}{(1+H_{11}G_{11}')(1+H_{32}CL_2'G_{32}')} .$$

Thus, after cancellation

$$\left.\frac{x_1}{x_{1c}}\right|_{3CL} \approx \frac{H_{11}G_{11}'}{1 + H_{11}G_{11}'} = T_1'. \qquad (4.28)$$

Effective crossfeeds eliminate all coupling effects of loop #2 and loop #3 on x_1.

f) Determine the coupling effects: x_{3c} on x_1, and x_{1c} on x_2 and x_3

The coupling in each output due to commands in the other loops will be examined using Eqs. (4.12) - (4.14). The relevant transfer functions will be presented one at a time.

First, from Eq. (4.12),

$$\left.\frac{x_1}{x_{3c}}\right|_{3CL} = \frac{1}{\Delta_{3CL}} \left[\frac{H_{32}CL_2'G_{12}'}{1+H_{11}G_{11}'}\right] .$$

From remarks made in Sections 3.3.2 and 4.2 concerning desired sizes of CL_2' and G_{12}', this transfer function will probably be small for effective choice of crossfeeds. An additional help is that, if H_{32} is designed so that $CL_2'G_{32}'$ is large at frequencies up to ω_{B_3} (where $\omega_{B_3} << \omega_{B_1}$), H_{32} will likely be very small at frequencies higher than ω_{B_3}. Of course, as might be expected this is a tradeoff situation since H_{32} may be large at very low frequencies. In any case, for well designed crossfeeds and well designed H_{11} (so that $H_{11}G_{11}'$ is large), x_1/x_{3c} will likely be small at frequencies up to near the loop #1 bandwidth.

Next, from Eq. (4.13),

$$\left.\frac{x_2}{x_{1c}}\right|_{3CL} = \frac{1}{\Delta_{3CL}}\left[\frac{CL_1'G_{21}'}{1+H_{22}G_{22}'} + H_{32}CL_2'\left(G_{32}'G_{21}' - G_{22}'G_{31}'\right)\right]$$

With effective crossfeeds, and well designed H_{11} and H_{22}, the first term will be small at frequencies at least up to near ω_{B_2}. The second term may cause some difficulties. For well designed H_{32}, $H_{32}CL_2'G_{32}'$ is large at frequencies up to ω_{B_3}. Thus, over very low frequencies ($0 < \omega < \omega_{B_3}$), $H_{32}CL_2'G_{32}'G_{21}'$ may be large even if G_{21}' is quite small. For $\omega_{B_3} < \omega < \omega_{B_2}$ however, this term should be small. The last term, $-H_{32}CL_2'G_{22}'G_{31}'$, will be small if the crossfeeds can be chosen to keep G_{31}' small at least from zero frequency to ω_{B_3}. Since $CL_2'G_{22}' = T_2' \approx 1$ for $0 < \omega < \omega_{B_2}$, and H_{32} — as noted previously — may be very small for $\omega > \omega_{B_3}$, the only time this third term may be large is for $0 < \omega < \omega_{B_3}$. Thus, the desire is to keep G_{31}' small for $0 < \omega < \omega_{B_3}$. This amplifies this same specification as found for step c).

In summary then, x_2/x_{1c} will be small if G_{21}' is small (especially for $0 < \omega < \omega_{B_3}$) and if G_{31}' is small (especially for $0 < \omega < \omega_{B_3}$).

The final system coupling due to a command input is, from Eq. (4.14),

$$\left.\frac{x_3}{x_{1c}}\right|_{3CL} = \frac{1}{\Delta_{3CL}}\left[CL_1'G_{31}' - CL_1'CL_2'G_{32}'G_{21}'\right]$$

For this coupling to be small, some of the requirements already made to reduce other couplings are just reiterated. The first term will be small for well designed H_{11} and for a small G_{31}' in the frequency range of interest for x_3. The latter term will be small for well designed H_{11} and H_{22}, and very very small values of G_{21}' in the frequency range of interest for x_3. It is noted that G_{21}' should be very small in this range since one of the crossfeed considerations is that G_{32}' be large in this same frequency range.

g) Determine the effects of disturbance inputs

As noted in Section 2.2, the disturbance input transfer functions, Eqs. (4.17) - (4.25), do not lend themselves easily to qualitative study of their magnitudes. Each of the nine transfer functions depends on three different open loop disturbance transfer functions. That is, each transfer functions is affected by the three open loop transfer functions which relate that output to each of the three disturbance inputs.

The only specification on the disturbance transfer functions is that each be small in its particular frequency range of interest. Not knowing what the open loop G_{ijd}'s might be, it is impossible to determine if the rules already established for the crossfeeds and compensators will adversely or benefically affect these transfer functions. Furthermore, even when the open loop disturbance transfer functions are known, it may be fairly difficult to get numerical values for Eqs. (4.17) - (4.25), since these equations involve sums of products of several transfer functions, each of which may be fairly high order. The high order factorizations necessary are at least tedious and possibly troublesome even on a computer.

The analysis of Eqs. (4.17) - (4.25) is taken up for a numerical problem in the following chapter.

The following table is presented to summarize the desired conditions for the design procedure, i.e., good closed loop response and effective decoupling.

Quantity	Magnitude	Frequency Range
G_{11}'	large	$0 < \omega < \omega_{B_1}$
G_{22}'	large	$0 < \omega < \omega_{B_2}$
G_{12}'	small	$0 < \omega < \omega_{B_1}$
G_{21}'	small	$0 < \omega < \omega_{B_2}$
	very small	$0 < \omega < \omega_{B_3}$
G_{31}'	small	$0 < \omega < \omega_{B_1}$
	very small	$0 < \omega < \omega_{B_3}$
G_{32}'	large	$0 < \omega < \omega_{B_3}$

Table 4.1 Desired Values for the New Plant as Concluded from the Design Procedure

4.3.3 Choosing Crossfeeds H_{12} and H_{21}

Criteria for the choice of crossfeeds were developed in Section 3.3.2 for the two-input two-output system. These criteria basically specified a reduction in G_{12}' and G_{21}' while hopefully maintaining or increasing the magnitudes and stability of G_{11}' and G_{22}', all over specified frequency ranges. The additional consideration introduced by the third output in this 3x2 system is the effect that desired values for G_{31}' and G_{32}' will have on choosing crossfeeds. That is, do the desired values for G_{31}' and G_{32}' as presented in Table 4.1 conflict with other requirements on H_{12} and H_{21}?

Table 4.1 lists all the major requirements observed in the design procedure. Compromises may be necessary. The decision as to which are the most important requirements will depend on the specifications of the particular system being designed. In order to determine how serious the compromises may have to be, the potentials of H_{12} and H_{21} to satisfy as many of the requirements on G_{12}', G_{21}', G_{31}', and G_{32}' as possible will now be investigated.

As demonstrated earlier in this chapter,

$$\begin{aligned} G_{31}' &= G_{31} + H_{21}G_{32} \\ G_{32}' &= G_{32} + H_{12}G_{31} \end{aligned} \tag{4.2}$$

The effect of H_{12} and H_{21} on G_{31} and G_{32} can be described almost exactly in the same manner as was the crossfeed effect on G_{11}' and G_{22}' in Section 3.3.2. That is, the signs and magnitudes of the crossfeeds affect G_{31} and G_{32} in ways that also depend directly on the particular nature of the dynamics of these transfer functions. Using the parameter plot however, some general comments can be made which will assist the designer in weighing the various (and sometimes conflicting) demands made upon the crossfeeds.

As usual, an example best illustrates the argument. Suppose H_{21} is such that to reduce G_{21}, its product with G_{32} is negative and has a phase angle (at frequencies up to ω_{B_2}) of about -180°. Concurrently,

suppose G_{31} is positive and has a phase angle (in the same frequency range) of between 0° and 90°. Then G_{31}' will be the result of a vector difference operation, with a phase difference between the two vectors of between 90° and 180°. A vector diagram such as is illustrated in Appendix B indicates that this will result in G_{31}' being larger than G_{31}. Were the product $H_{21}G_{32}$ of positive sign, the result would be the opposite. This example, which indicates a fair amount of interdependence of factors in the choice of the crossfeeds, is somewhat simplified in that phase angles often change considerably with frequency. That is, it is possible (even probable) that even though $G_{31}' < G_{31}$ at one frequency, it may happen that $G_{31}' > G_{31}$ at another frequency.

In sum, by observing whether G_{31}' and G_{32}' are the results of vector sums or differences, and what the phase differences are (all dependent indirectly on the magnitudes, signs, and phases of G_{12} and G_{21}), one can determine whether or not G_{31}' is reduced and G_{32}' increased. Only by studying the particular plant dynamics can it be accurately determined if the various requirements on the crossfeeds will conflict with one another. The designer must decide which demands on H_{12} and H_{21} are most important for the particular system being designed. All of these factors are considered in the following application.

CHAPTER 5

APPLICATION OF THE DESIGN PROCEDURE FOR CRUISE CONTROL OF THE SPACE SHUTTLE ORBITER

5.1 Introduction

The expansion of the design procedure for a general 3x2 plant, as developed in the previous chapter, is directly applied here to the lateral control of the MSC 040A space shuttle orbiter. As will be seen, the lateral control of an aircraft is particularly well suited to a formulation with three outputs and two inputs.

As noted above, the design procedure as presented in this thesis assumes a knowledge of the plant. In designing a control system for cruising flight, linear perturbation equations of motion can be used, and the constant coefficients in these equations can be quite accurately determined. Thus, for the problem chosen, the plant is well known and is presented — in the form of transfer functions and frequency responses — in Appendix C.

In this chapter, specifications are given for the lateral control of the space shuttle, crossfeeds and feedbacks are designed to meet these specifications, and the amount of coupling in the system is examined. Finally, the system response to gust disturbances is evaluated.

5.2 Specifications for Lateral Control of the Space Shuttle Orbiter

The three lateral output variables are sideslip angle, roll angle, and heading rate. The inputs are aileron and rudder surface deflections. For this system, the desired objectives are to maintain a zero sideslip angle and to respond well to a heading rate command.

As noted in Section 4.2.1, a basic assumption made in designing a 3x2 system is that two outputs must be closely related in some way. It is apparent from the open loop frequency responses that ϕ (roll angle)

and $\dot{\psi}$ (heading rate) are related by merely a gain factor at low frequency. Roll angle and heading rate loops can, therefore, be closed around the same control. Actually, this kind of occurrence should generally be predicted before the analysis begins, so that it is known that a 3x2 system can be designed. This insight comes initially from a knowledge of the physics of the plant. Since heading rate is a desired output, and since a roll angle is obtained only to generate a steady state heading rate for an aircraft, the roll angle loop will be made an inner loop for heading rate.

The conclusions of Section 2.3 give direction for choosing loop closure sequence. One conclusion is that, if certain output quantities should be suppressed, they should be made inner loops. Since it is desired that β (sideslip) be equal to zero, a β loop will be an inner loop. Another conclusion of Section 2.3 is that the command loop be made the outer loop. Since $\dot{\psi}$ is of interest, the $\dot{\psi}$ loop will be made the third loop, and of course the ϕ loop becomes the second loop. Since roll is controlled by the ailerons (δa), the control for the second and third loops will be δa. Thus, β controlled with δr (rudder) is the first loop closed. The open loop frequency responses indicate that the Dutch roll mode frequency of 1.23 rad/sec governs the crossover frequencies of most of the transfer functions. Only $G_{\dot{\psi}\delta r}$, $G_{\dot{\psi}\delta a}$, and $G_{\beta\delta a}$ could be said to have smaller crossover frequencies. Since $G_{\dot{\psi}\delta a}$ is the loop #3 transfer function, the conclusion that inner loops have highest bandwidths is at least somewhat satisfied.

Thus the lateral plant is

$$G = \begin{bmatrix} G_{11} & G_{12} \\ G_{21} & G_{22} \\ G_{31} & G_{32} \end{bmatrix} = \begin{bmatrix} G_{\beta\delta r} & G_{\beta\delta a} \\ G_{\phi\delta r} & G_{\phi\delta a} \\ G_{\dot{\psi}\delta r} & G_{\dot{\psi}\delta a} \end{bmatrix} \qquad (5.1)$$

Since the aerodynamic forces and moments on the aircraft are dependent on perturbations in the motions relative to the atmosphere, the disturbance inputs ($\underline{x}_d$) may be modeled as atmospheric gusts ($\underline{x}_g$).

Lateral aerodynamic gusts are side velocity gust v_g and rolling velocity gust p_g. Rotary gusts can physically be regarded as being due to the spatial distributions of linear gust velocities (Ref. 6). That is, $\dot{\phi}_g = p_g = \partial w_g/\partial y$ and $r_g = sv_g/U_o = s\beta_g$, where w_g is the vertical velocity gust, y is the spanwise direction, and $r_g = \dot{\psi}_g$ is the yaw rate gust. Since $\dot{\psi}_g = s\beta_g$, for lateral dynamics there are only two physical gust inputs: $\beta_g(x_{1g})$ and $p_g(\dot{x}_{2g})$.

For the lateral dynamics plant with disturbances modeled as wind gusts, C(s) in the equations of motion, Eq. (2.1), is composed of the aerodynamic coefficients of β and $\dot{\phi}$. After using Cramer's rule, the gust input transfer functions are:

$$G_d = \begin{bmatrix} G_{11g} & G_{12g} \\ G_{21g} & G_{22g} \\ G_{31g} & G_{32g} \end{bmatrix} = \begin{bmatrix} G_{\beta\beta_g} & sG_{\beta p_g} \\ G_{\phi\beta_g} & sG_{\phi p_g} \\ G_{\dot{\psi}\beta_g} & sG_{\dot{\psi} p_g} \end{bmatrix} \qquad (5.2)$$

All of the frequency responses to follow, as well as gust input analyses, are done using β_g and p_g as inputs since a ϕ_g is physically meaningless. The open loop transfer functions and frequency responses are given in Appendix C.

The block diagram for this lateral control system — for the moment neglecting gusts — is given in Fig. 5.1. The system is shown with crossfeeds already chosen.

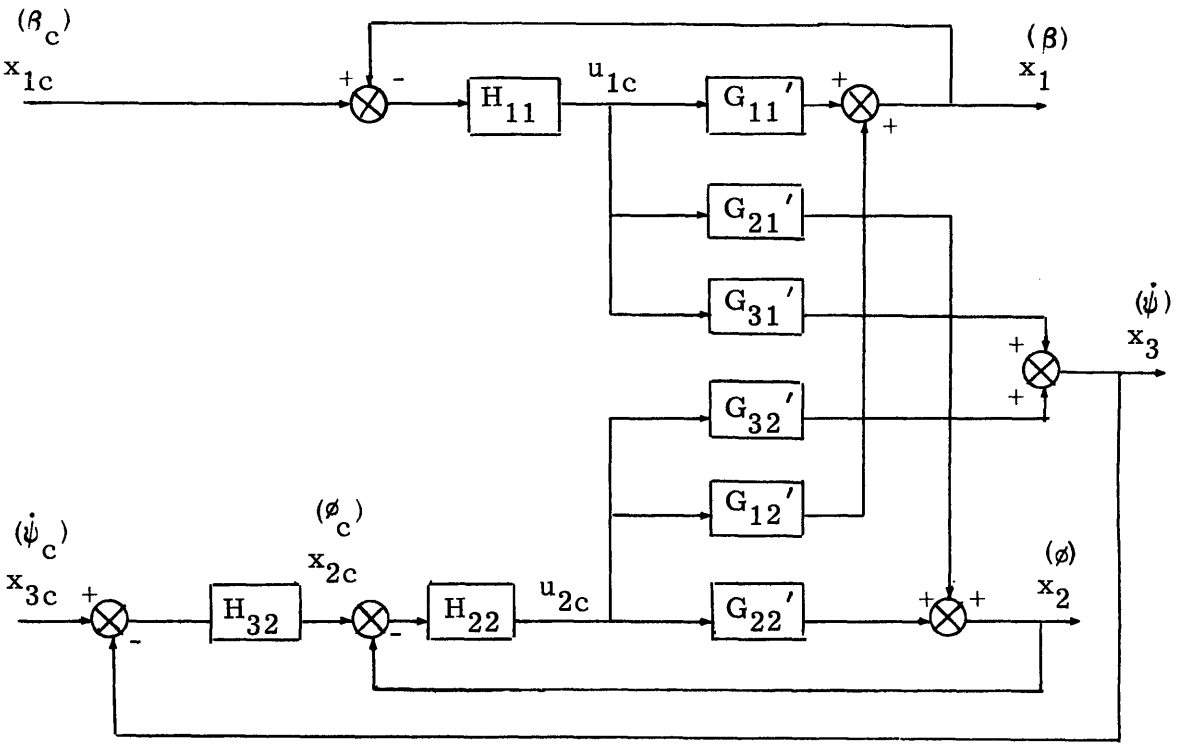

Figure 5.1 Block Diagram of Lateral Control System for the Space Shuttle Orbiter

5.3 Design Procedure for the Space Shuttle Orbiter

5.3.1 Choosing the Crossfeeds H_{12} and H_{21}

In all the qualitative discussions of the design procedure, specifications for the choice of crossfeeds were always developed last. The insights gained from first following steps b) - g) in the design procedure were thus used to formulate crossfeed requirements. This is a logical sequence to use for a qualitative analysis. However, for the actual physical problem at hand, the crossfeeds must be chosen first. Choosing the crossfeeds is, in fact, the first step in the design procedure. Use will of course be made of all the specifications derived so far.

The design procedure is presented in this and the next two subsections.

a) Choose the crossfeeds and derive the "new plant"

Generally, the most desirable situation is "exact decoupling" discussed in Section 3.3 2, where the crossfeeds are such that loops #1 and #2 are completely decoupled. This choice of crossfeeds was used for the space shuttle lateral dynamics plant, following very closely the design procedure as previously developed.

For exact decoupling,

$$G_{21}' = G_{21} + H_{21}G_{22} = 0 \Rightarrow H_{21} = -\frac{G_{21}}{G_{22}}$$

$$G_{12}' = G_{12} + H_{12}G_{11} = 0 \Rightarrow H_{12} = -\frac{G_{12}}{G_{11}}$$

which results in, for the space shuttle,

$$H_{21} = +.305\ \frac{(s-.8671)(s+1.0411)}{(s+.1913+j.8170)(s+.1913-j.8170)} \qquad (5.3)$$

$$H_{12} = +.341\ \frac{(s+.1654)(s+.4541)(s+108.33)}{(s+.00124)(s+.82156)(s+30.365)} \qquad (5.4)$$

This choice for the crossfeeds should now be examined, using the arguments of Sections 3.3.2 and 4.3.3, to see if its effects on G_{11}, G_{22}, G_{31}, and G_{32} are beneficial or detrimental. Bode sketches — magnitude and phase plots as functions of frequency — can easily be done and are sufficient for this purpose.

While this initial analysis is an approximate one, it gives an indication as to whether or not the "exact decoupling" choice of crossfeeds will cause any serious problems for this plant. The Bode plots for G_{11}, G_{22}, G_{31} and G_{32} are contained in Appendix C. The Bode plots for $H_{21}G_{12}$, $H_{12}G_{21}$, $H_{21}G_{32}$, and $H_{12}G_{31}$ for the above choice for H_{21} and H_{12} are contained in Figs. 5.2 and 5.3. The procedure is as follows.

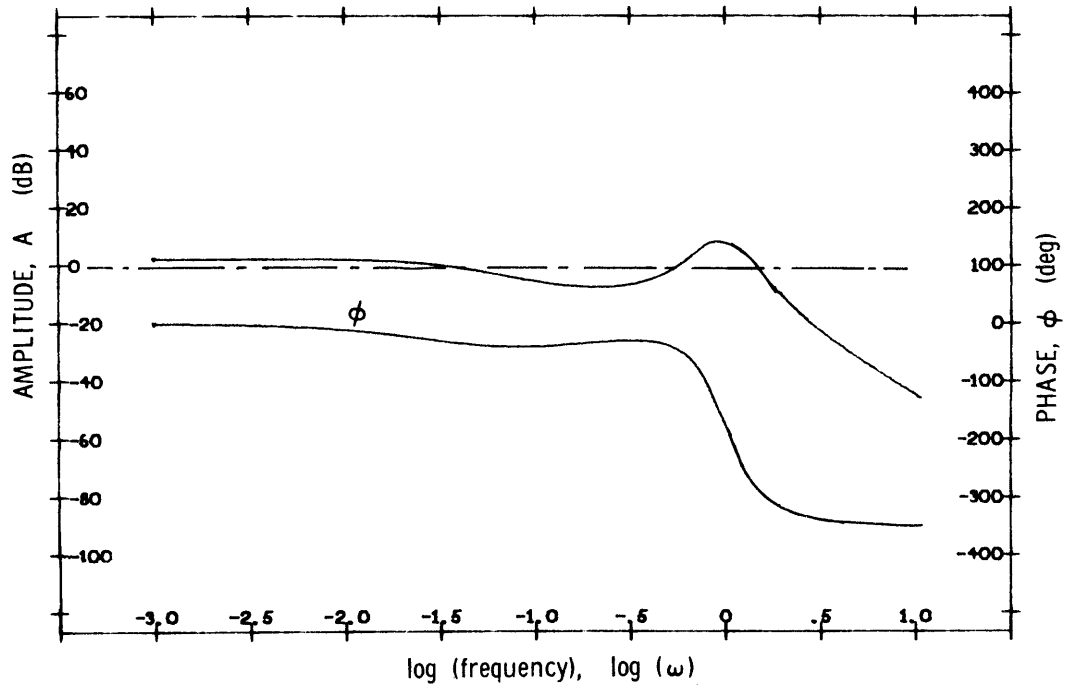

Fig. 5.2a Frequency Plot of $H_{21}G_{12}$

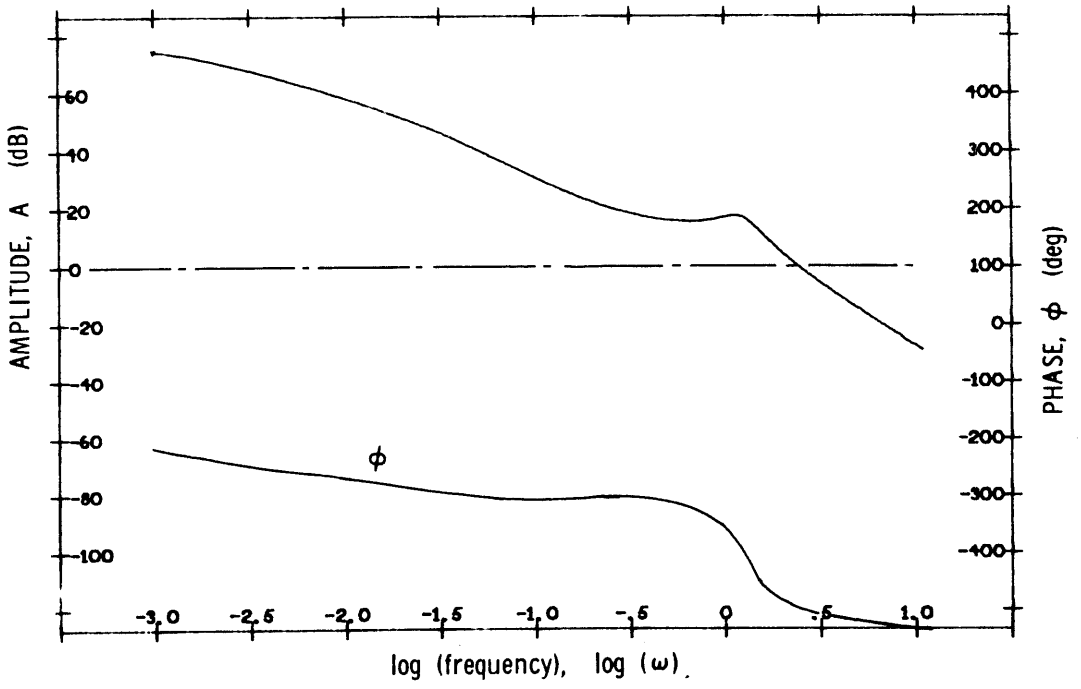

Fig. 5.2b Frequency Plot of $H_{12}G_{21}$

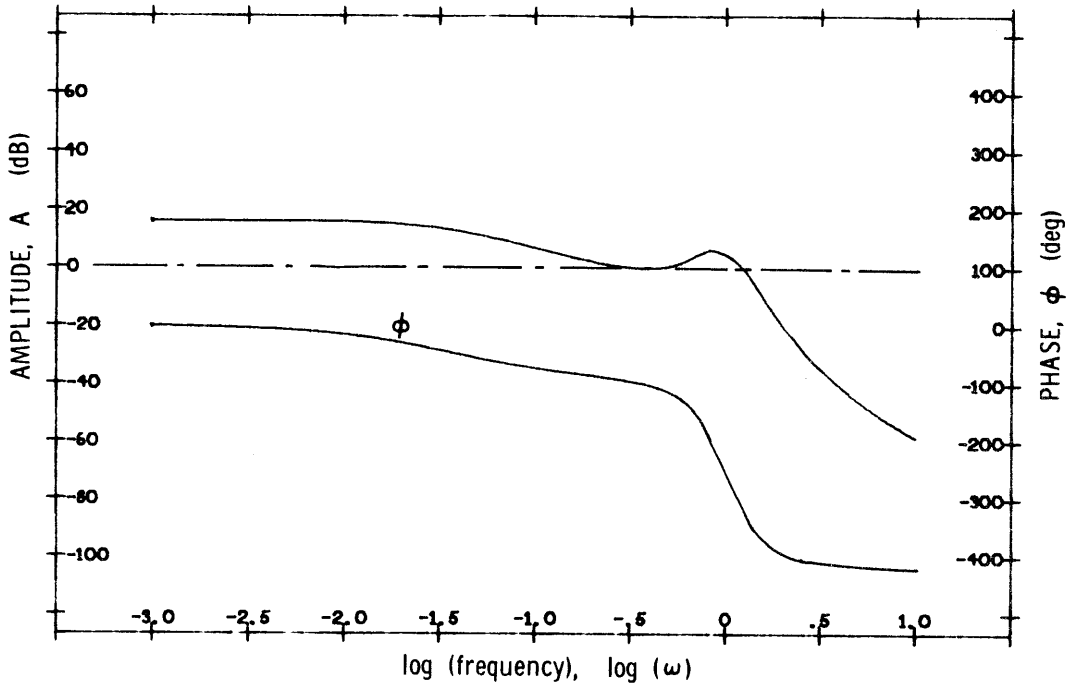

Fig. 5.3a Frequency Plot of $H_{21}G_{32}$

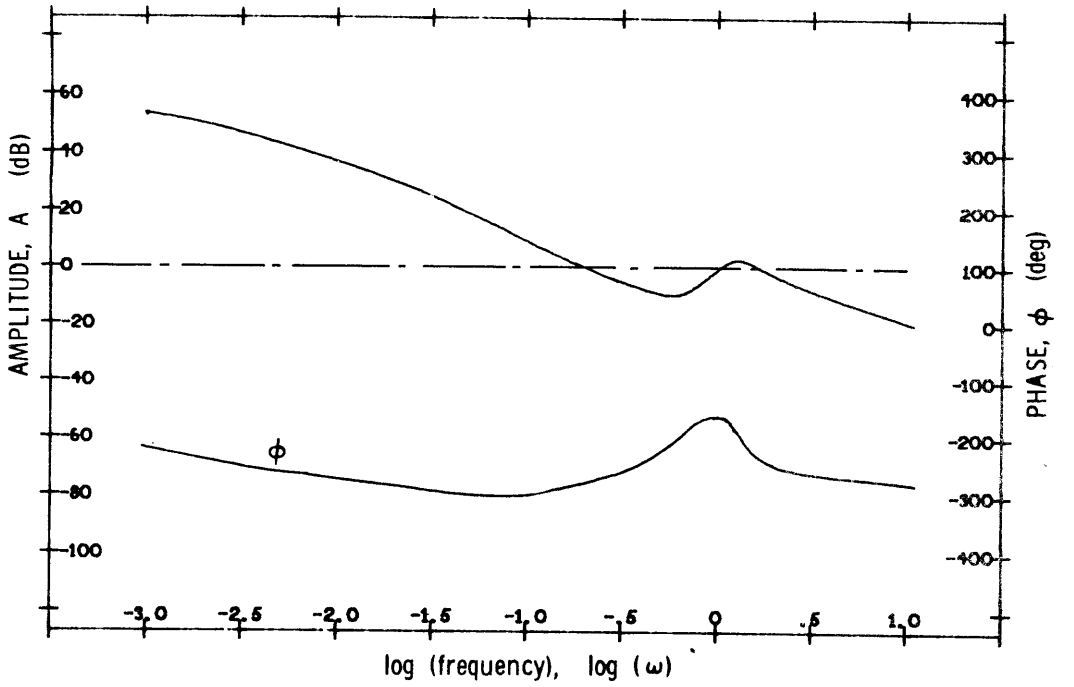

Fig. 5.3b Frequency Plot of $H_{12}G_{31}$

1. $$G_{11}' = G_{11} + H_{21}G_{12}$$

$$-90° < \phi_{G_{11}} < 90° \qquad \text{for} \quad 0 < \omega < 1.2$$

$$\phi_{H_{21}G_{12}} < -180° \qquad \text{for} \quad 0 < \omega$$

where

$$\phi_{G_{11}} = \text{phase angle of } G_{11}$$

$$\phi_{H_{21}G_{12}} = \text{phase angle of } H_{21}G_{12}$$

Since $G_{11} > 0$* and $H_{12}G_{12} < 0$, G_{11}' is the result of a vector difference for a phase difference, ϕ, which is greater than 90°. Thus $G_{11}' > G_{11}$ over the frequency range $0 < \omega < 1.2$

2. $$G_{22}' = G_{22} + H_{12}G_{21}$$

$$-90° < \phi_{G_{22}} < 0° \qquad \text{for} \quad 0 < \omega < 1.2$$

$$\phi_{H_{12}G_{21}} < -180° \qquad \text{for} \quad 0 < \omega$$

Since $G_{22} < 0$ and $H_{12}G_{21} > 0$, G_{22}' is the result of a vector difference for $\phi > 90°$. Thus $G_{22}' > G_{22}$ over the frequency range $0 < \omega < 1.2$.

3. $$G_{31}' = G_{31} + H_{21}G_{32}$$

$$-90° < \phi_{G_{31}} < 0° \qquad \text{for} \quad 0 < \omega$$

---

* By "$G_{ij} > 0$" is meant merely that the leading gain factor has a positive sign. For example, since G_{12} has a negative leading gain factor (see Appendix C) and H_{21} has a positive one (see Eq. 5.3), then $H_{21}G_{12} < 0$.

$$-90^\circ < \phi_{H_{21}G_{32}} < 0^\circ \quad \text{for} \quad 0 < \omega < .25$$

$$-180^\circ < \phi_{H_{21}G_{32}} < -90^\circ \quad \text{for} \quad .25 < \omega < .80$$

Since $G_{31} < 0$ and $H_{21}G_{32} > 0$, G_{31}' is the result of a vector difference for $\phi < 90^\circ$ over small frequencies. Thus $G_{31}' < G_{31}$ over very low frequencies ($\omega < .25$). Also, since $\phi > 90^\circ$ over higher frequencies, $G_{31}' > G_{31}$ for $.25 < \omega$.

4.

$$G_{32}' = G_{32} + H_{12}G_{31}$$

$$-270^\circ < \phi_{G_{32}} < -180^\circ \quad \text{for} \quad 0 < \omega < .70$$

$$-120^\circ < \phi_{H_{12}G_{31}} < 0^\circ \quad \text{for} \quad 0 < \omega < .70$$

Since $G_{32} > 0$ and $H_{12}G_{31} < 0$, G_{32}' is the result of a vector difference for $\phi > 90^\circ$. Thus $G_{32}' > G_{32}$ for $\omega < .70$.

These approximate results indicate that this choice of crossfeeds results in a new plant which satisfies most of the specifications of Table 4.1. In addition, the fact that $G_{12}' = G_{21}' = 0$ somewhat eases the strictness of the requirements on other new plant transfer functions. This suggests that Eqs. (5.3) and (5.4) are indeed very good choices for the crossfeeds. As the analysis continues, this will be seen to be precisely the case.

One important advantage of the "exact decoupling" choice for the crossfeeds is the great numerical simplification it affords in the calculation of G_{11}', G_{22}', G_{31}' and G_{32}'. The reason for this is that, for this choice of crossfeeds, the Multiloop Analysis coupling numerators can be used. As an example, consider G_{11}'.

$$G_{11}' = G_{11} + H_{21}G_{12} = G_{11} - \frac{G_{21}}{G_{22}} G_{12}$$

$$= \frac{G_{11}G_{22} - G_{21}G_{12}}{G_{22}}$$

From Appendix A,

$$\Delta(G_{11}G_{22} - G_{21}G_{12}) = N_{u_1u_2}^{x_1x_2}$$

As noted in Section 4.2.1, the coupling numerator is easily obtained by Cramer's rule from the original plant dynamics and is generally of low order. Rather than subtract two products of third and fourth order numerators and denominators, the new plant transfer functions can be quickly found (for exact decoupling choices of H_{12} and H_{21}) as:

$$G_{11}' = \frac{G_{11}G_{22} - G_{12}G_{21}}{G_{22}} = \frac{N_{u_1u_2}^{x_1x_2}}{N_{u_2}^{x_2}}$$

$$G_{22}' = \frac{G_{11}G_{22} - G_{12}G_{21}}{G_{11}} = \frac{N_{u_1u_2}^{x_1x_2}}{N_{u_1}^{x_1}}$$

$$G_{31}' = \frac{G_{31}G_{22} - G_{21}G_{32}}{G_{22}} = \frac{N_{u_1u_2}^{x_3x_2}}{N_{u_2}^{x_2}}$$

$$G_{32}' = \frac{G_{11}G_{32} - G_{12}G_{31}}{G_{11}} = \frac{N_{u_1u_2}^{x_1x_3}}{N_{u_1}^{x_1}}$$

If one were actually to perform the operations $G_{11}G_{22} - G_{12}G_{21}$, for instance, he would find the result to be a transfer function with ninth order numerator and tenth order denominator. However, an eighth order factor is common to the numerator and denominator. This factor is Δ^2. The resulting transfer function (G_{11}') has a first order numerator and second order denominator. Thus,

$$G_{11}' = \frac{N_{\delta r \delta a}^{\beta\ \phi}}{N_{\delta a}^{\phi}} = .0435\ \frac{(s+21.2014)}{(s+.1913+j.81701)(s+.1913-j.81701)} \quad (5.5)$$

$$G_{22}' = \frac{N_{\delta r \delta a}^{\beta\ \phi}}{N_{\delta r}^{\beta}} = -10.482\ \frac{(s+21.2014)}{(s+.00129)(s+.82156)(s+30.365)} \quad (5.6)$$

$$G_{31}' = \frac{N_{\delta r \delta a}^{\dot{\psi}\ \phi}}{N_{\delta a}^{\phi}} = -.935\ \frac{(s+.21125)}{(s+.1913+j.81701)(s+.1913-j.81701)} \quad (5.7)$$

$$G_{32}' = \frac{N_{\delta r \delta a}^{\beta\ \dot{\psi}}}{N_{\delta r}^{\beta}} = -.297\ \frac{(s+.5434)(s+114.70)}{(s+.00129)(s+.82156)(s+30.365)} \quad (5.8)$$

Frequency plots of these new plant transfer functions are given in Figs. 5.4 - 5.7. To this point, it has been assumed that the crossfeeds should reduce the coupling as much as possible. However, in dealing with a plant as complex as an aircraft, there may be reasons why having a small amount of coupling between controls is desirable. In order to get some notion as to actually what is desirable, aircraft handling qualities specifications can be translated into "ideal" transfer functions. This somewhat arbitrary and approximate procedure, along with the final results for the ideal transfer functions, are presented in Appendix D. It is indeed gratifying to observe how well the new plant frequency responses

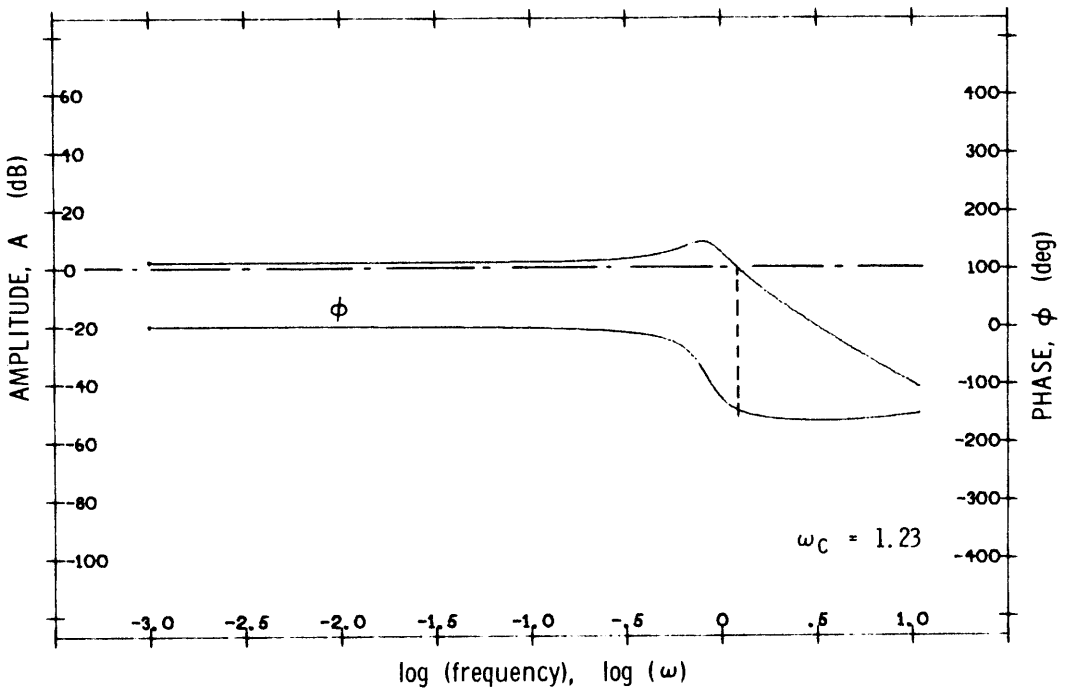

Fig. 5.4 Frequency Plot of G_{11}'

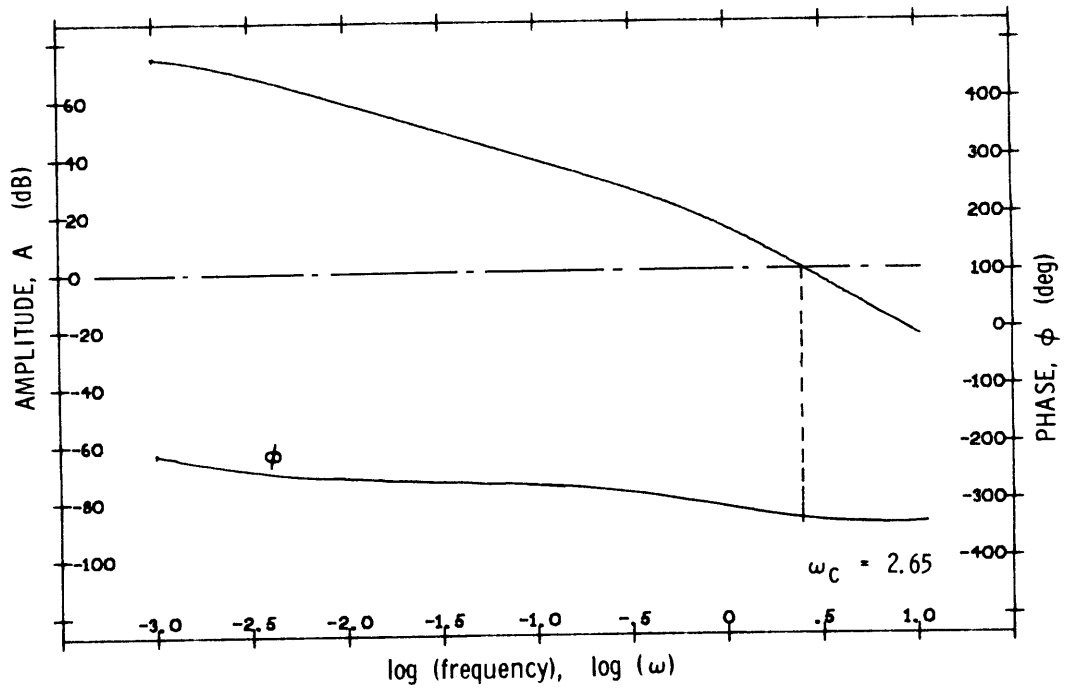

Fig. 5.5 Frequency Plot of G_{22}'

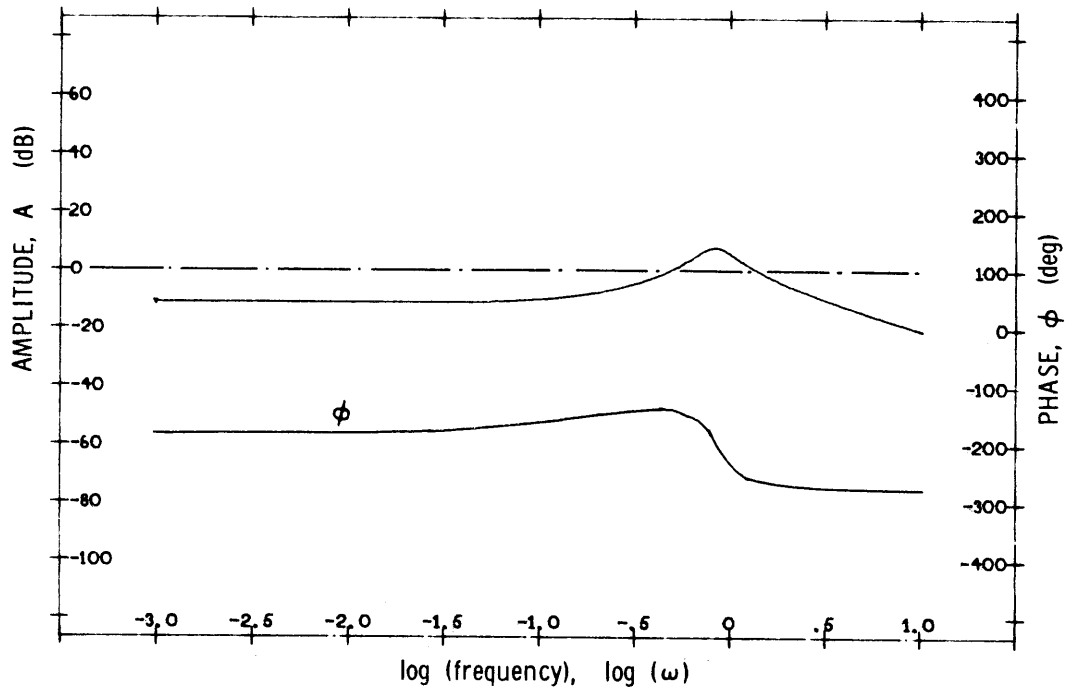

Fig. 5.6 Frequency Plot of G_{31}'

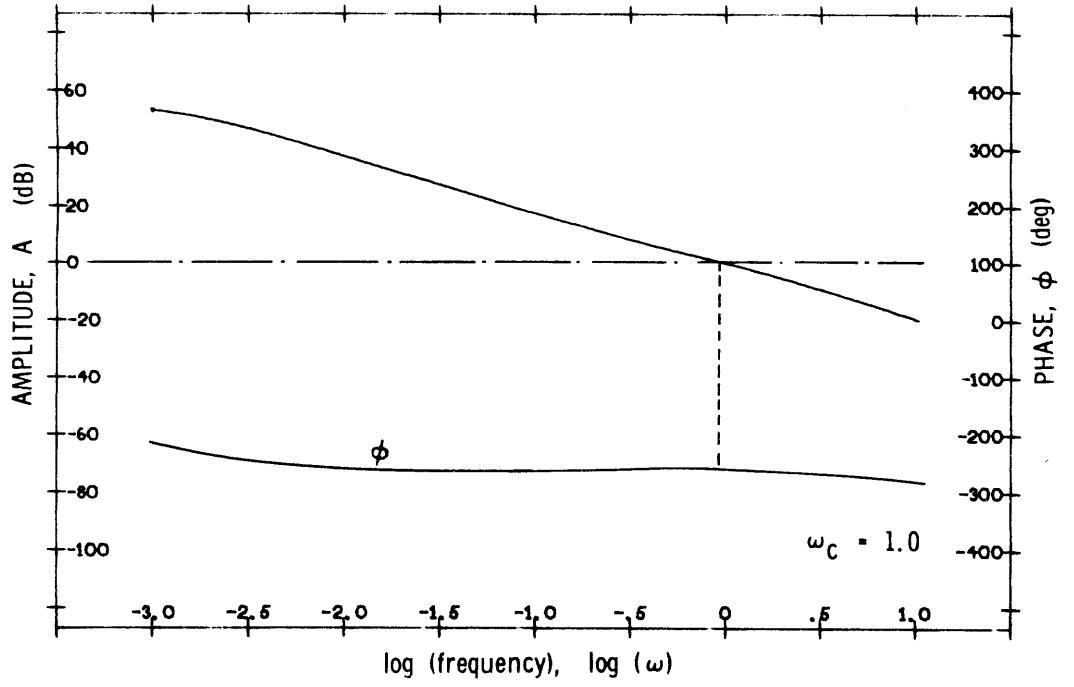

Fig. 5.7 Frequency Plot of G_{32}'

(Figs. 5.4 - 5.7),* resemble the "ideal" frequency responses (Figs. D.1 - D.6). This indicates, of course, that the exact decoupling choice for the crossfeeds achieves the desired results. The possibility of control system failure and resulting pilot takeover makes it desirable to have an open loop plant which closely models a pilot-rated "ideal" plant. This "ideal" plant also closely matches — as it should for easy design — the frequency and magnitude specifications of Table 4.1.

5.3.2 Designing Feedback Compensations

Having chosen the crossfeeds, the designer is ready to continue in the design procedure, the next steps being the design of feedback compensations. Several general comments will be made before proceeding with steps b), c), and d) of the design procedure.

The loop compensations are designed to meet the specifications of Section 5.2. The design will be carried out entirely in the frequency domain, using plots of magnitude and phase versus frequency.

It might be well here to review the criteria used in frequency domain design. For good closed loop response, i.e., output following input or,

$$\frac{x}{x_c} = \frac{HG}{1 + HG} \approx 1,$$

the designer wants high gain in the forward loop transfer function (HG) at frequencies up to crossover. As usual, in this design it is assumed that the crossover frequency is close to the closed loop bandwidth. In addition, the phase angle of HG should be sufficiently above -180° to ensure stability. This requirement for large phase margin ensures a small closed loop peak resonance. This is particularly important in that it signifies that any

---

* The only responses not showing resemblance are G_{21}' and the "ideal" G_{21}. It should be remembered, however, that "ideal" was defined for specific purposes. G_{21} is the transfer function $\phi/\delta r$, and large values of it at low frequency in the "ideal" analysis probably indicate the arbitrary nature of choosing the control derivatives. For normal relatively short duration rudder inputs, in fact, there will not result any large values of roll angle. It is relevant to note that the $\phi/\delta r$ transfer function has low gain at all frequencies.

overshoot in the time response to a step input will be small.

Continuing with the design procedure:

b) Close loop #1

Using Fig. 5.4, H_{11} is designed so that, as outlined above, the open loop gain $H_{11}G_{11}'$ is large at frequencies up to crossover, and so that the bandwidth is large. Since this first loop is the sideslip loop, it should have very high gain at zero frequency to keep steady state sideslip equal to zero. Also, the bandwidth should be as large as possible so that the inner loop bandwidths may not be too restricted. It may then be desirable to increase the crossover frequency, if it can be done without losing needed phase margin.

Thus, H_{11} is chosen to have a high gain factor, an integrator for infinite steady state gain, a low frequency phase lead, and a lead-lag at higher frequencies to extend the crossover while retaining sufficient phase margin for stability.

$$H_{11} = 22.1\frac{(s+.05)(s+1.2)}{s(s+5.1)} \tag{5.9}$$

$H_{11}G_{11}'$ is plotted in Fig. 5.8.

The closed loop response is shown in Fig. 5.9. The requirements presented above for good closed loop response are clearly satisfied.

c) Analyze and design loop #2 with loop #1 closed

Using Fig. 5.5, H_{22} is designed so that $H_{22}G_{22}'$ is large at frequencies up to crossover, and so that the bandwidth is large. Since G_{22}' has a net minus sign, H_{22} is chosen to be negative for stability. An alternative would be to have positive H_{22} and positive feedback. For uniformity in analysis, the former method is chosen. Since G_{22}' has large magnitude itself, H_{22} is designed merely as a lead-lag to increase the phase margin at crossover.

$$H_{22} = -\frac{(s+2.0)}{(s+4.4)} \tag{5.10}$$

Figs. 5.10 and 5.11 show the frequency plots for $H_{22}G_{22}'$ and $\left.\frac{x_2}{x_{2c}}\right|_{2CL}$ respectively.

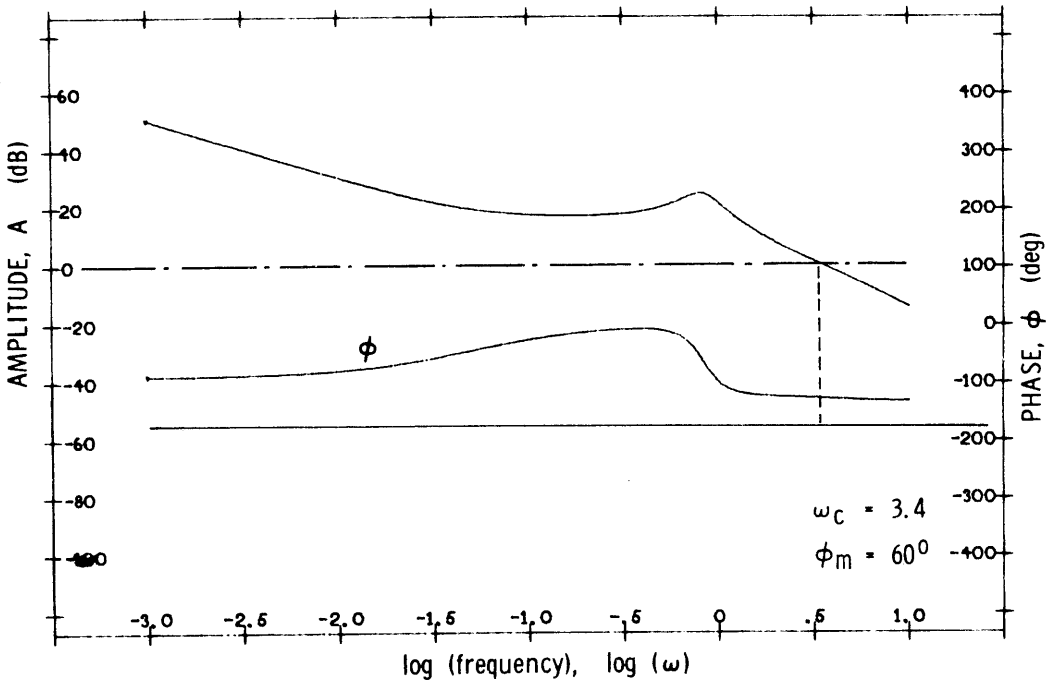

Fig. 5.8 Frequency Plot of $H_{11}G_{11}'$

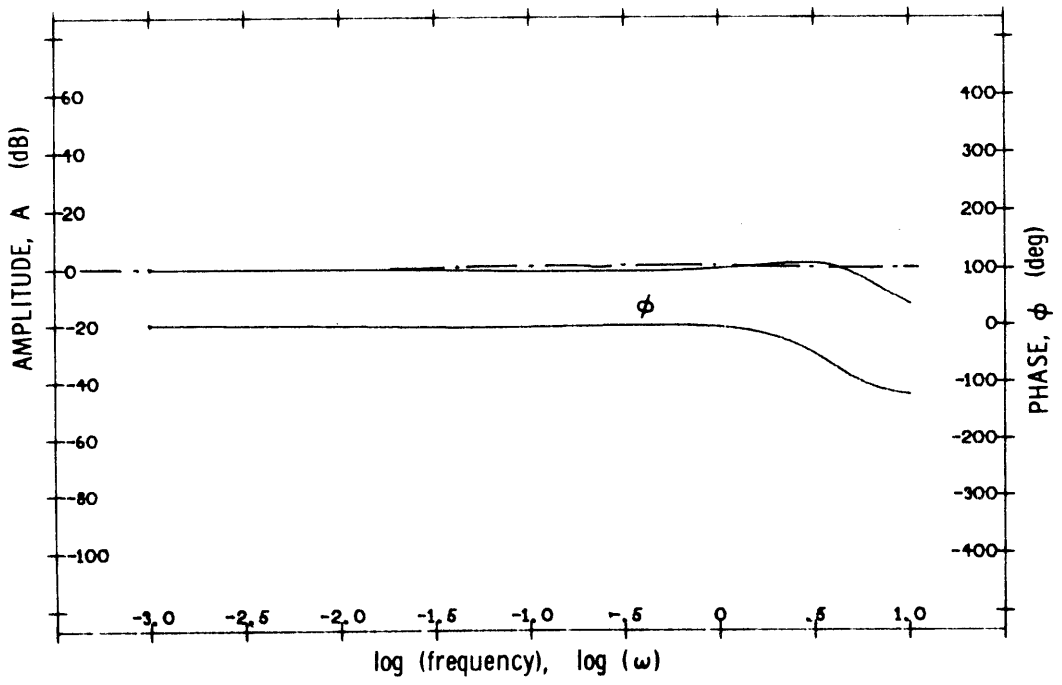

Fig. 5.9 Frequency Plot of $\left.\frac{x_1}{x_{1c}}\right|_{1CL}$

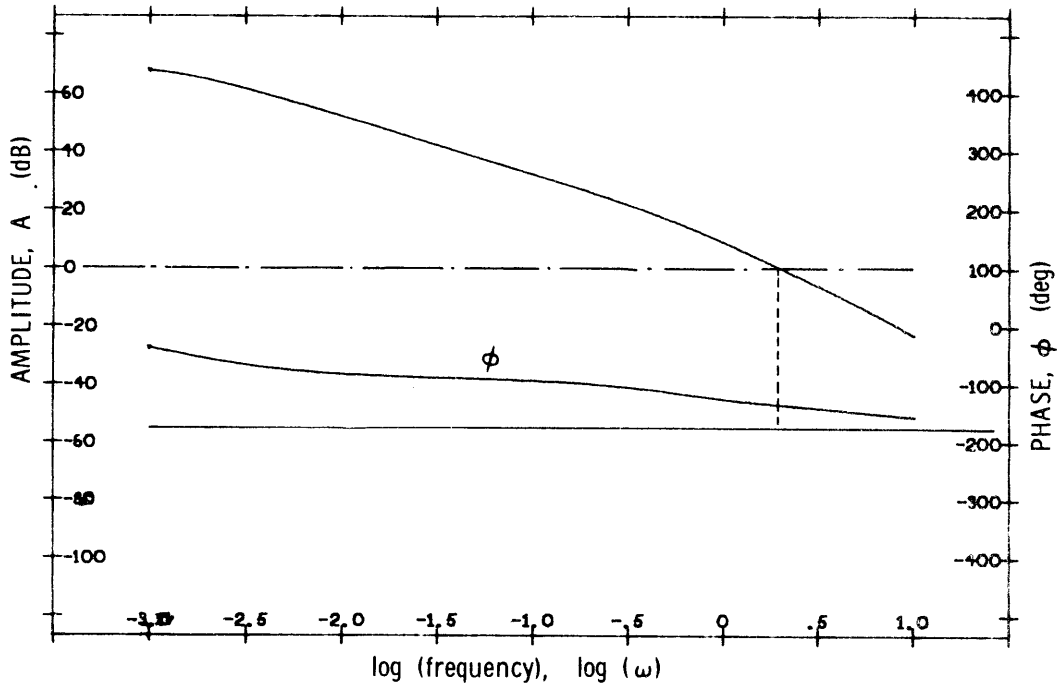

Fig. 5.10 Frequency Plot of $H_{22}G_{22}'$

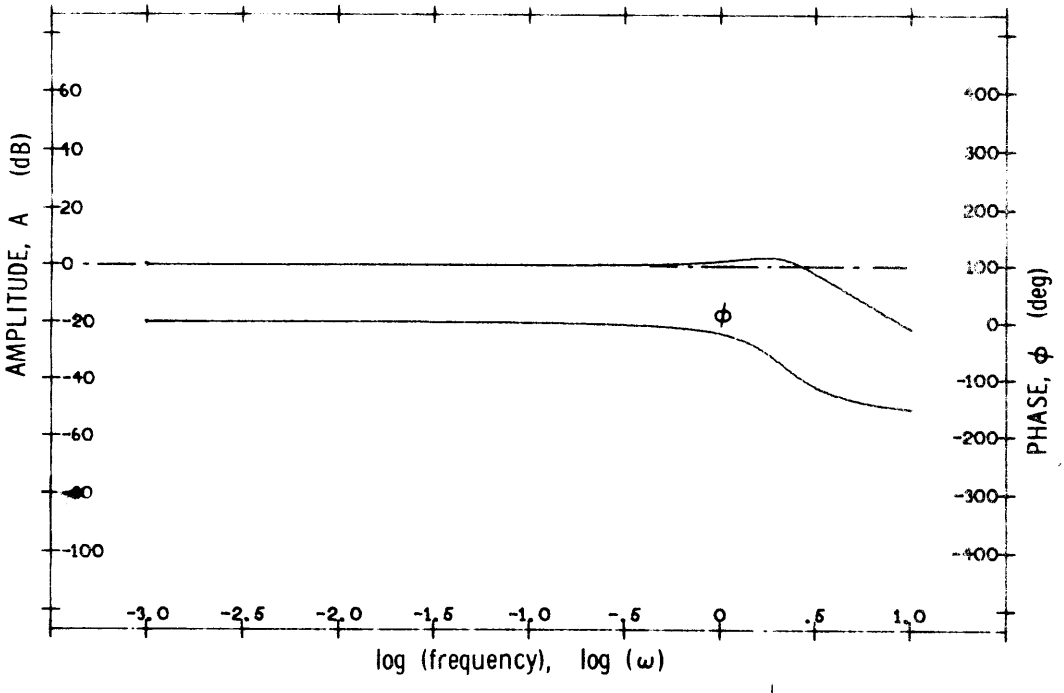

Fig. 5.11 Frequency Plot of $\left.\frac{x_2}{x_{2c}}\right|_{1CL}$

The design procedure specifies that at this point, having designed H_{22} assuming no coupling, the designer should return to the total transfer function and determine if the coupling from loop #1 is large. For this exact decoupling case, the coupling term $-H_{22}G_{12}'CL_1G_{21}'$ (from Eq. (4.10)) is exactly zero. Thus, loop #1 has no effect in the response in x_2 to an x_{2c}.

d) Analyze and design loop #3 with loop #1 and loop #2 closed

Since loop #3 is closed around loop #2, the open loop uncompensated transfer function for loop #3 is $CL_2'G_{32}'$. It is plotted in Fig. 5.12. Neglecting all coupling, H_{32} is designed to meet the same criteria as H_{11} and H_{22} except for one important consideration. The bandwidth of this third loop should be quite small to avoid possible coupling, as mentioned briefly above in Secion 4.3.1. That is, its bandwidth should be considerably smaller than that of loop #1 or loop #2. A term with CL_1', for instance, as one of its factors may grow very large near ω_{B_1} where $CL_1' \approx H_{11}$. If ω_{B_3} is small, then H_{32} will be very small at higher frequencies, which in many cases (see Section 4.3.2) will compensate for the increase in factors like CL_1'. The final choice for H_{32} is shown in Fig. 5.13.

$$H_{32} = .64\,\frac{(s+.10)}{s(s+.015)}. \tag{5.11}$$

Having designed H_{32}, the design procedure now specifies that the complete transfer function x_3/x_{3c} be studied. Since terms containing G_{12}' or G_{21}' are zero for exact decoupling, the complete transfer function x_3/x_{3c} is, as demonstrated in Section 4.3.1:

$$\frac{x_3}{x_{3c}} = \frac{H_{32}[CL_2'G_{32}'(1+H_{11}G_{11}')]}{(1+H_{11}G_{11}')[1+H_{32}G_{32}'CL_2']}$$

$$= \frac{H_{32}CL_2'G_{32}'}{1+H_{32}CL_2'G_{32}'}.$$

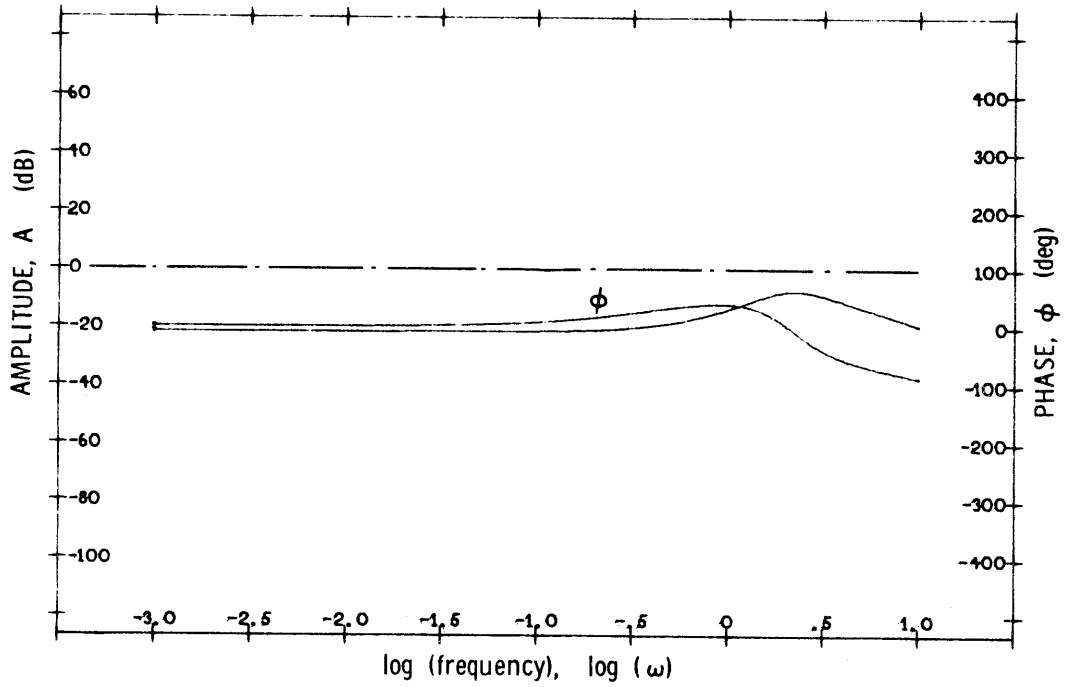

Fig. 5.12 Frequency Plot of $G_{32}'CL_2'$

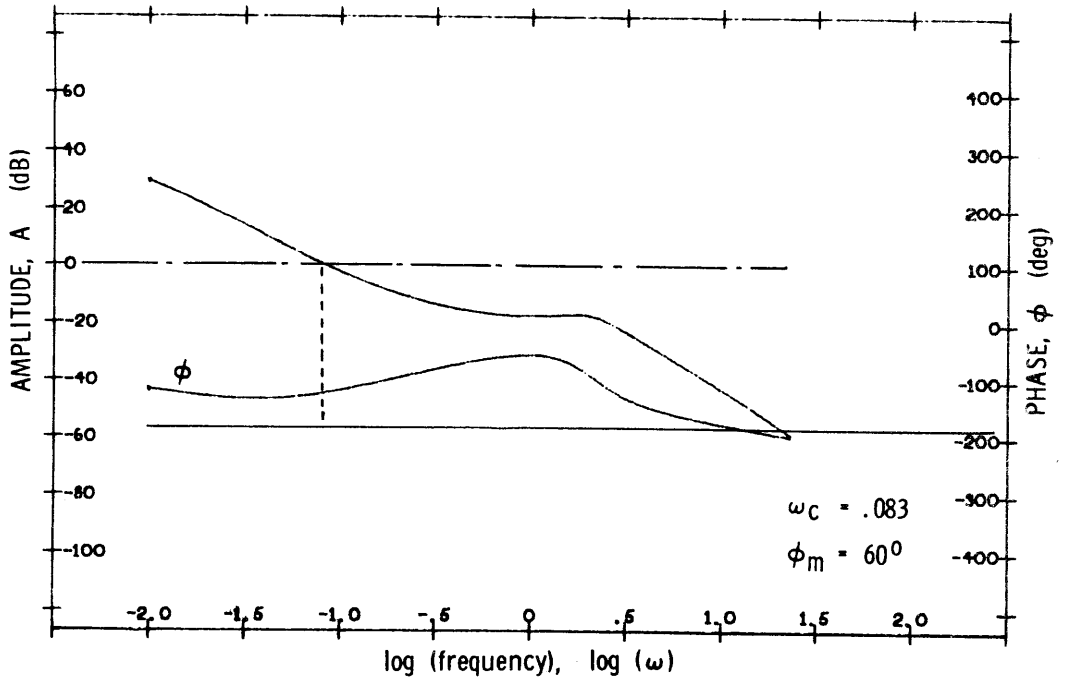

Fig. 5.13 Frequency Plot of $H_{32}G_{32}'CL_2'$

Thus exact decoupling eliminates any coupling in the heading rate response to a heading rate command. Figure 5.14 gives the closed loop response for loop #3.

5.3.3 Evaluating Couplings

The final steps of the design procedure involve the evaluation of couplings in the system and the response of the system to gust disturbances.

e) Determine the effect of loop #2 on loop #1, and loop #3 on loop #1

For exact decoupling, all terms containing G_{12}' and G_{21}' are zero and there is no effect from loop #2 or loop #3 on x_1 due to an x_{1c}. That is,

$$\left.\frac{x_1}{x_{1c}}\right|_{3CL} = \frac{H_{11}G_{11}'}{1 + H_{11}G_{11}'} = T_1'.$$

The response of x_1 to x_{1c} can, in general, be used to give information regarding the response in x_1 to initial conditions. However, for the lateral control system this is the only practical use for x_1/x_{1c}, since $\beta_c = x_{1c} = 0$ always. Thus, since it is desired that $\beta = 0$, $\underline{x_1 \text{ due to an } x_{1c}}$ is always zero, regardless of coupling.

f) Determine the coupling effects: x_{3c} on x_1, and x_{1c} on x_2 and x_3

Substituting $G_{12}' = 0$ and $G_{21}' = 0$ in Eqs. (4.13) and (4.14) results in:

$$\left.\frac{x_2}{x_{1c}}\right|_{3CL} = -\frac{H_{32}T_2CL_1'G_{31}'}{1 + H_{32}CL_2'G_{32}'} \qquad (5.12)$$

which, for small G_{31}' and small H_{32} at higher frequencies (near ω_{B_2}) is quite small.

$$\left.\frac{x_3}{x_{1c}}\right|_{3CL} = \frac{CL_1'G_{31}'}{1 + H_{32}CL_2'G_{32}'}. \qquad (5.13)$$

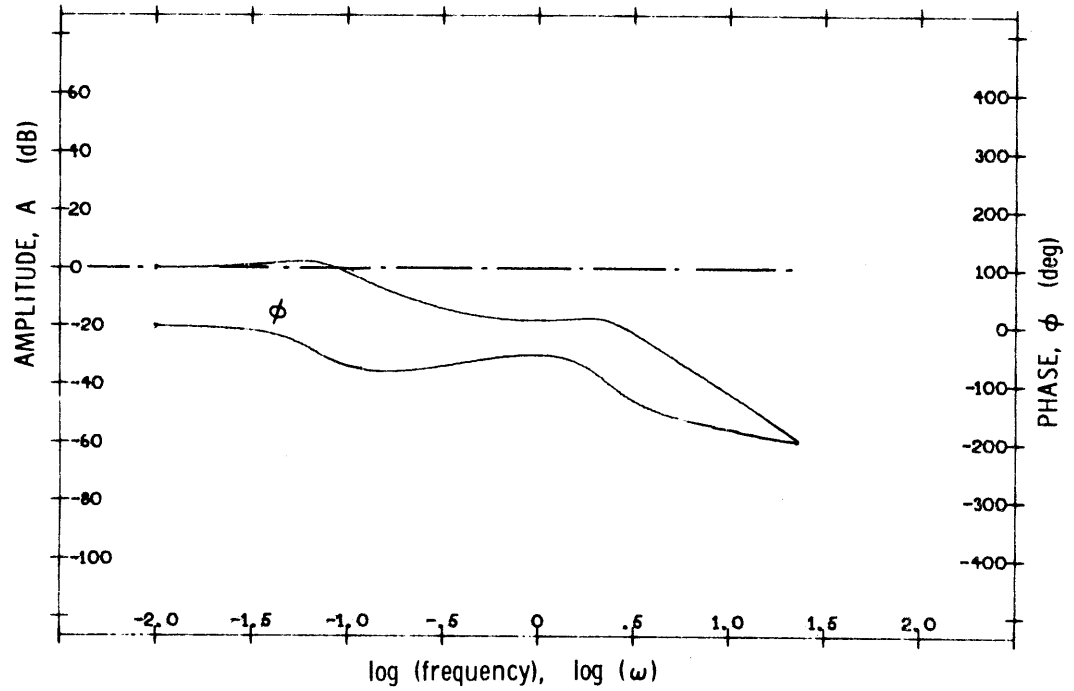

Fig. 5.14 Frequency Plot of $\left.\frac{x_3}{x_{3c}}\right|_{3CL}$

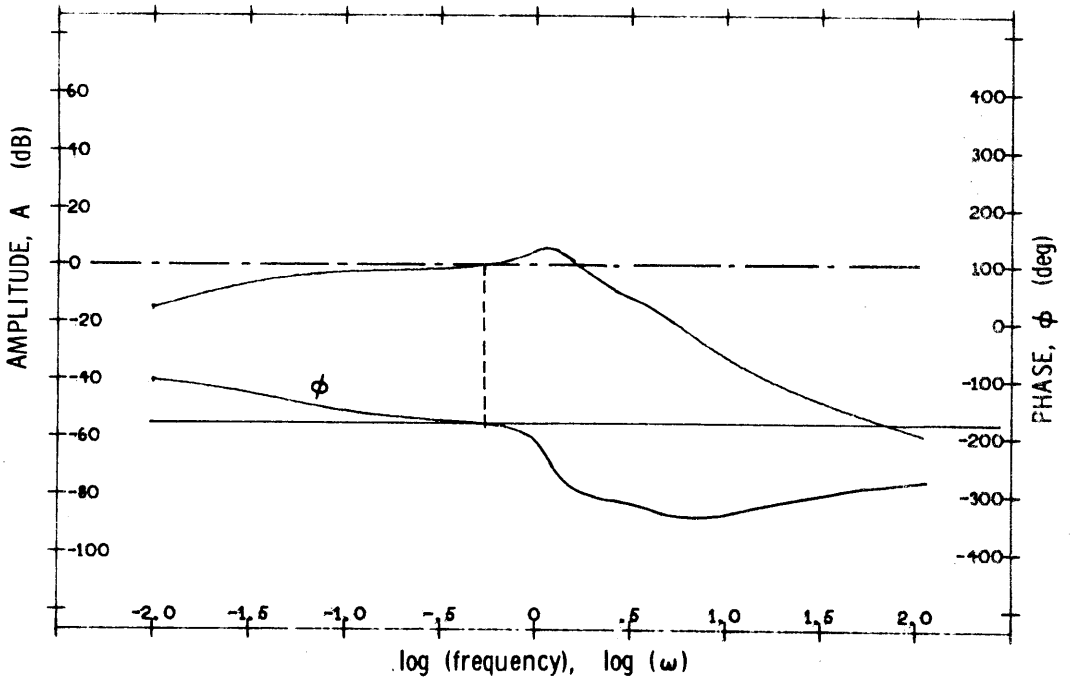

Fig. 5.15 Frequency Plot of $\frac{x_1}{x_{1g}}$

Eq. (5.13), for small values of G_{31}' at low frequencies, will be small. Again, these general comments are not really necessary for the present application since $x_{1c} = \beta_c = 0$.

Finally, from Eq. (4.12),

$$\left.\frac{x_1}{x_{3c}}\right|_{3CL} = \frac{1}{\Delta_{3CL}}\left[\frac{H_{32}CL_2'G_{12}'}{1+H_{11}G_{11}'}\right]$$

which, for exact decoupling, is exactly zero.

Thus, the exact decoupling choice for the crossfeeds eliminates all coupling in each output due to commands in other loops.

g) Determine the effects of disturbance inputs

As a final check on the design, it is well to examine the system response to disturbance inputs. As noted previously, the system response to disturbances is not easily analyzed qualitatively since it depends so much on individual open loop responses.

The disturbances to the space shuttle are modeled as gusts. The gust open loop transfer functions and frequency plots are given in Appendix C. Since, for this particular control system, the outputs of interest are β and $\dot{\psi}$ (x_1 and x_3 respectively), and since the only physical gusts are β_g and p_g (x_{1g} and $\dot{x}_{2g}$ respectively), the only system transfer functions of interest are x_1/x_{1g}, $x_1/\dot{x}_{2g}$, x_3/x_{1g}, and $x_3/\dot{x}_{2g}$. Using Eqs. (4.18), (4.19) (4.23) and (4.24) for exact decoupling, the system transfer functions become:

$$\left.\frac{x_1}{x_{1g}}\right|_{3CL} = \frac{G_{11g}}{1 + H_{11}G_{11}'} \tag{5.14}$$

$$\left.\frac{x_1}{\dot{x}_{2g}}\right|_{3CL} = \frac{G_{12g}}{s(1 + H_{11}G_{11}')} \tag{5.15}$$

$$\left.\frac{x_3}{x_{1g}}\right|_{3CL} = \frac{G_{31g} - G_{32}'CL_2'G_{21g} - G_{31}'CL_1'G_{11g}}{1 + H_{32}CL_2'G_{32}'} \qquad (5.16)$$

$$\left.\frac{x_3}{\dot{x}_{2g}}\right|_{3CL} = \frac{G_{32g} - G_{32}'CL_2'G_{22g} - G_{31}'CL_1'G_{12g}}{s(1 + H_{32}CL_2'G_{32}')} \qquad (5.17)$$

The numerical values for Eqs. (5.16) and (5.17) are not quickly and easily obtained. Multiloop Analysis offers no assistance because several terms have been set equal to zero by virtue of exact decoupling and the remaining terms do not combine to form coupling numerators. The tedious procedure to follow is to multiply the various factors in each term together and add the resultant polynomials until the final transfer function is obtained. The frequency responses for these system transfer functions are given in Figs. 5.15 - 5.18.

It can be seen from the frequency plots that the responses to gust disturbances, with one exception, are quite small over the frequency range of interest for each output variable. This one exception is the $\dot{\psi}$ response to a rolling gust, Fig. 5.18.

However, due to the random nature of gust disturbances, it is necessary to consider more than merely the transfer function in order to get an accurate picture of an aircraft's response to gusts. The power spectral density will be used here as a statistical description of the airplane's response. Assuming no correlation between command and disturbance inputs, and isolating the rolling rate gust, the power spectral density of the output, $\dot{\psi}$, may be written in terms of the power spectral density of p_g as:

$$\Phi_{\dot{\psi}\dot{\psi}}(\omega) = |G_{\dot{\psi}p_g}(\omega)|_{3CL}|^2 \Phi_{p_g p_g}(\omega) = \left|\frac{H_{32}CL_2'G_{32}'}{1+H_{32}CL_2'G_{32}'}\right|^2 \Phi_{p_g p_g}(\omega) \qquad (5.18)$$

What is needed now is the value of $\Phi_{p_g p_g}(\omega)$.

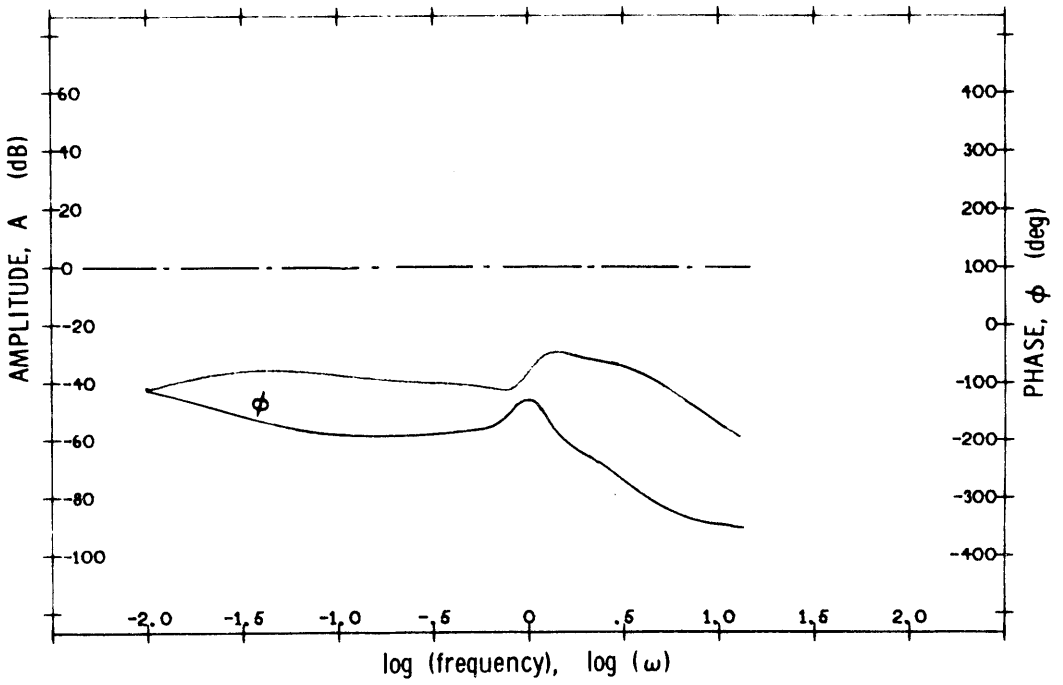

Fig. 5.16 Frequency Plot of $\frac{x_1}{\dot{x}_{2g}}$

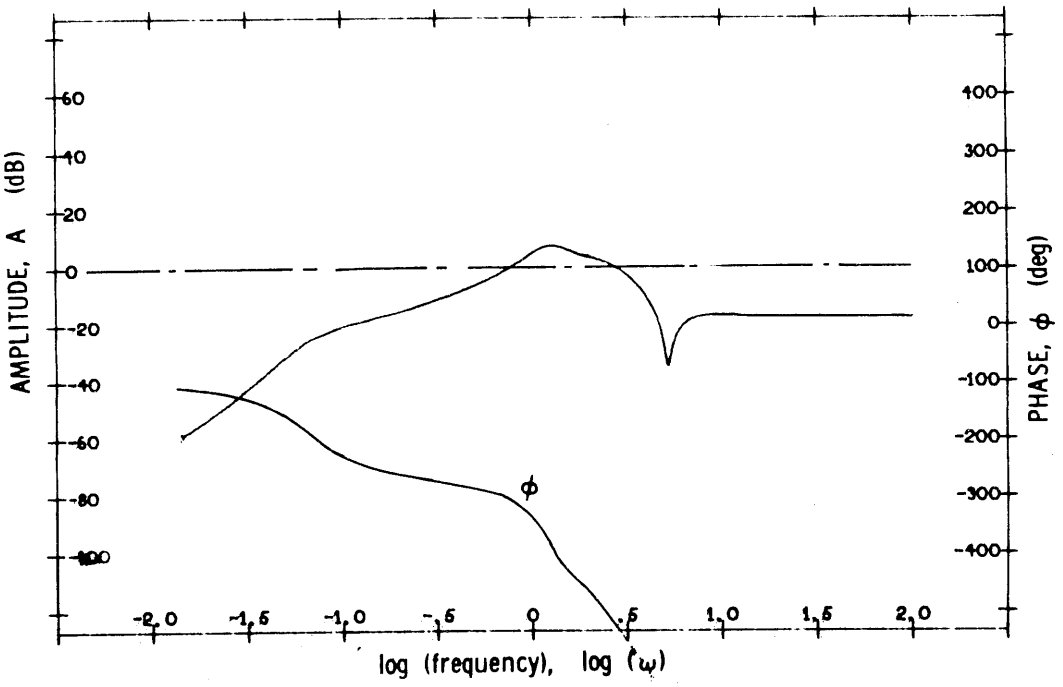

Fig. 5.17 Frequency Plot of $\frac{x_3}{x_{1g}}$

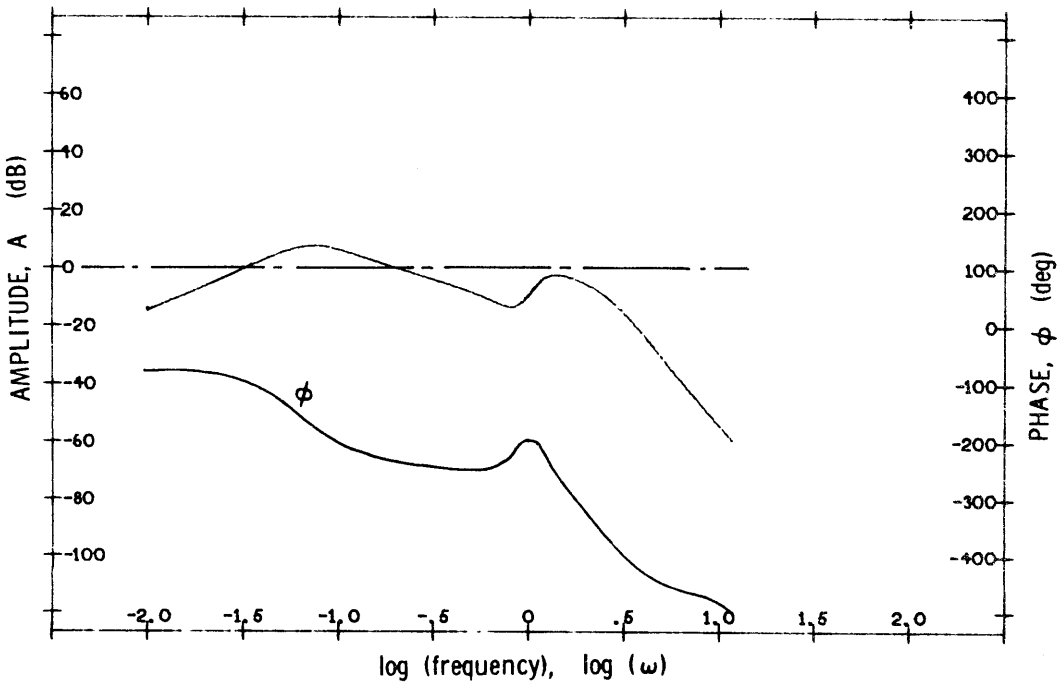

Fig. 5.18 Frequency Plot of $\frac{x_3}{\dot{x}_{2g}}$

For high altitudes, the statistical description of turbulence is greatly simplified over the near-ground description. This is due mostly to the assumption of isotropy at high altitudes, where the turbulence field characteristics are invariant with direction (Refs. 3 and 8). Also, this gust field possesses stationarity and homogeneity. Because the assumption of isotropy is valid, use can be made of the Dryden spectral model (Fig. 5.19), which gives the power spectral density as a function of spatial frequency (Ω), turbulence scale length (L), and root-mean-square value (σ). Taylor's hypothesis relates the component of spatial frequency along the flight path (Ω_x) to the angular frequency (ω) by,

$$\Omega_x = \frac{\omega}{V_o}$$

where V_o is the total forward velocity. For lateral-directional dynamics, the power spectral densities of interest are those for gust velocities normal to the flight path. The one-dimensional Dryden models (i.e., for spatial frequencies only along the flight path, Ω_x) are:

$$\Phi_{v_g v_g}(\Omega_x) = \frac{L}{\pi} \sigma_{v_g}^2 \frac{1+3L^2\Omega_x^2}{(1+L^2\Omega_x^2)^2} \tag{5.19}$$

$$\Phi_{w_g w_g}(\Omega_x) = \frac{L}{\pi} \sigma_{w_g}^2 \frac{1+3L^2\Omega_x^2}{(1+L^2\Omega_x^2)^2} \tag{5.20}$$

where σ_{v_g} = rms value of side velocity gust and σ_{w_g} = rms value of vertical velocity gust. Due to isotropy, $\sigma_{v_g}^2 = \sigma_{w_g}^2$. Also $L_{v_g} = L_{w_g} = L$. Thus, the spectra Eqs. (5.19) and (5.20) are exactly the same (at high altitudes) and Fig. 5.19 can be read as a plot of either.

Use is made of the fact that (as presented in Section 5.2) rotary gusts are due to spanwise distributions of linear velocity gusts, to obtain the power spectral density of p_g. The result is (Ref. 8, Section 3.7.5),

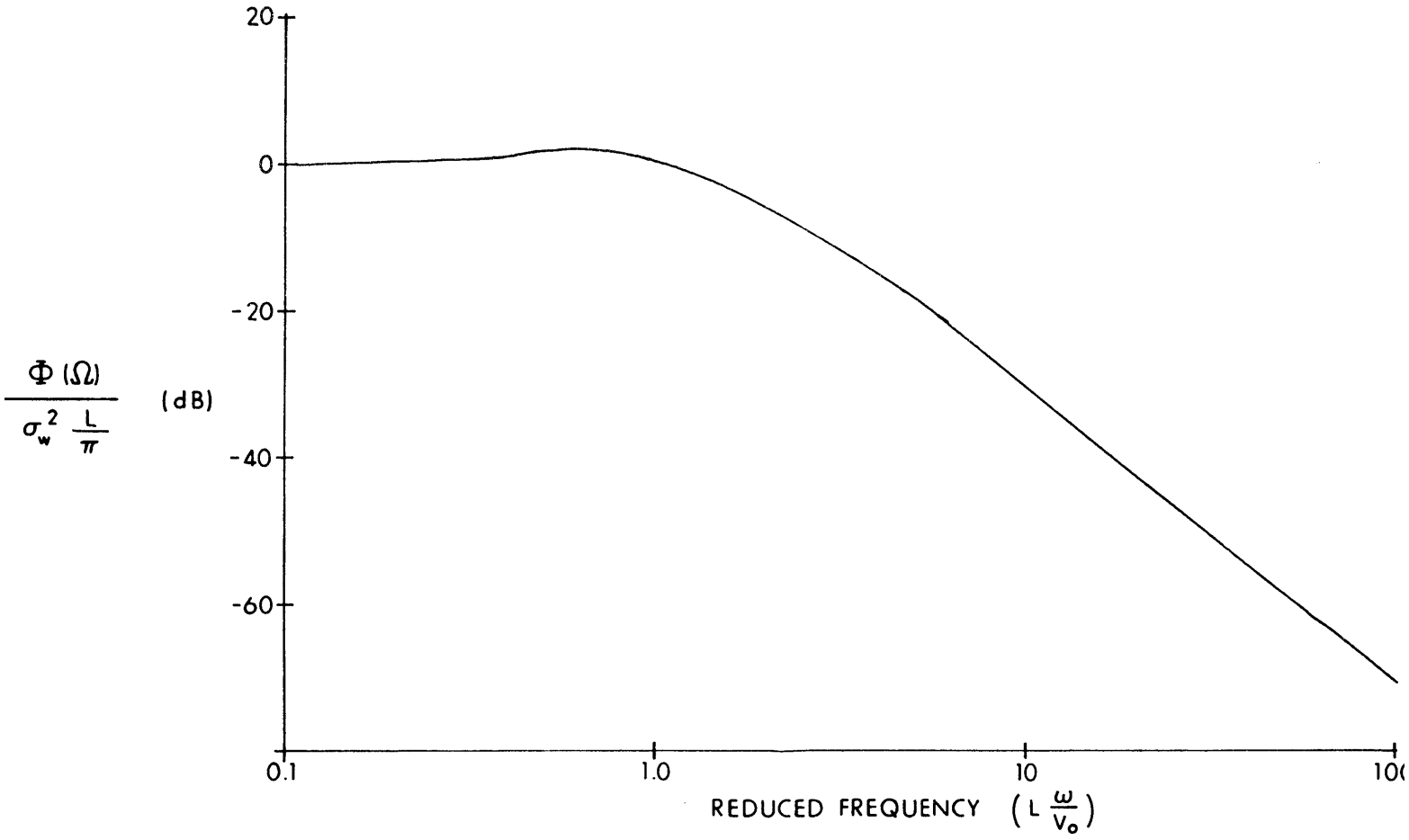

Fig. 5.19 Power Spectral Density — The Dryden Model

$$\Phi_{p_g p_g}(\Omega_x) = \frac{\sigma_{w_g}^2}{L_{w_g}} \frac{0.8\left(\frac{\pi L_{w_g}}{4b}\right)^{1/3}}{1 + \left(\frac{4b}{\pi}\Omega_x\right)^2} \tag{5.21}$$

where b = wing span.

Since $\Omega_x = \omega/V_o$, the conversion from spatial frequency to radian frequency is made by

$$\Phi_{ii}(\omega) = \frac{1}{V_o} \Phi_{ii}\left(\Omega = \frac{\omega}{V_o}\right). \tag{5.22}$$

The mean square turbulence value is then

$$\sigma_i^2 = \int_o^\infty \Phi_{ii}(\omega)\, d\omega. \tag{5.23}$$

Generally accepted values for this 5000 ft altitude flight condition were found to be σ = 5.7 ft/sec and L between 1750 ft and 2500 ft.* For a choice of L = 2000 ft, with the shuttle wingspan (b) = 73.5 ft, Eq. (5.22) gives:

$$\Phi_{p_g p_g}(\Omega) = \frac{.0360}{1 + 8757.8\,\Omega^2} \quad \text{ft/sec}^2$$

Using Eq. (5.22) finally,

$$\Phi_{p_g p_g}(\omega) = \frac{1}{V_o} \frac{.0360}{1 + 8757.8\left(\frac{\omega}{V_o}\right)^2} = \frac{.000090}{1 + (.2339\,\omega)^2} \quad \frac{\text{rad/sec}^2}{\text{rad/sec}} \tag{5.24}$$

This power spectral density is plotted in Fig. 5.20. It is seen that the

---

* See Ref. 8 and Saldana, "Gust Model for Digital SSV Landing Simulations", NASA MSC Memo EG2-71-182, 9/14/71.

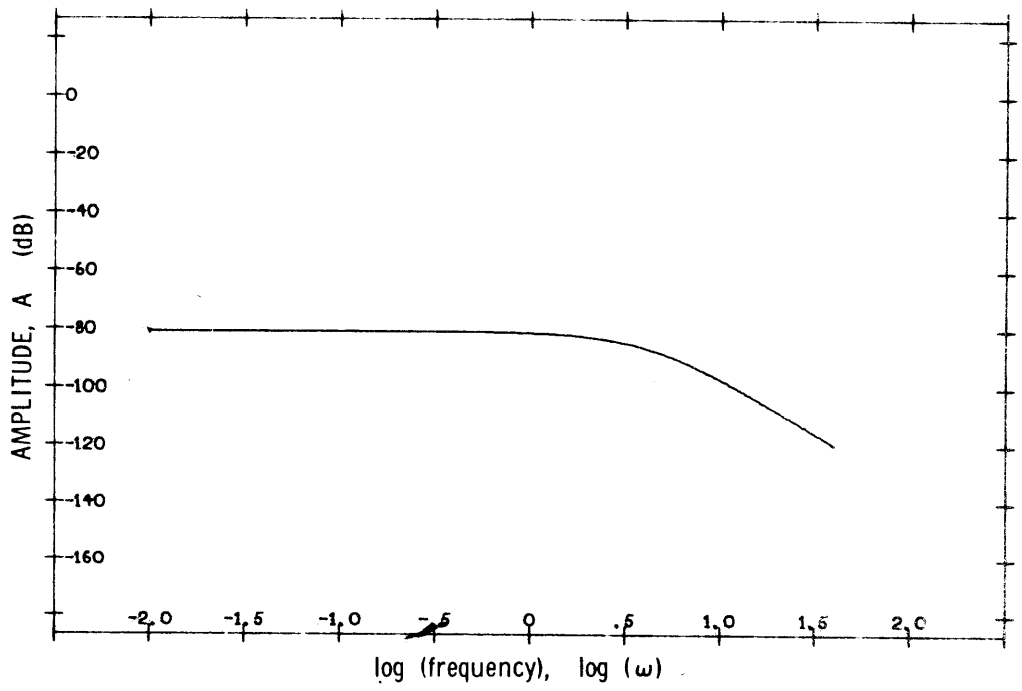

Fig. 5.20 Power Spectral Density of a Rolling Gust — $\Phi_{p_g p_g}$

power for this gust disturbance is contained in the very low frequencies (and even there the magnitude is extremely small) and drops off rapidly at frequencies above 4-6 rad/sec. Also, from Eq. (5.23),

$$\sigma_{p_g}^2 = \int_0^\infty 9 \times 10^{-5} \frac{d\omega}{1 + (.2339\,\omega)^2}$$

$$= 9 \times 10^{-5} \left[\frac{1}{.2339} \tan^{-1} .2339\,\omega \right]_0^\infty$$

$$\sigma_{p_g}^2 = 1.92\pi \times 10^{-4} \text{ (rad/sec)}^2 \tag{5.25}$$

These values for $\Phi_{p_g p_g}(\omega)$ and $\sigma_{p_g}^2$ seem to be sufficiently small to indicate that there is no significant influence in $\dot{\psi}$ due to p_g. However, in order to complete this analysis, using Eq. (5.18):

$$\Phi_{\dot{\psi}\dot{\psi}}(\omega) = \left[G_{\dot{\psi} p_g}(\omega) \Big|_{3CL} \right]^2 \frac{9 \times 10^{-5}}{1 + (.2339\,\omega)^2}.$$

Since $G_{\dot{\psi} p_g}(\omega)\Big|_{3CL}$ is a fairly complicated function of ω and since it has a peak in the frequency range of interest, a useful relationship is

$$\overline{\dot{\psi}^2} = \int_0^\infty |G_{\dot{\psi} p_g}(\omega)| \Phi_{p_g p_g}(\omega) d\omega \leq |G_{\dot{\psi} p_g}(\omega)|_{max}^2 \int_0^\infty \Phi_{p_g p_g}(\omega) d\omega$$

$$= |G_{\dot{\psi} p_g}(\omega)|_{max}^2 \sigma_{p_g}^2 .$$

Thus,

$$\overline{\dot{\psi}^2} \leq |G_{\dot{\psi} p_g}(\omega)|_{max}^2 \sigma_{p_g}^2 . \tag{5.26}$$

From Fig. 5.16,

$$|G_{\dot{\psi} p_g}(\omega)|_{max} = 2.12 \quad \text{at} \quad \omega = .07 \text{ rad/sec}$$

Therefore

$$\overline{\dot{\psi}^2} \leq (2.12)^2 (1.92\pi \times 10^{-4})$$

$$\overline{\dot{\psi}^2} \leq .00272 \text{ (rad/sec)}^2 \tag{5.27}$$

This amount of heading rate due to a roll rate gust is certainly small enough to be considered negligible in the system.

Although the transfer function $G_{\dot{\psi} \beta_g}$ is small at frequencies of interest, (see Fig. 5.17), it is still worthwhile to do the same frequency analysis for β_g inputs as done above for p_g inputs. Since, by definition $\beta_g = v_g/V_o$, then in terms of one-dimensional spectra (Ref. 8),

$$\Phi_{\beta_g \beta_g}(\Omega_x) = \frac{1}{V_o^2} \Phi_{v_g v_g}(\Omega_x)$$

and

$$\sigma_{\beta_g} = \frac{1}{V_o} \sigma_{v_g}.$$

Thus, using Eqs. (5.19) and (5.22),

$$\Phi_{p_g \beta_g}(\Omega_x) = \frac{L\sigma_{v_g}^2}{\pi V_o^2} \frac{1+3L^2\Omega_x^2}{(1+L^2\Omega_x^2)^2} \tag{5.28}$$

and

$$\Phi_{\beta_g \beta_g}(\omega) = \frac{L\sigma_{v_g}^2}{\pi V_o^3} \frac{1+3\left(\frac{L}{V_o}\right)^2 \omega^2}{\left(1+\left(\frac{L}{V_o}\right)^2 \omega^2\right)^2}. \tag{5.29}$$

Using the values given above for L and σ_{v_g},

$$\Phi_{\beta_g \beta_g}(\omega) = .000324 \frac{1 + 75\omega^2}{(1 + 25\omega^2)^2} \tag{5.30}$$

From above,

$$\sigma_{\beta_g} = \frac{1}{V_o} \sigma_{v_g} = .01425 \text{ rad} \tag{5.31}$$

Using the relationship

$$\overline{\dot{\psi}^2} \leq |G_{\dot{\psi}\beta_g}(\omega)|^2_{max} \sigma_{\beta_g}^2 \tag{5.32}$$

and, from Fig. 5.17,

$$|G_{\dot{\psi}\beta_g}(\omega)|_{max} = 2.29 .$$

The final result is

$$\overline{\dot{\psi}^2} \leq (2.29)^2 .01425$$

$$\overline{\dot{\psi}^2} \leq .0748 \text{ (rad/sec)}^2 \tag{5.33}$$

This amount of heading rate due to a sideslip gust is probably small enough to be neglected. It should be remembered that the $|G_{\dot{\psi}\beta_g}(\omega)|_{max}$ used above occurs at a frequency higher than the $\dot{\psi}$-loop bandwidth. Within this third loop bandwidth, $|G_{\dot{\psi}\beta_g}(\omega)|_{max} \approx .20$ and

$$\overline{\dot{\psi}^2} \leq (.20)^2 .01425$$

$$\overline{\dot{\psi}^2} \leq .00057 \text{ (rad/sec)}^2 \tag{5.34}$$

It is apparent that the heading rate due to a sideslip gust is a negligible quantity.

In summary, it is apparent that, for this lateral airplane dynamics example, the design procedure using exact decoupling has been quite successful. Also, due to the beneficial effect of the exact decoupling choice on the direct transfer functions G_{11}, G_{22}, G_{31}, and G_{32}, it might be expected that a choice for crossfeeds that was not exact decoupling might also be successful.

CHAPTER 6

SUMMARY AND CONCLUSIONS

The central aim in this thesis is to propose a procedure which will decouple (or nearly decouple) the outputs of a multiloop system and design that system to meet certain desired objectives. In order to accomplish the desired degree of decoupling, crossfeeds are used between the controls. The design procedure for coupled multiloop systems rests, to a great extent, on the successful selection of the crossfeeds. In fact, unless the crossfeeds achieve a desired reduction in coupling, the design procedure may not result in a "good" closed loop system.

Some general conclusions are drawn from a qualitative examination of the steps in the design procedure. These conclusions — which are validated throughout the thesis — specify that, if the open loop coupling between output x_i and control u_j is large at frequencies of interest for x_i, then the closed loop coupling in x_i due to a command x_{jc} may be large. Also, rules are established to guide the designer in the application of the design procedure. The most important of these rules state that the first loop to be closed should be a high frequency loop, and that the first loop transfer function should have high open loop gain.

Conclusions can be drawn as to desirable values for the open loop transfer functions after the crossfeeds are closed — the so called "new plant". Each step in the design procedure offers insight into what these desirable values might be. Table 4.1 summarizes these conclusions. The fact that this implies specifications on other than coupling transfer functions leads to additional demands on the crossfeeds. That is, since the crossfeeds affect all outputs of the plant, these effects (in addition to the effects on couplings) should be considered when choosing crossfeeds. Potential conflicts in selecting crossfeeds thus may arise. No general conclusions can be made as to when and where conflicts may occur.

Due to the potentially conflicting demands made on the crossfeeds, compromises in their design will often have to be made. However, in the application of the design procedure in Chapter 5, nearly all of the specifications of Table 4.1 were met remarkably well by the "exact decoupling" choice for the crossfeeds. In fact, it was seen that this choice of crossfeeds resulted in a plant which closely matched a pilot-rated "ideal" plant.

The application of the design procedure to the lateral control of the space shuttle resulted, not only in successful design in terms of the crossfeeds, but also in a very well-behaved closed loop system. That is, loop gains are high, stability is good, responses to commands are accurate, and responses to disturbance inputs are generally suppressed.

Since the results of the design procedure using the "exact decoupling" choice for the crossfeeds are so good, there is reason to believe that a choice of crossfeeds that was slightly different might also give good results. The investigation of such a choice for crossfeeds is the next logical step in this analysis. Also, since the "exact decoupling" choice can only be made if the plant parameters are precisely known and constant, a different choice for crossfeeds would be one method of determining how well the design procedure performs in the presence of parameter variations.

APPENDIX A

MULTILOOP ANALYSIS – USING "COUPLING NUMERATORS"

A method is derived in this Appendix for quickly finding closed loop transfer functions for multiloop systems. The method is based on applications of Cramer's rule to the determinant of state coefficients (the left hand side of Eq. (2.1)).

The technique to be developed for the general multiloop vehicular control system shown in Fig. A.1 follows Ashkenas, McRuer, and Graham and consists of a vehicle and control equipment, including sensing, equalization and actuating elements. For this system, the Laplace-transformed linearized vehicle equations of motion, in matrix form, are

$$\begin{bmatrix} a_{11} & a_{12} & a_{13} \\ a_{21} & a_{22} & a_{23} \\ a_{31} & a_{32} & a_{33} \end{bmatrix} \begin{bmatrix} x_1 \\ x_2 \\ x_3 \end{bmatrix} = \begin{bmatrix} b_{11} & b_{12} \\ b_{21} & b_{22} \\ b_{31} & b_{32} \end{bmatrix} \begin{bmatrix} u_1 \\ u_2 \end{bmatrix} + \begin{bmatrix} c_{11} & c_{12} & c_{13} \\ c_{21} & c_{22} & c_{23} \\ c_{31} & c_{32} & c_{33} \end{bmatrix} \begin{bmatrix} x_{1_d} \\ x_{2_d} \\ x_{3_d} \end{bmatrix} \tag{A.1}$$

or

$$A(s)\underline{x}(s) = B(s)\underline{u}(s) + c(s)\underline{x}_d(s) \tag{A.2}$$

where a, b, and c are functions of the Laplace operator, s, and the vehicle stability derivatives. A is defined as the "coefficient matrix of motion variables" and $\underline{u}$ is a matrix of control inputs.

Consider a simple two-input, two-output example of the technique to be used. From Fig. A.1, ignoring disturbances $\underline{x}_d$ for simplicity, the equations of motion may be written:

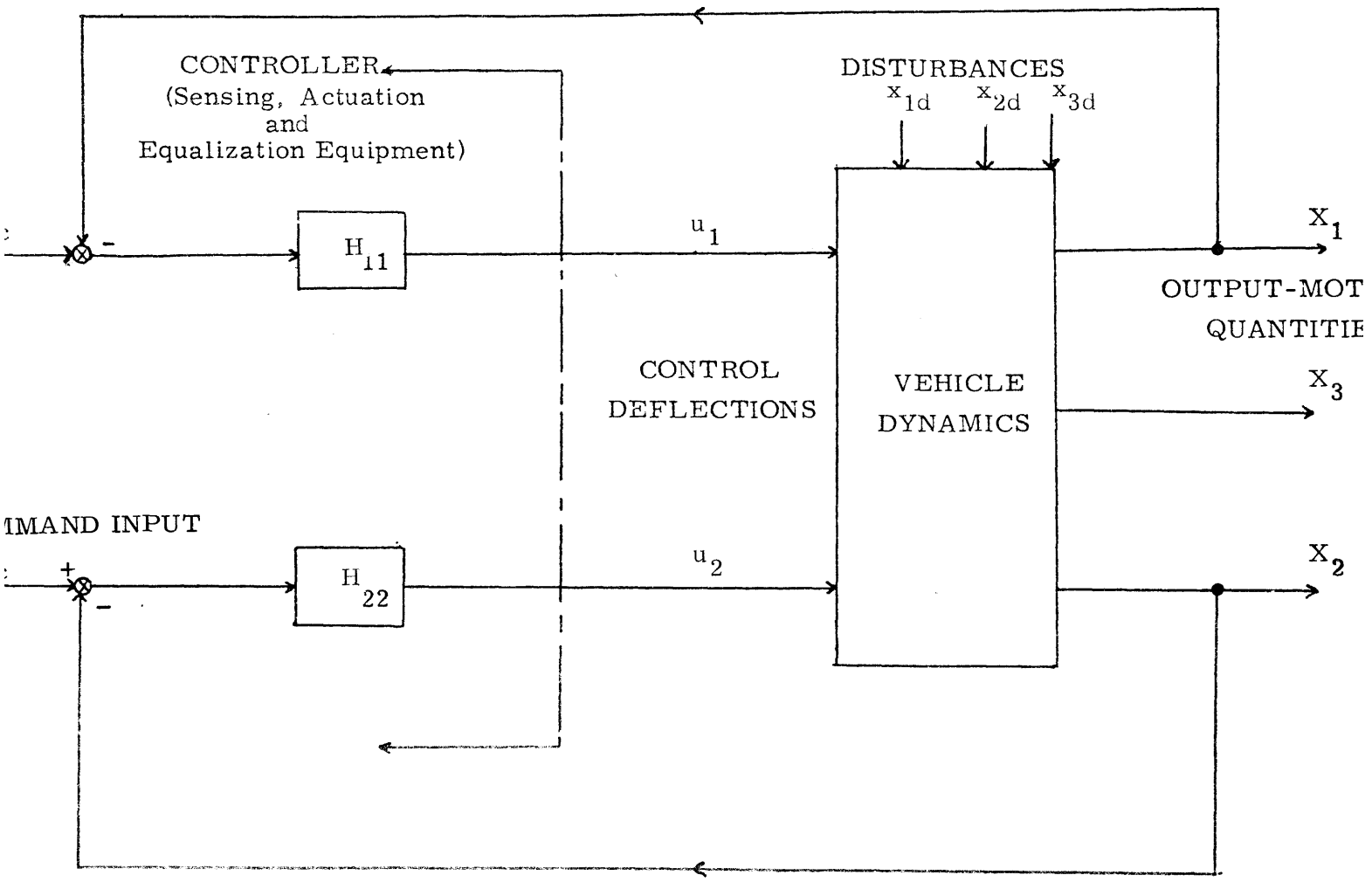

Figure A. 1. MULTILOOP VEHICULAR CONTROL SYSTEM

(From Ashkenas, McRuer, Graham, p. 3-62)

$$\begin{bmatrix} a_{11} & a_{12} \\ a_{21} & a_{22} \end{bmatrix} \begin{bmatrix} x_1 \\ x_2 \end{bmatrix} = \begin{bmatrix} b_{11} & b_{12} \\ b_{21} & b_{22} \end{bmatrix} \begin{bmatrix} u_1 \\ u_2 \end{bmatrix} \tag{A.3}$$

or

$$\begin{aligned} a_{11}x_1 + a_{12}x_2 &= b_{11}u_1 + b_{12}u_2 \\ a_{21}x_1 + a_{22}x_2 &= b_{21}u_1 + b_{22}u_2 \end{aligned} \tag{A.4}$$

Open loop transfer functions are obtained from these equations by a simple application of Cramer's rule. That is,

$$G_{11} = \frac{x_1}{u_1} = \frac{\begin{vmatrix} b_{11} & a_{12} \\ b_{21} & a_{22} \end{vmatrix}}{\begin{vmatrix} a_{11} & a_{12} \\ a_{21} & a_{22} \end{vmatrix}} = \frac{N_{u_1}^{x_1}}{\Delta}, \quad G_{21} = \frac{x_2}{u_1} = \frac{\begin{vmatrix} a_{11} & b_{11} \\ a_{21} & b_{21} \end{vmatrix}}{\begin{vmatrix} a_{11} & a_{12} \\ a_{21} & a_{22} \end{vmatrix}} = \frac{N_{u_1}^{x_2}}{\Delta}, \text{ etc.}$$

Also, from Fig. A.1, by inspection

$$u_1 = -H_{11}x_1 \qquad u_2 = -H_{22}x_2$$

where H_{ij} is a feedback matrix for the loop $x_j \rightarrow u_i$ including gain and equalization.

If we first close the upper loop ($x_1 \rightarrow u_1$) in Fig. A.1, then we may substitute $-H_{11}x_1$ for u_1 in the equation of motion (A.4):

$$\begin{aligned} a_{11}x_1 + a_{12}x_2 &= -b_{11}H_{11}x_1 + b_{12}u_2 \\ a_{12}x_1 + a_{22}x_2 &= -b_{21}H_{11}x_1 + b_{22}u_2 \end{aligned} \tag{A.5}$$

These equations represent the vehicle equations of motion with the first loop ($x_1 \rightarrow u_1$) closed.

Rearranging Eq. (A.5):

$$(a_{11} + b_{11}H_{11})x_1 + a_{12}x_2 = b_{12}u_2$$
$$(a_{21} + b_{21}H_{11})x_1 + a_{22}x_2 = b_{22}u_2 \qquad \text{(A.6)}$$

Now a straightforward application of Cramer's rule yields the open-loop transfer function for the second loop ($x_2 \rightarrow u_2$) with the first loop closed.

$$\left.\frac{x_2}{u_2}\right|_{x_1 \rightarrow u_1} = \frac{\begin{vmatrix} a_{11} + b_{11}H_{11} & b_{12} \\ a_{21} + b_{21}H_{11} & b_{22} \end{vmatrix}}{\begin{vmatrix} a_{11} + b_{11}H_{11} & a_{12} \\ a_{21} + b_{21}H_{11} & a_{22} \end{vmatrix}} \qquad \text{(A.7)}$$

Equation (A.7) can be rewritten with the aid of the following rules of determinants:

1. If each element in one column is expressed as the sum of two terms, then the determinant is equal to the sum of two determinants, in each of which one of the two terms is deleted in every element of that column.

2. If all elements of one column of a square matrix are multiplied by a number k, the determinant is multiplied by k.*

The application of these rules results in:

$$\left.\frac{x_2}{u_2}\right|_{x_1 \rightarrow u_1} = \frac{\begin{vmatrix} a_{11} & b_{12} \\ a_{21} & b_{22} \end{vmatrix} + H_{11}\begin{vmatrix} b_{11} & b_{12} \\ b_{21} & b_{22} \end{vmatrix}}{\begin{vmatrix} a_{11} & a_{12} \\ a_{21} & a_{22} \end{vmatrix} + H_{11}\begin{vmatrix} b_{11} & a_{12} \\ b_{21} & a_{22} \end{vmatrix}} \qquad \text{(A.8)}$$

* Francis B. Hildebrand, Methods of Applied Mathematics, second ed., (Englewood Cliffs, N. J.). p. 10.

It will be helpful at this point to define a convenient shorthand notation for determinants to be used throughout.

$N_{u_i}^{x_j}$ ≡ a numerator, obtained by replacing the j^{th} column of the coefficient matrix (A) by the column of u_i coefficients from the right hand side of Eq. (A.3).

Δ ≡ $|A|$; the characteristic determinant; that is, the determinant of the coefficients of the lefthand side of Eq. (A.3).

$N_{u_i u_k}^{x_j x_\ell}$ ≡ a "coupling numerator", obtained by replacing both the j^{th} and ℓ^{th} columns of the coefficient matrix by the columns of u_i and u_k coefficients respectively from the right hand side of Eq. (A.3).

$N_{u_i u_k x_{d_m}}^{x_j x_\ell x_n}$ ≡ a possible "type-two coupling numerator", obtained by replacing the j^{th}, ℓ^{th} and n^{th} columns of the coefficient matrix by the columns of u_i, u_k, and x_{d_m} coefficients respectively from the right hand side of Eq. (A.2).

Note that, by the rules of determinants, an important simplification often occurs. The determinant of any matrix with two equal columns is equal to zero. Thus, for instance,

$$N_{u_1 u_1}^{x_2 x_3} \equiv 0, \quad \text{or} \quad N_{u_1 u_2 u_2}^{x_2 x_1 x_3} \equiv 0, \quad \text{or} \quad N_{u_1 u_2}^{x_2 x_2} \equiv 0, \quad \text{etc.}$$

Using this notation, the above transfer function can be rewritten directly as:

$$\left.\frac{x_2}{u_2}\right|_{x_1 \to u_1} = \frac{N_{u_2}^{x_2} + H_{11} N_{u_1 u_2}^{x_1 x_2}}{\Delta + H_{11} N_{u_1}^{x_1}} \qquad (A.9)$$

The next step is to close the second loop and repeat the above procedure in order to obtain a transfer function for the system with both loops closed.

From the block diagram of Fig. A.1, the following equation for the controller characteristics may be written:

$$\begin{bmatrix} u_1 \\ u_2 \end{bmatrix} = \begin{bmatrix} 0 & 0 \\ 0 & H_{22} \end{bmatrix} \begin{bmatrix} x_{1c} \\ x_{2c} \end{bmatrix} - \begin{bmatrix} H_{11} & 0 \\ 0 & H_{22} \end{bmatrix} \begin{bmatrix} x_1 \\ x_2 \end{bmatrix}$$

$$\underline{u} = H(\underline{x}_x - \underline{x}) \tag{A.10}$$

Substituting Eq. (A.10) into the equations of motion Eq. (A.6) for the first loop closed and using Cramer's rule together with rules 1 and 2 of determinants as above, results in the transfer function

$$\left.\frac{x_2}{x_{2c}}\right|_{\substack{x \to u_1 \\ x \to u_2}}.$$

The steps are:

equations of motion:

$$\begin{aligned} (a_{11} + b_{11}H_{11})x_1 + a_{12}x_2 &= b_{12}u_2 \\ (a_{21} + b_{21}H_{11})x_1 + a_{22}x_2 &= b_{22}u_2 \end{aligned} \tag{A.6}$$

Substituting $u_2 = H_{22}(x_{2c} - x_2)$:

$$\begin{aligned} (a_{11} + b_{11}H_{11})x_1 + (a_{12} + b_{12}H_{22})x_2 &= b_{12}H_{22}x_{2c} \\ (a_{21} + b_{21}H_{11})x_1 + (a_{22} + b_{22}H_{22})x_2 &= b_{22}H_{22}x_{2c} \end{aligned} \tag{A.11}$$

Then, by Cramer's rule:

$$\left.\frac{x_2}{x_{2c}}\right|_{\substack{x_1 \to u_1 \\ x_2 \to u_2}} = \frac{\begin{vmatrix} a_{11} + b_{11}H_{11} & b_{12}H_{22} \\ a_{21} + b_{21}H_{11} & b_{22}H_{22} \end{vmatrix}}{\begin{vmatrix} a_{11} + b_{11}H_{11} & a_{12} + b_{12}H_{22} \\ a_{21} + b_{21}H_{11} & a_{22} + b_{22}H_{22} \end{vmatrix}} \qquad \text{(A.12)}$$

$$= \frac{H_{22}\begin{vmatrix} a_{11} & b_{12} \\ a_{21} & b_{22} \end{vmatrix} + H_{22}H_{11}\begin{vmatrix} b_{11} & b_{12} \\ b_{21} & b_{22} \end{vmatrix}}{\begin{vmatrix} a_{11} & a_{12} \\ a_{21} & a_{22} \end{vmatrix} + H_{11}\begin{vmatrix} b_{11} & a_{12} \\ b_{21} & a_{22} \end{vmatrix} + H_{22}\begin{vmatrix} a_{11} & b_{12} \\ a_{21} & b_{22} \end{vmatrix} + H_{11}H_{22}\begin{vmatrix} b_{11} & b_{12} \\ b_{21} & b_{22} \end{vmatrix}} \qquad \text{(A.13)}$$

Finally,

$$\left.\frac{x_2}{x_{2c}}\right|_{\substack{x_1 \to u_1 \\ x_2 \to u_2}} = \frac{H_{22}\left(N_{u_2}^{x_2} + H_{11}N_{u_1u_2}^{x_1x_2}\right)}{\Delta + H_{11}N_{u_1}^{x_1} + H_{22}N_{u_2}^{x_2} + H_{11}H_{22}N_{u_1u_2}^{x_1x_2}} \qquad \text{(A.14)}$$

We should be reminded that the numerator and denominator of Eq. (A.14), despite having terms that we know, are not yet polynomials. The terms are matrices or ratios. Obtaining the actual numerator and denominator polynomials involves expanding the determinants of the various numerator matrices (N) and cross multiplying the numerator and denominator terms of the compensation functions (H). In particular, this means that the poles of the feedback transfer function (H_{ij}) appear as zeros of the closed loop transfer function.

Naturally this simple two-loop example can be generalized to an n-loop system with m inputs and ℓ outputs.

It would be desirable to be able to write all the terms of the transfer function of the final loop closure without going through the intermediate steps outlined above. This is, in fact, possible to do, by first noticing the apparent pattern of the numerator and denominator terms in Eq. (A.14).

Generalizing from this pattern the following rules may be stated for writing the numerator and denominator terms of the closed-loop transfer function of the n^{th} loop of a multiloop system:

1. The effective denominator is equal to:
   a. The open-loop denominator,
   b. Plus the sum of all the feedback transfer functions, each one multiplied by the appropriate numerator,
   c. Plus the sum of all the feedback transfer functions taken two at a time, each pair multiplied by the appropriate coupling numerator,
   d. Plus the sum of all the feedback transfer functions taken three at a time, each combination multiplied by the appropriate type-two coupling numerator, etc.
2. The effective numerator is equal to:
   a. The open-loop numerator,
   b. Plus the sum of all the feedback transfer functions, each one multiplied by the appropriate coupling numerator,
   c. Plus the sum of all the feedback transfer functions taken two at a time, each pair multiplied by the appropriate type-two coupling numerator, etc.

Looking at the transfer function x_2/x_{2c} again, we can write:

$$\frac{x_2}{x_{2c}} = \frac{H_{22}(N_{u_2}^{x_2} + H_{11} N_{u_1 u_2}^{x_1 x_2})}{\Delta + H_{11} N_{u_1}^{x_1} + H_{22} N_{u_2}^{x_2} + H_{11} H_{22} N_{u_1 u_2}^{x_1 x_2}}$$

$$= \frac{H_{22} \dfrac{N_{u_2}^{x_2}}{\Delta} \left(1 + H_{11} \dfrac{N_{u_1 u_2}^{x_1 x_2}}{N_{u_2}^{x_2}}\right)}{1 + H_{11} \dfrac{N_{u_1}^{x_1}}{\Delta} + H_{22} \dfrac{N_{u_2}^{x_2}}{\Delta} \left(1 + H_{11} \dfrac{N_{u_1 u_2}^{x_1 x_2}}{N_{u_2}^{x_2}}\right)}$$

$$= \frac{H_{22} N}{D + N}. \qquad \text{(A.15)}$$

This clearly shows that this closed-loop transfer function follows from a root locus of N/D — the transfer function of the first loop closure. That is, x_2/x_{2c} is the closed-loop transfer function corresponding to the open loop N/D.

While the application of this procedure to analysis is apparent, its utility in the design of multiloop systems should not be overlooked. The design of an outer loop after inner loops have been closed is handled with considerable ease by this method. Also the design complexities involved in adding to a control system with one input u_1, a second input u_2, are somewhat alleviated by this method.

APPENDIX B

PARAMETER PLOT

Any quantity which possesses both magnitude and phase must follow vector rules for addition and subtraction. If, for instance, the magnitudes of two vectors are the same but their phase angles are quite different, the difference of these two vectors could be substantial. Similarly, for a large phase angle difference, the sum of two vectors with large magnitudes could be quite small.*

In order to compare relative sizes of transfer functions, which possess both magnitude and phase, the parameter plot (Fig. B.1) is presented. The following vector diagram indicates the notation used on the included plot. The parameter plot shows the magnitude V and phase θ of the difference of two vectors (transfer functions) $\underline{M}_1$ and $\underline{M}_2$ as functions of the ratio (parameter) $M_1/M_2 = P$, and the phase difference $\phi = \phi_{\underline{M}_1} - \phi_{\underline{M}_2}$. The plot is presented in polar coordinates.

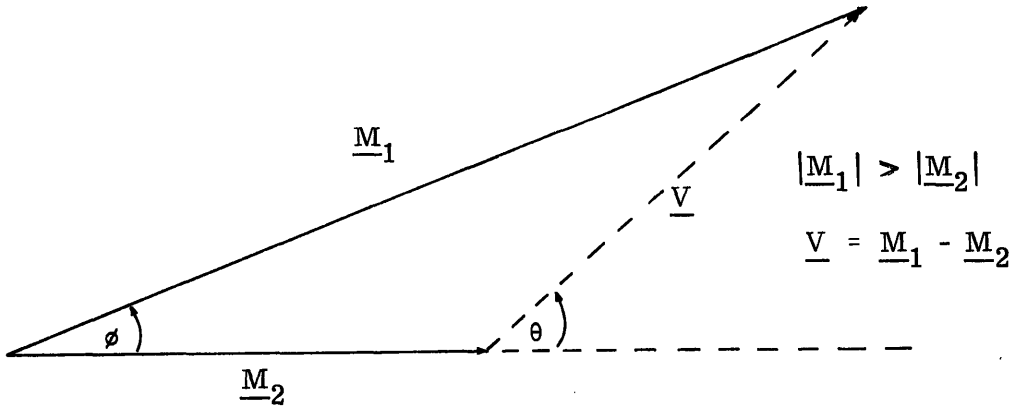

Figure B.1 Vector Diagram for the Parameter Plot

* For transfer functions, it is found that the main contributor to large phase differences is the presence of right-half plane factors in one of the transfer functions.

Briefly, the parameter plot is generated by using trigonometric relations for Fig. B.1. The result is just a plot of the law of cosines. That is,

$$V^2 = P^2 + 1 - 2P \cos \phi \tag{B.1}$$

$$\theta = \tan^{-1} \left(\frac{\sin \phi}{\cos \phi - P} \right) \tag{B.2}$$

Lines of constant V are the dashed lines while the solid lines are lines of constant θ.

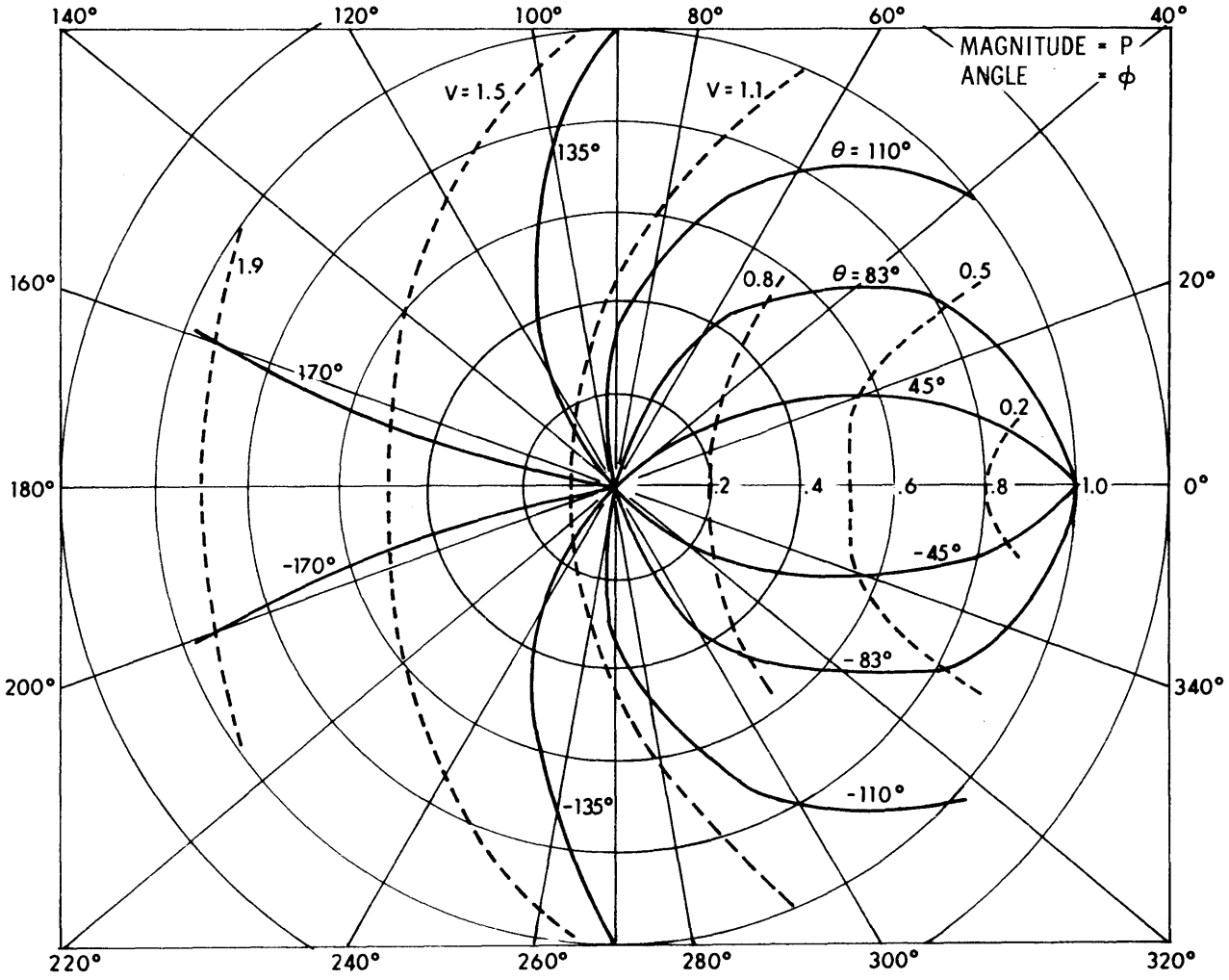

Fig. B.1 Parameter Plot

APPENDIX C

LATERAL AERODYNAMIC DATA FOR THE NASA MSC 040A SPACE SHUTTLE ORBITER

This Appendix presents the data used for the application problem for this thesis. The transfer functions were generated from data for the NASA MSC 040A space shuttle orbiter* for a cruise flight condition of 5000 ft. altitude and V = 392 ft/sec, using linearized perturbation equations of motion.

The open loop transfer functions, gust input transfer functions, and coupling numerators (see Appendix A), derived from linearized lateral perturbation equations of motion, are as follows.
Open loop transfer functions:

$$G_{11} = G_{\beta\delta r} = .0486\,[(s + .00129)(s + .82156)(s + 30.365)]/\Delta$$

$$G_{12} = G_{\beta\delta a} = -.0166\,[(s + .4541)(s + .1654)(s + 108.33)]/\Delta$$

$$G_{21} = G_{\phi\delta r} = 3.57[(s - .8671)(s + 1.0411)]/\Delta$$

$$G_{22} = G_{\phi\delta a} = -11.7\,[(s + .1913 + j.8170)(s + .1913 - j.8170)]/\Delta$$

$$G_{31} = G_{\dot{\psi}\delta r} = -.938[(s+.7306)(s+.2359+j.5780)(s+.2359-j.5780)]/\Delta$$

$$G_{32} = G_{\dot{\psi}\delta a} = .0229[(s+.5629)(s+4.9615)(s-10.2607)]/\Delta$$

Gust input transfer function:

---

* David W. Gilbert, "Proposed Near-term Test Schedule and Math Model to support MSC 040A Configuration on the CRALS", NASA MSC Memo EG 6-71-107, October 29, 1971.

$$G_{11g} = G_{\beta\beta_g} = -.1138[(s+.0345)(s+.7121)(s+14.715)]/\Delta$$

$$\frac{1}{s}G_{12g} = G_{\beta p_g} = -.16443[(s+.5008)(s+.1384)]/\Delta$$

$$G_{21g} = G_{\phi\beta_g} = .001998[(s-.000354)(s+.2203)(s-3092.5)]/\Delta$$

$$\frac{1}{s}G_{22g} = G_{\phi p_g} = -1.0275[(s+.1934+j.7843)(s+.1934-j.7893)]/\Delta$$

$$G_{31g} = G_{\dot{\psi}\beta_g} = -.1396[(s-.000549)(s-.1276)(s+.8815)(s-4.426)]/\Delta$$

$$\frac{1}{s}G_{32g} = G_{\dot{\psi}p_g} = .01072[(s+.5586)(s+2.8215)(s-3.1285)]/\Delta$$

where

$$\Delta = (s+.03497)(s+.78056)(s+.3021+j1.1905)(s+.3021-j1.1905)$$

Coupling numerators:

$$N^{x_1x_2}_{u_1u_2} = N^{\beta\ \phi}_{\delta_r\delta_a} = -.5130\,(+21.2014)$$

$$N^{x_1x_3}_{u_1u_2} = N^{\beta\ \dot{\psi}}_{\delta_r\delta_a} = -.0144\,(s+.5434)(s+114.70)$$

$$N^{x_3x_2}_{u_1u_2} = N^{\dot{\psi}\ \phi}_{\delta_r\delta_a} = 10.95\,(s+.21125)$$

Frequency responses for the open loop control and gust input transfer functions are presented in Figs. C.1-C.12.

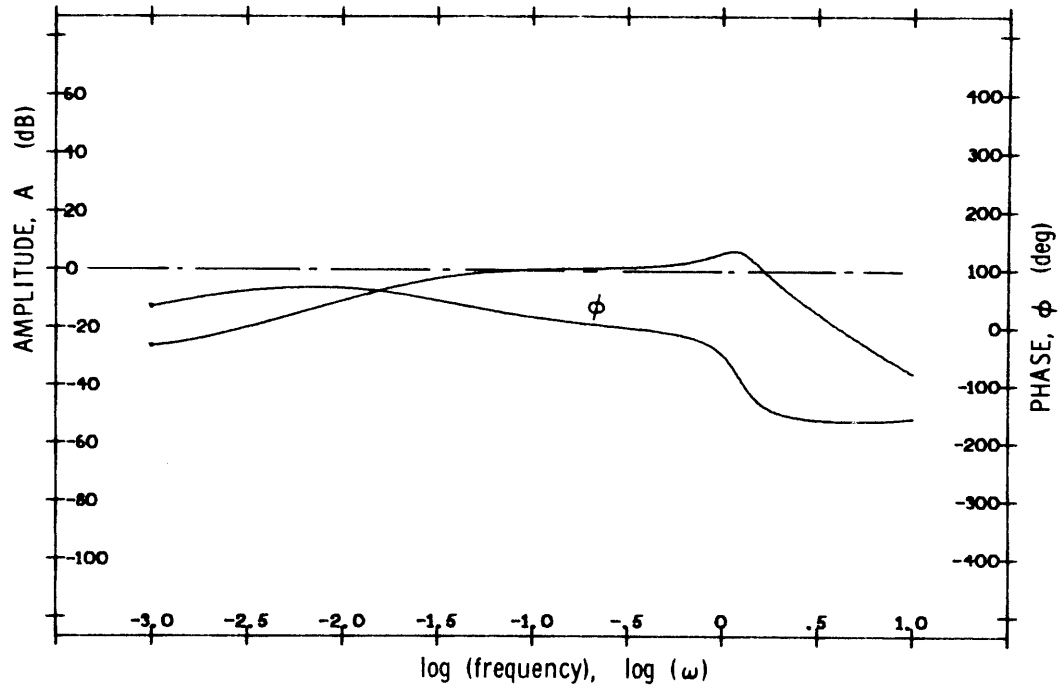

Fig. C.1 Frequency Plot of G_{11}

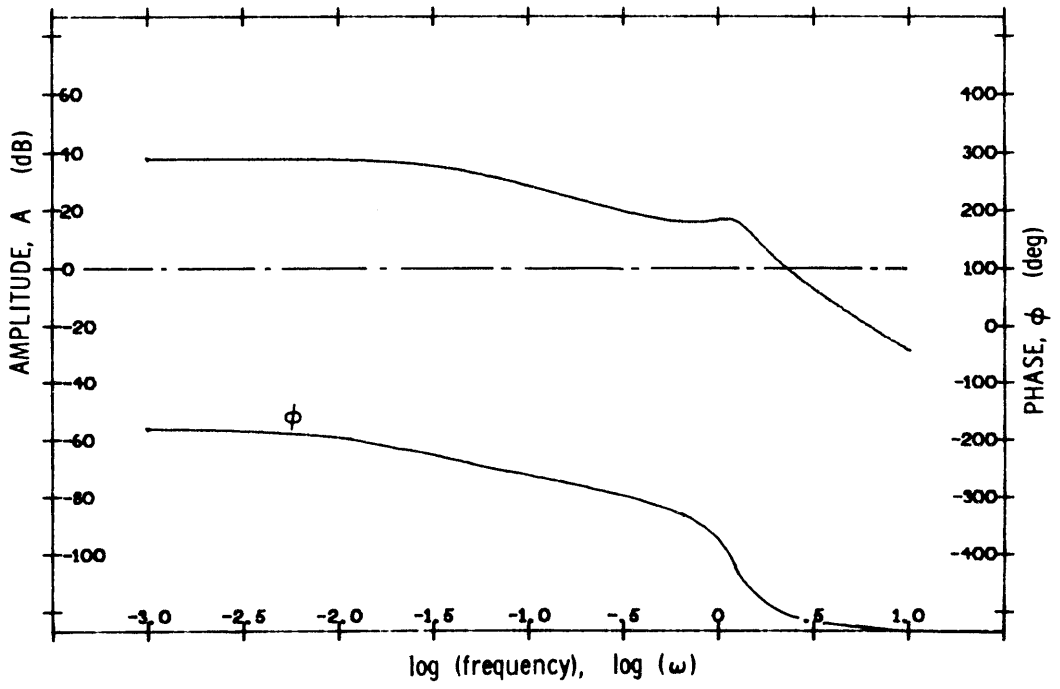

Fig. C.2 Frequency Plot of G_{21}

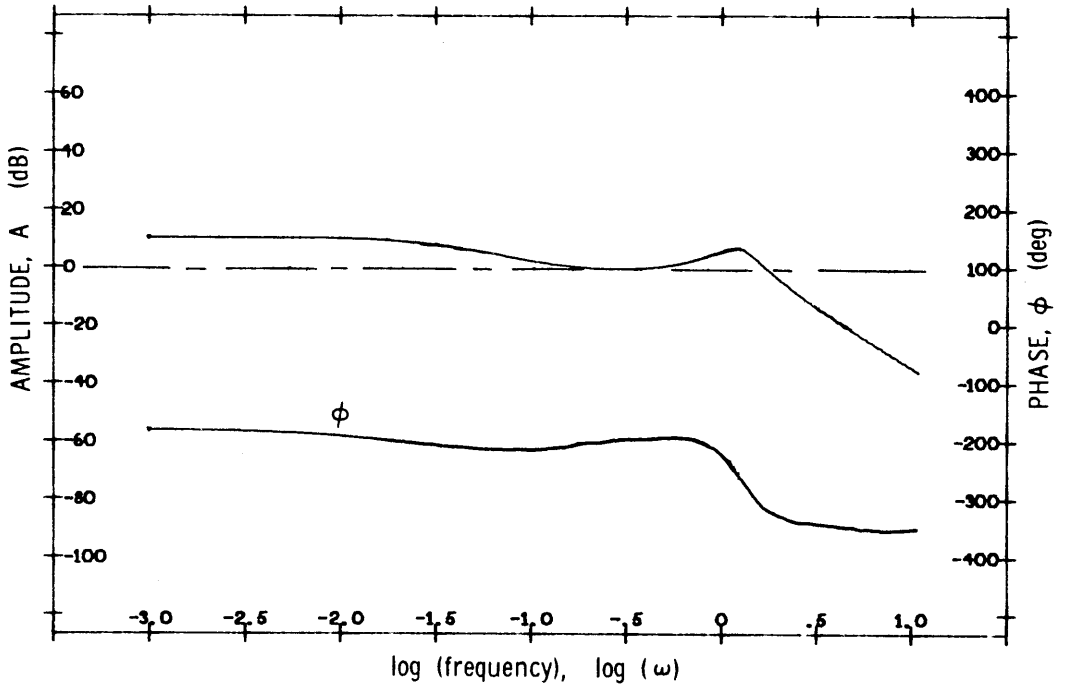

Fig. C.3 Frequency Plot of G_{12}

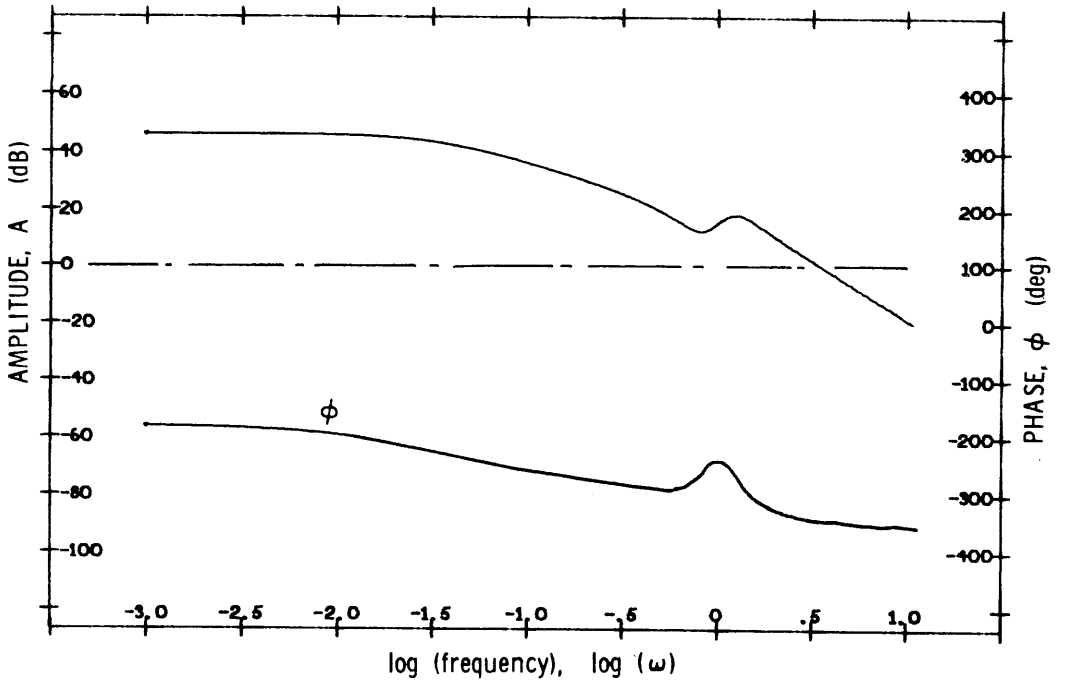

Fig. C.4 Frequency Plot of G_{22}

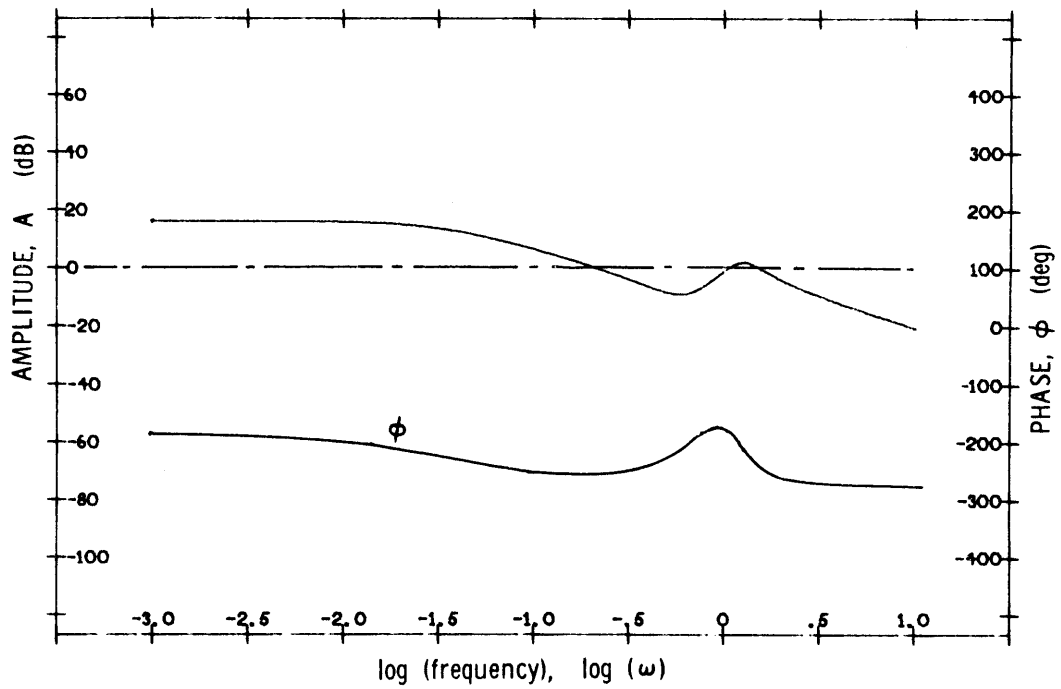

Fig. C.5 Frequency Plot of G_{31}

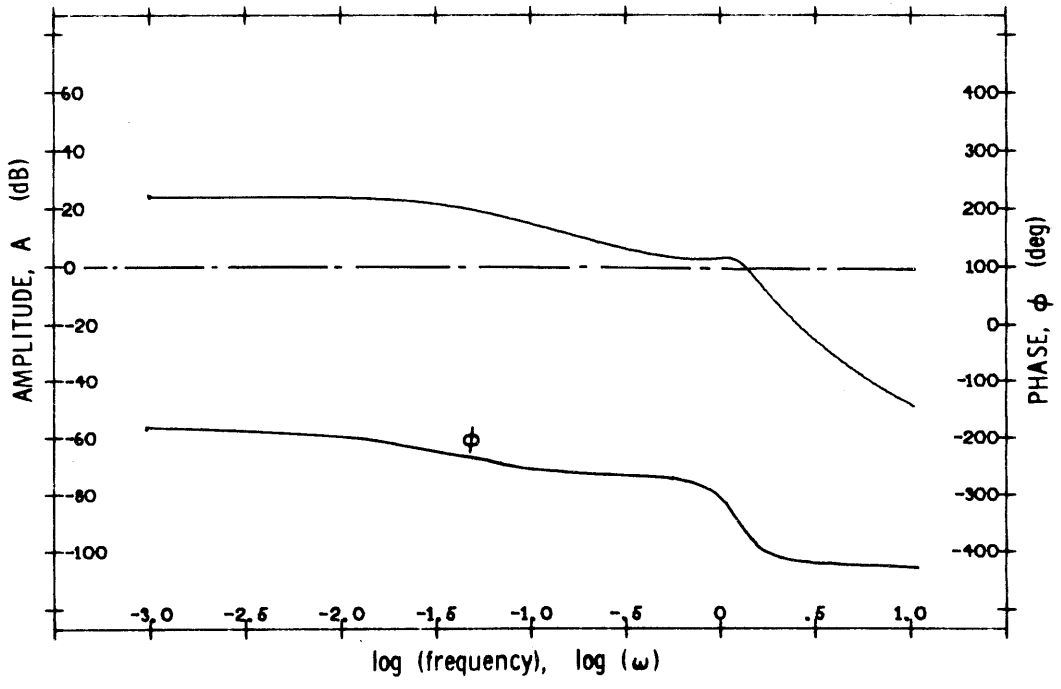

Fig. C.6 Frequency Plot of G_{32}

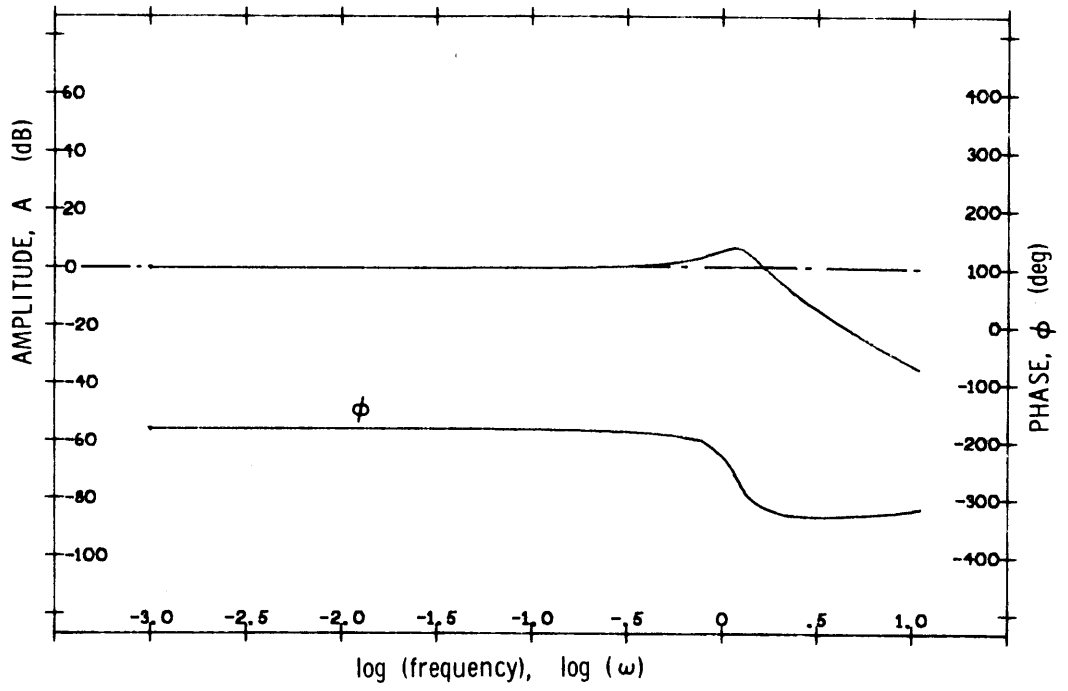

Fig. C. 7 Frequency Plot of G_{11g}

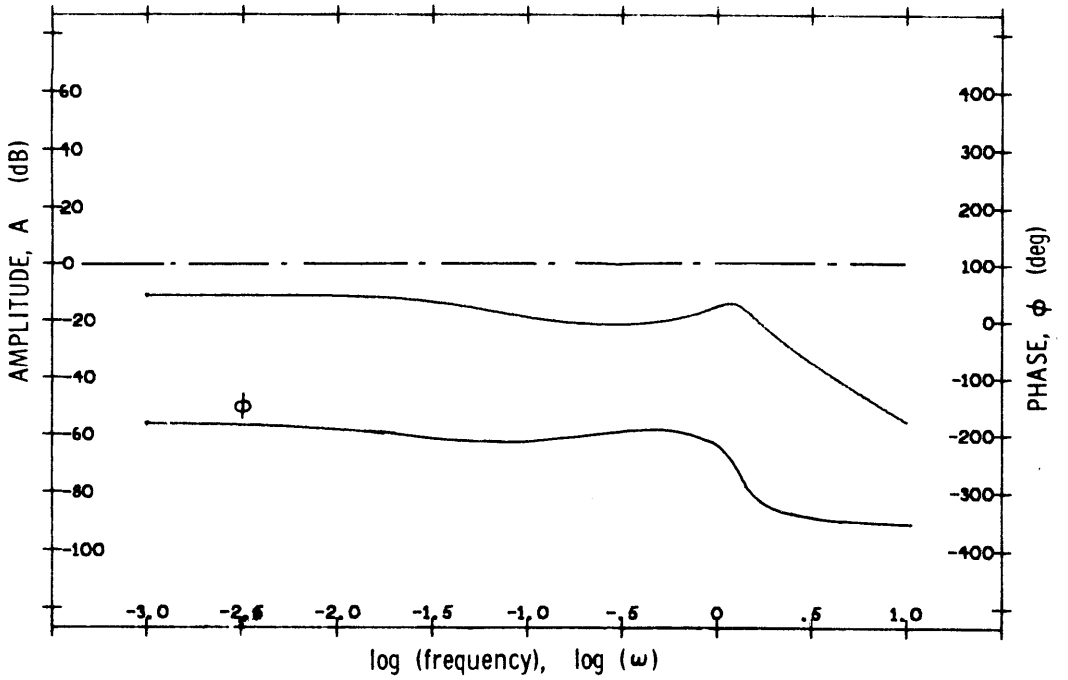

Fig. C. 8 Frequency Plot of G_{12g}/s

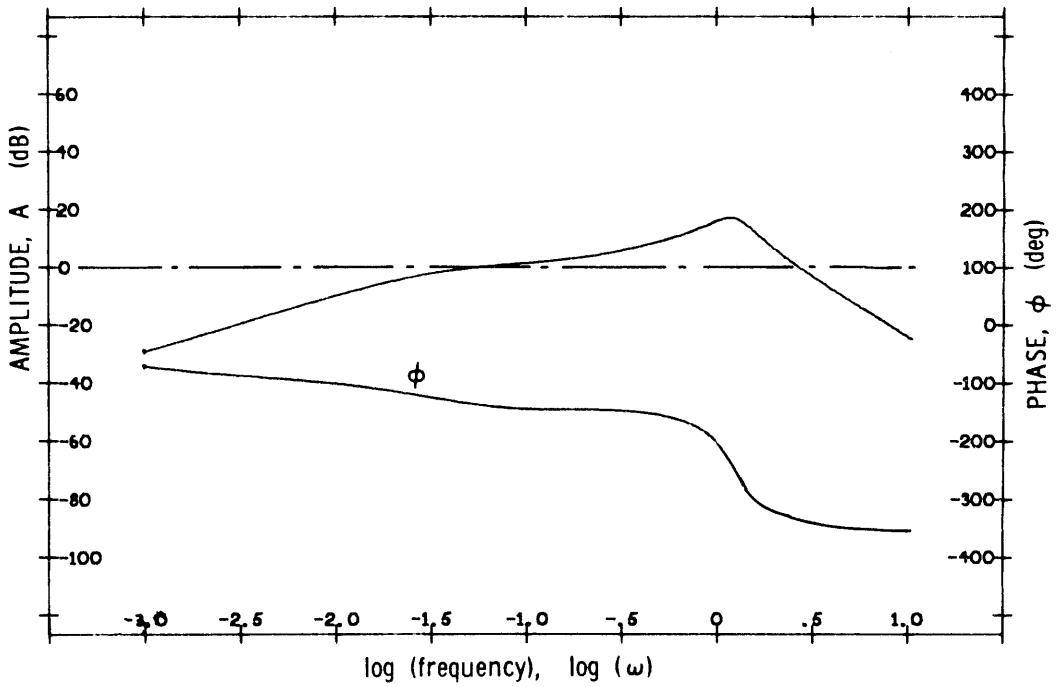

Fig. C.9 Frequency Plot of G_{21g}

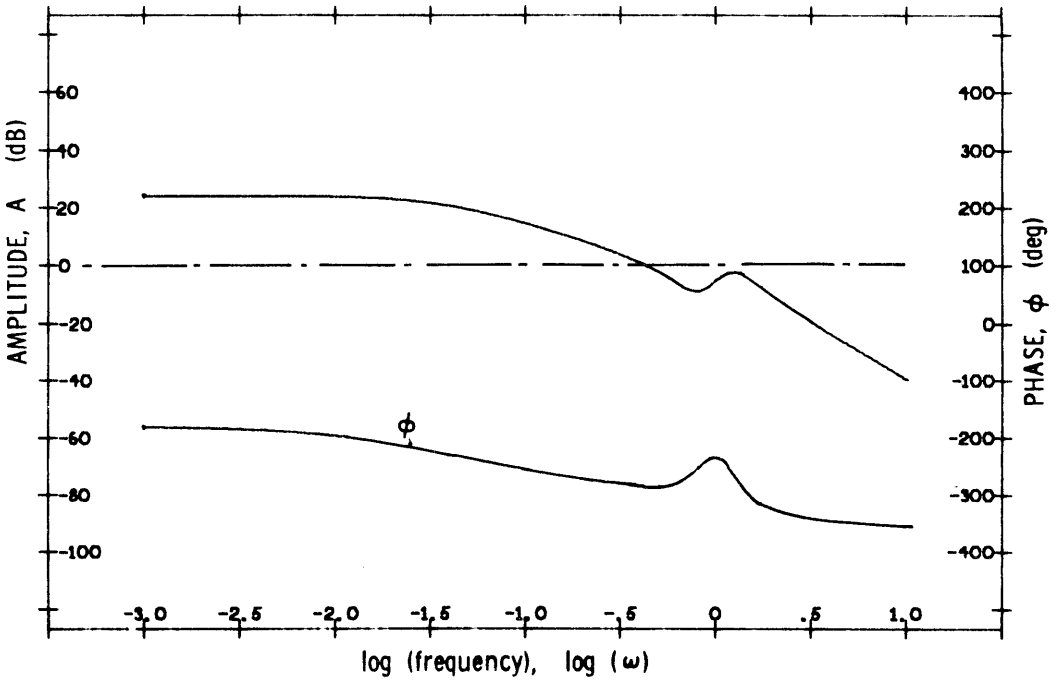

Fig. C.10 Frequency Plot of G_{22g}/s

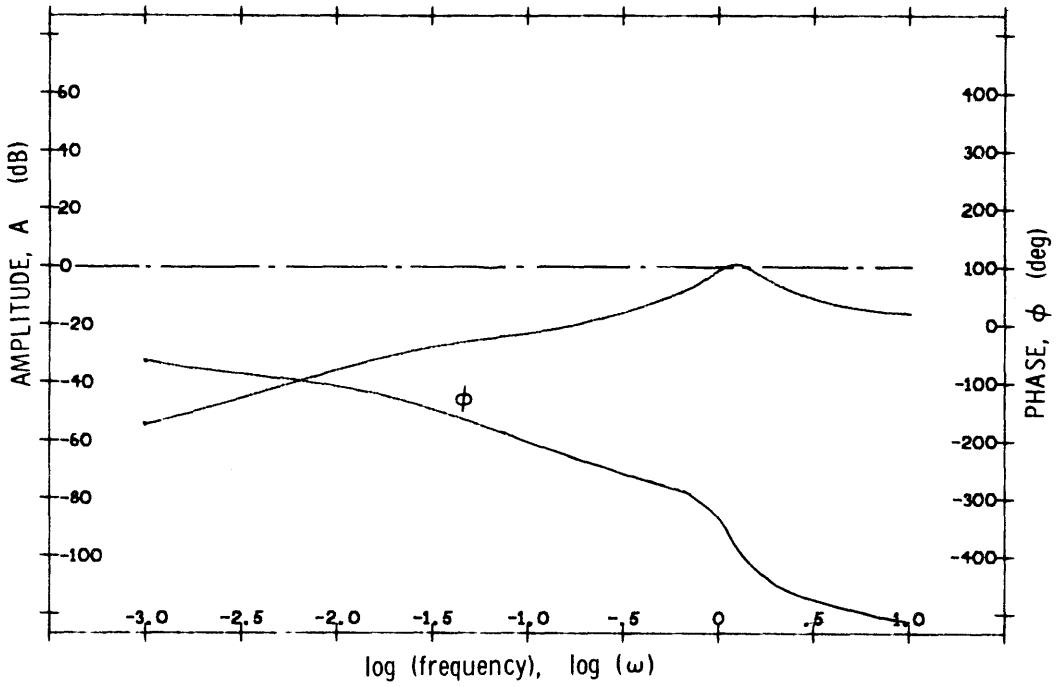

Fig. C.11 Frequency Plot of G_{31g}

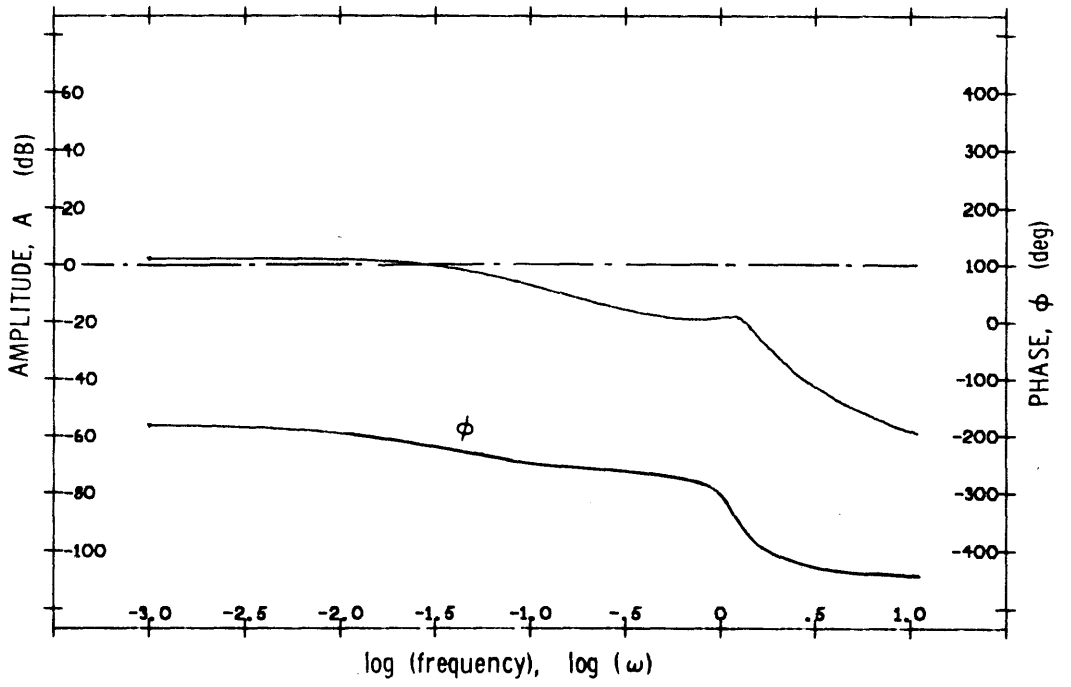

Fig. C.12 Frequency Plot of G_{32g}/s

APPENDIX D

THE "IDEAL" LATERAL AIRPLANE

The objective here is to translate optimum aircraft handling qualities specifications into "ideal" transfer functions. Handling qualities (Ref. 8) are specified most often in terms of limits on frequencies and dampings of motions, time constants, or desirable† s-plane positions of poles or zeros of transfer functions. No direct handling qualities requirements are placed on transfer functions.

In terms of dimensional stability derivatives, the linearized, Laplace-transformed perturbation equations of motion may be presented in matrix form as follows:

$$\underline{Ax} = \underline{Bu}$$

$$\begin{bmatrix} (-Y_{\phi} - Y_p^{*}s) & (1 - Y_r^{*}) & (s - Y_v) \\ s(s - L_p') & -L_r' & -L_\beta' \\ -N_p' & (s - N_r') & -N_\beta' \end{bmatrix} \begin{bmatrix} \phi \\ \dot{\psi} \\ \beta \end{bmatrix} = \begin{bmatrix} Y_{\delta_a} & Y_{\delta_r} \\ L_{\delta_a}' & L_{\delta_r}' \\ N_{\delta_a}' & N_{\delta_r}' \end{bmatrix} \begin{bmatrix} \delta_a \\ \delta_r \end{bmatrix} \quad \text{(D. 1)}$$

The following arguments were used to obtain ideal values for the various stability derivatives (from Ref's. 1 and 5). $Y_p^{*} = Y_r^{*} = L_r' = N_p' = 0$ since they represent undesirable dynamic couplings between sideslip, yaw, and roll motions. Positive dihedral ($L_\beta' < 0$) is desirable for static stability and to help with Dutch roll damping, but it must not be too large. In order to ensure neutral spiral stability, the term $-N_r'Y_\phi$ will be added to the yawing moment equation. N_β' must be positive for directional stability and N_r' must be large and negative, since it is the main contributor to Dutch roll damping. These specifications result in, for the ideal lateral matrix of stability derivatives:

†"Desirable" is generally defined by highest pilot rating.

$$A_{ideal} = \begin{bmatrix} -Y_{\phi} & 1 & (s - Y_v) \\ s(s - L_p') & 0 & -L_{\beta}' \\ N_r'Y_{\phi} & (s - N_r') & -N_{\beta}' \end{bmatrix}$$

The characteristic equation $\det(A_{ideal}) = 0$ has the approximate factorization:

$$\lambda(\lambda - L_p')[\lambda^2 + (-Y_v - N_r')\lambda + (N_{\beta}' + Y_v N_r' + Y_{\phi} L_{\beta}'/L_p')] = 0$$

where $\lambda = 0$ corresponds to the neutral spiral mode, $\lambda = L_p'$ corresponds to the roll mode, and the quadratic term

$$\lambda^2 + (-Y_v - N_r')\lambda + (N_{\beta}' + Y_v N_r' + Y_{\phi} L_{\beta}'/L_p') = \lambda^2 + 2(\zeta\omega)_d \lambda + \omega_d^2$$

represents the oscillatory Dutch roll motion.

The strictest handling qualities specifications were chosen to derive the "ideal" plant. It is desirable for the rolling motion time constant to be from .5 - 1.0 sec with the lower value preferred. Since $T_R \approx 1/(L_p')$, this requirement implies $L_p' \leq -2.0$. $L_p' = -2$ is chosen. Also, according to a collection of pilot opinions, $\zeta_d > .15$, $.8 < \omega_d < 6.0$ and $(\zeta\omega)_d = .35$ for good handling qualities. A value of .48 was actually chosen for $(\zeta\omega)_d$ after some unsatisfactory attempts using $(\zeta\omega)_d = .35$. This larger value gave more desirable Dutch roll damping.

From the approximate factorization of the characteristic equation we have

$$\lambda_1 = 0$$

$$\lambda_2 = L_p' = -2$$

$$.96 = -Y_v - N_r' \qquad \text{(D.2)}$$

$$\omega_d^2 = N_\beta' + Y_v N_r' + Y_\phi L_\beta'/L_p' \qquad (D.3)$$

It is also desirable to have the frequency of the quadratic numerator of the yaw rate to rudder transfer function be much less than the Dutch roll frequency. If this is so, the closed loop Dutch roll damping can be very good. An approximation can be given as

$$\omega_r^2 \approx \frac{g}{U_o} \frac{L_\beta}{L_p} \qquad (D.4)$$

By definition $L_i = L_i' + (I_{xz}/I_x)N_i'$, and since I_{xz}/I_x is usually small (it is -.0143 for the space shuttle) we shall, for the purposes of this analysis, say $L_i = L_i'$. Equations (D.2) - (D.4) can be solved for N_β', L_β', Y_v and N_r' by using some intuition as to relatively how large each derivative is. For instance, $N_\beta' > (Y_v + N_r' + Y_\phi L_\beta'/L_p')$ since $\omega_d^2 = N_\beta'$ is often a valid approximation. The "ideal" matrix of stability derivatives given below was derived for:

$$Y_\phi = \frac{g \cos \gamma_o}{U_o} \approx .11$$

$$\omega_d = 1.3 \qquad \zeta_d = .40 \qquad (\zeta\omega)_d = .48$$

$$\omega_r = .25$$

Also, with the approximation

$$2\zeta_r \omega_r \approx -(Y_v - \frac{g}{U_o} \frac{L_\beta}{L_p^2})$$

a value of $\zeta_r = .297$ is obtained.

These values, of course, represent just one possible set of "ideal" dynamics, since the specifications are usually given as a range of "best" values.

In order to have direct control in one axis only for each aerodynamic control large values were chosen for L_{δ_a}' and N_{δ_r}' while the other control derivatives were set equal to zero. Thus $L_{\delta_a}' = 3$, $N_{\delta_r}' = 1$, and $Y_{\delta_r} = Y_{\delta_a} = L_{\delta_r}' = N_{\delta_a}' = 0$.

The final result then, for the "ideal" lateral airplane dynamics, is

$$\begin{bmatrix} -.11 & 1 & (s + .180) \\ s(s + 2.0) & 0 & 1.14 \\ -.0858 & (s + .780) & -1.36 \end{bmatrix} \begin{bmatrix} \phi \\ \dot{\psi} \\ \beta \end{bmatrix} = \begin{bmatrix} 0 & 0 \\ 3 & 0 \\ 0 & -1 \end{bmatrix} \begin{bmatrix} \delta_a \\ \delta_r \end{bmatrix} \quad (D.5)$$

By appropriate use of Cramer's rule, ideal transfer functions can be found from Eq. (D.5). Frequency responses are presented in Figs. D.1 - D.6.

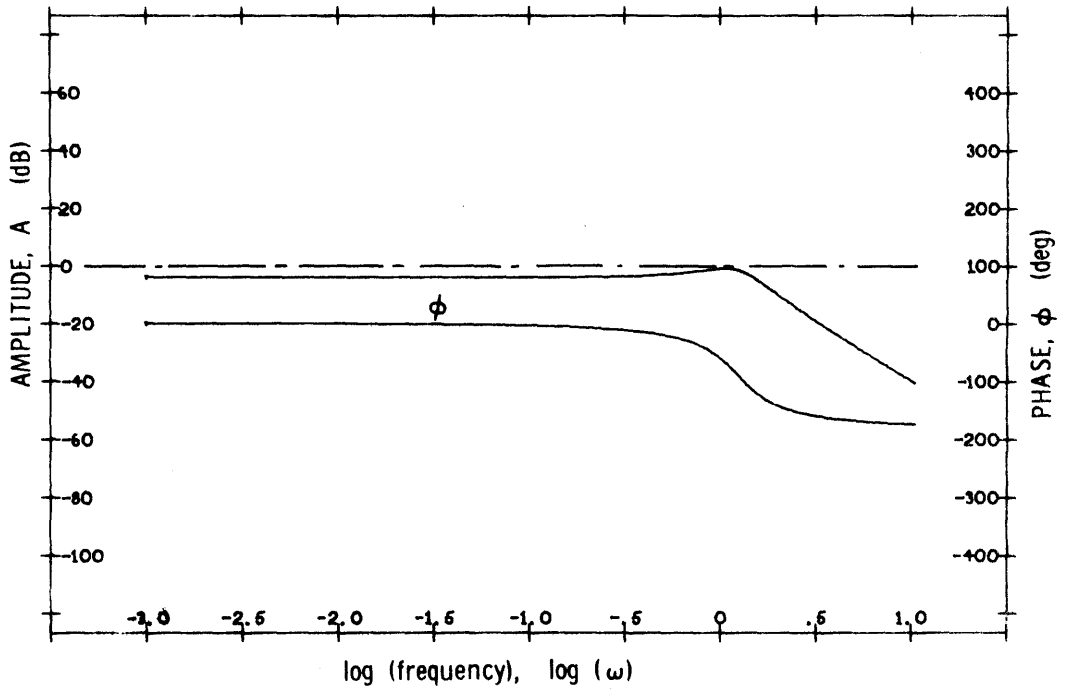

Fig. D.1 Frequency Plot of $G_{11_{ideal}}$

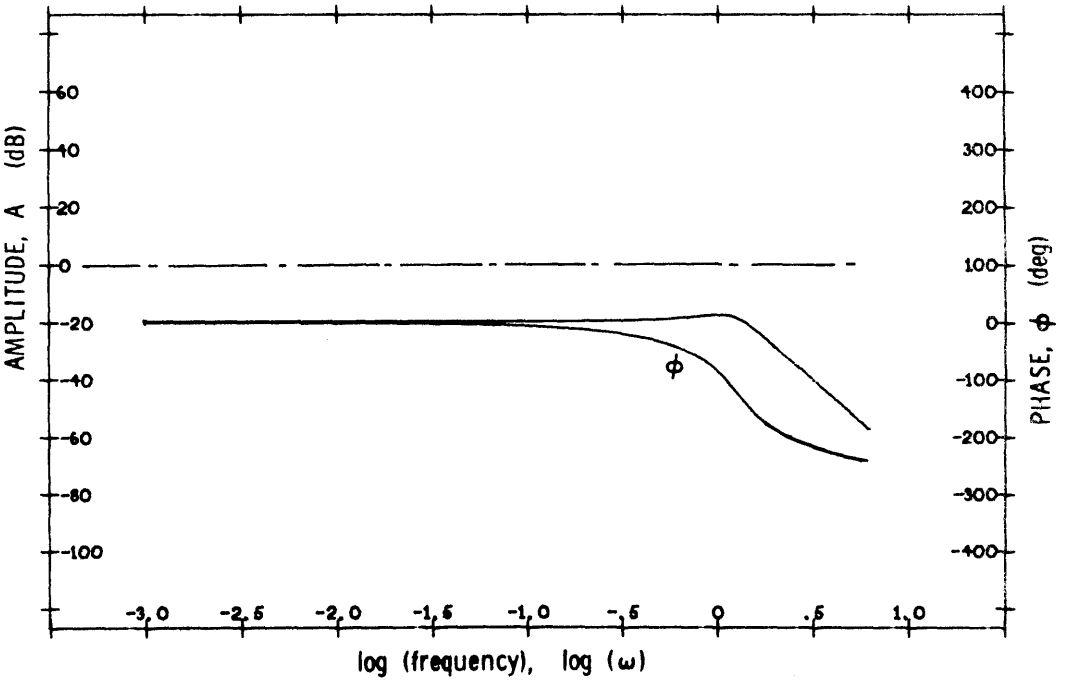

Fig. D.2 Frequency Plot of $G_{12_{ideal}}$

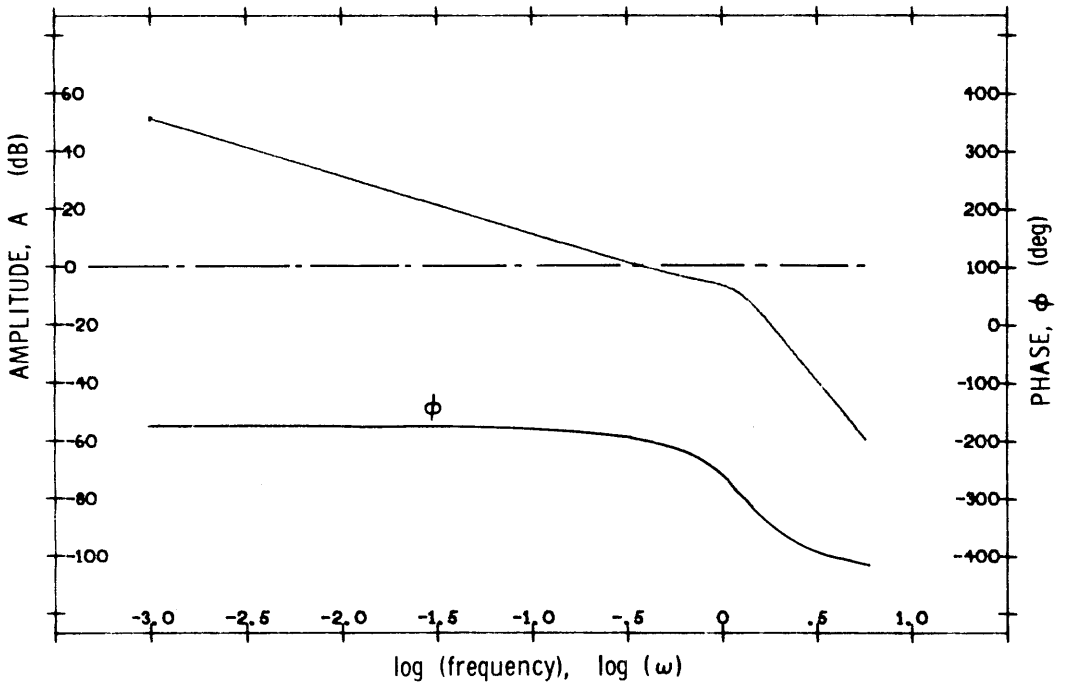

Fig. D.3 Frequency Plot of $G_{21_{ideal}}$

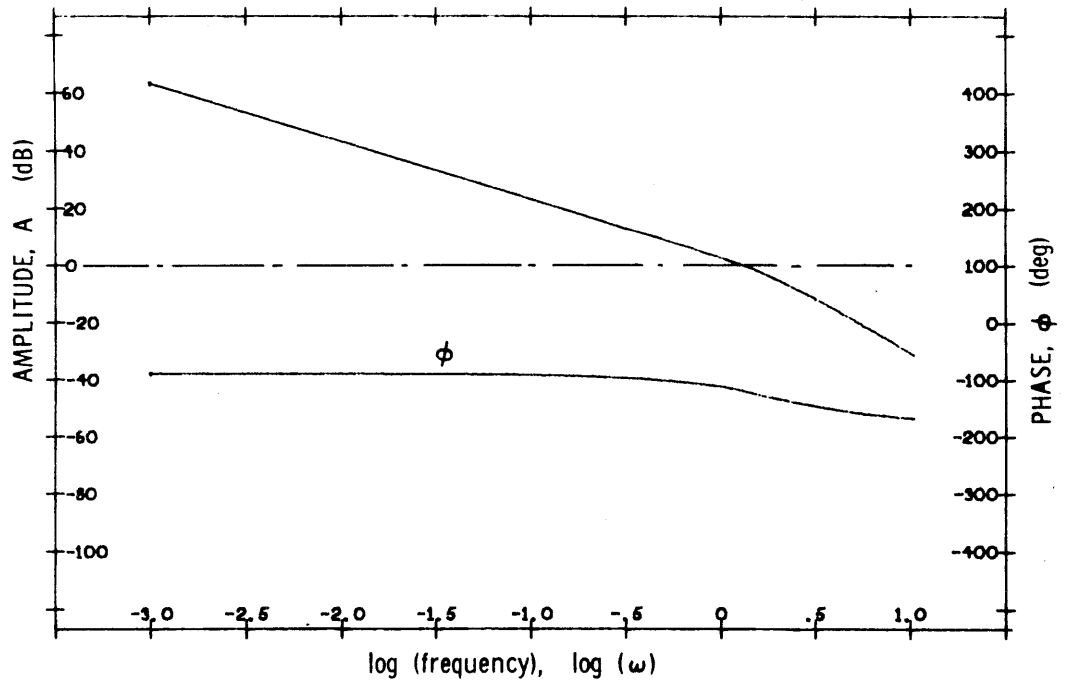

Fig. D.4 Frequency Plot of $G_{22_{ideal}}$

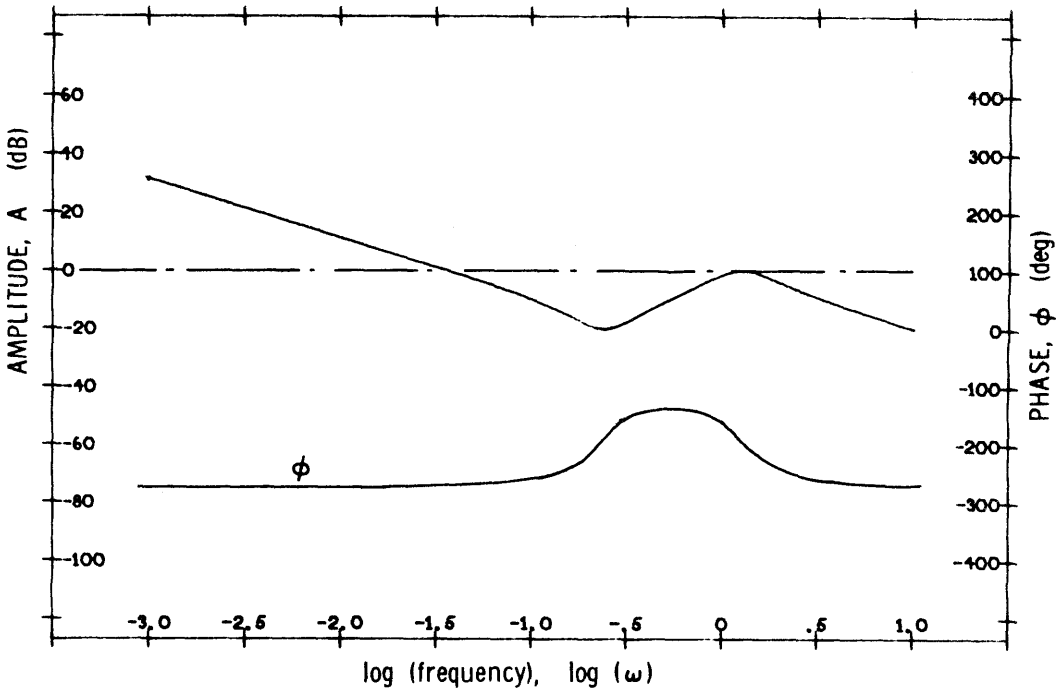

Fig. D.5 Frequency Plot of $G_{31_{ideal}}$

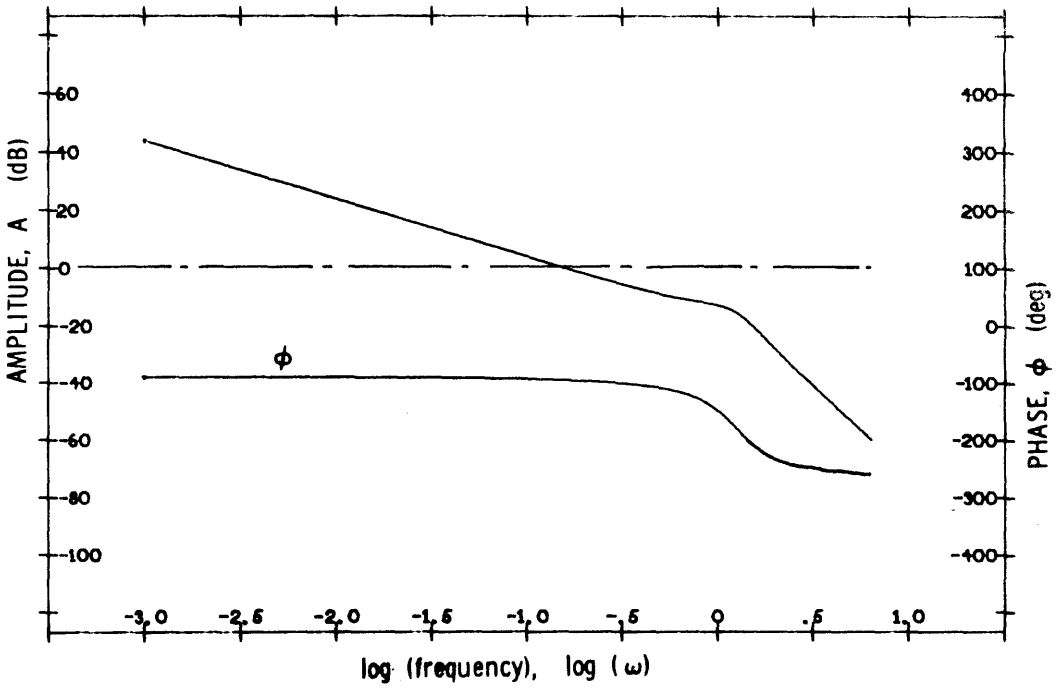

Fig. D.6 Frequency Plot of $G_{32_{ideal}}$

REFERENCES

1. Ashkenas, I. L., McRuer, D. T., and Pass, H. R., Analysis of Multiloop Vehicular Control Systems, ASD-TDR-62-1014, AF Flight Dynamics Lab, Wright-Patterson AFB, Ohio, March, 1964.

2. Cox, K. J., An Applied Synthesis Technique for Strongly Interacting Multivariable Control Systems, Ph.D. Thesis, Rice University, Houston, Texas, July, 1965.

3. Franklin, J. A., Turbulence and Lateral-Directional Flying Qualities, NASA CR-1718, prepared at Princeton University, Princeton, N. J., April, 1971.

4. Kavanagh, R. I., "The Application of Matrix Methods to Multi-Variable Control Systems", Journal, Franklin Institute, Phil., Pa., Nov., 1956.

5. Markland, C. A., "Design of Optimal and Suboptimal Stability Augmentation Systems", AIAA Journal, Vol. 8, No. 4, April, 1970.

6. McRuer, D. T., Ashkenas, I. L., Graham, D., Aircraft Dynamics and Automatic Control, Systems Technology, Inc., Hawthorne, Cal., August, 1968.

7. Morse, A. S., Wonham, W. M., "Decoupling and Pole Assignment by Dynamic Compensation", SIAM J. Control, Vol. 8, No. 3, August, 1970.

8. Woodcock, R. J., et al, "Background Information and User Guide for MIL-F-8785B (ASG), Military Specification — Flying Qualities of Piloted Airplanes", AFFDL-TR-69-72, August, 1969.